AD-A075 168 AIR WEATHER SERVICE SCOTT AFB IL F/G 4/1
ELECTRO-OPTICAL HANDBOOK. VOLUME I. WEATHER SUPPORT FOR PRECISI--ETC(U)
MAY 79 K G COTTRELL, P D TRY, D B HODGES
UNCLASSIFIED AWS/TR-79/002 NL

1 OF 2
ADA
075168

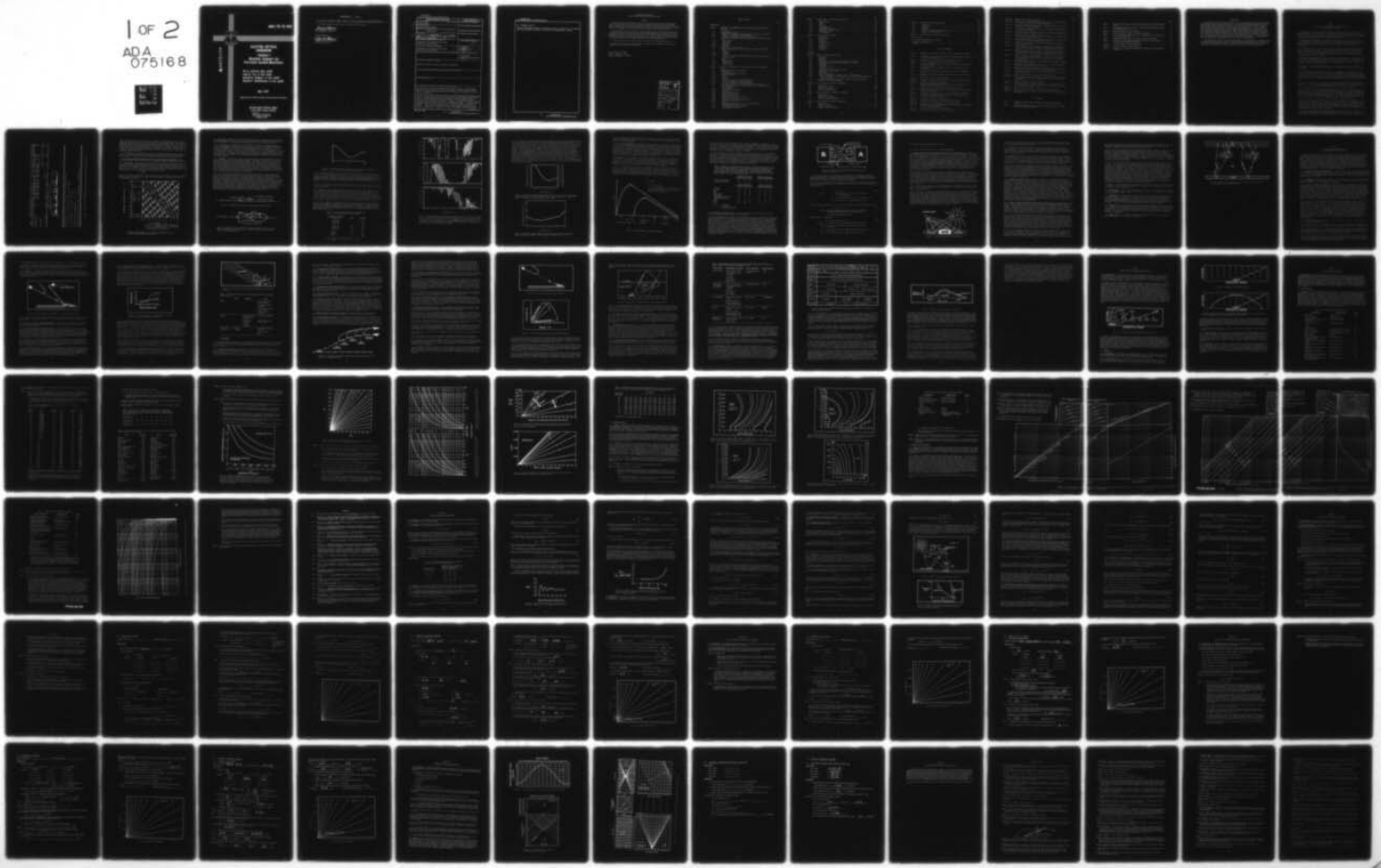

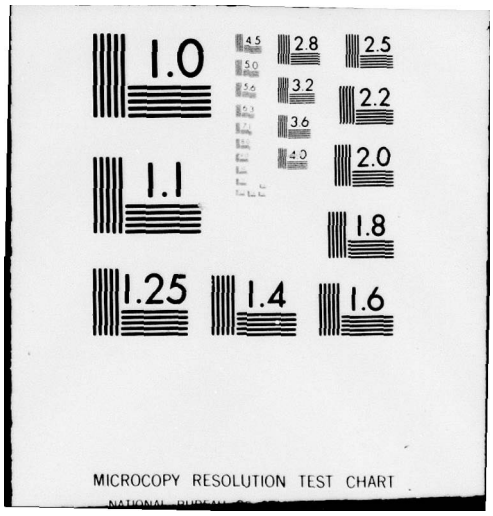
1.0
1.1
1.25
1.4
1.6
1.8
2.0
2.2
2.5
2.8
3.2
3.6
4.0
4.5
5.0
5.6
MICROCOPY RESOLUTION TEST CHART

AWS/TR-79/002

ELECTRO–OPTICAL HANDBOOK

Volume I
Weather Support for Precision Guided Munitions

Kit G. Cottrell, Maj, USAF
Paul D. Try, Lt Col, USAF
Donald B. Hodges, Lt Col, USAF
Ronald F. Wachtmann, Lt Col, USAF

May 1979

AIR WEATHER SERVICE (MAC)
Scott AFB, Illinois 62225

REVIEW AND APPR[illegible]NT

This report is approved for public release. There is no objection to unlimited distribution of the report to the public at large, or by DDC to the National Technical Information Service (NTIS).

This technical report has been reviewed and is approved for publication.

Gary D. Atkinson

GARY D. ATKINSON, Colonel, USAF
Asst DCS/Aerospace Sciences

FOR THE COMMANDER

Robert M Gottuso

ROBERT M. GOTTUSO, Colonel, USAF
DCS/Aerospace Sciences

UNCLASSIFIED

SECURITY CLASSIFICATION OF THIS PAGE *(When Data Entered)*

REPORT DOCUMENTATION PAGE	READ INSTRUCTIONS BEFORE COMPLETING FORM
1. REPORT NUMBER: AWS/TR-79/002 (14)	2. GOVT ACCESSION NO.
3. RECIPIENT'S CATALOG NUMBER	
4. TITLE *(and Subtitle)*: (6) ELECTRO-OPTICAL HANDBOOK. Volume I. Weather Support for Precision Guided Munitions	5. TYPE OF REPORT & PERIOD COVERED
	6. PERFORMING ORG. REPORT NUMBER
7. AUTHOR(s): (10) Kit G. Cottrell, ~~Maj, USAF~~; Paul D. Try, ~~Lt Col, USAF~~; Donald B. Hodges, Lt Col, USAF; Ronald F. Wachtmann, ~~Lt Col~~, USAF	8. CONTRACT OR GRANT NUMBER(s)
9. PERFORMING ORGANIZATION NAME AND ADDRESS: Headquarters Air Weather Service (MAC), Scott AFB, Illinois 62225	10. PROGRAM ELEMENT, PROJECT, TASK AREA & WORK UNIT NUMBERS: (12) 1A8
11. CONTROLLING OFFICE NAME AND ADDRESS: Headquarters Air Weather Service (MAC), Scott AFB, Illinois 62225 (11)	12. REPORT DATE: May 1979
	13. NUMBER OF PAGES: 105
14. MONITORING AGENCY NAME & ADDRESS *(if different from Controlling Office)*	15. SECURITY CLASS. *(of this report)*: Unclassified
	15a. DECLASSIFICATION/DOWNGRADING SCHEDULE

16. DISTRIBUTION STATEMENT *(of this Report)*

Approved for public release; distribution unlimited.

17. DISTRIBUTION STATEMENT *(of the abstract entered in Block 20, if different from Report)*

18. SUPPLEMENTARY NOTES

19. KEY WORDS *(Continue on reverse side if necessary and identify by block number)*

Electro-Optics; Precision Guided Munitions; Weather Support; Electromagnetic Radiation; Radiative Energy; Guidance System Types; Electro-optical sensors; Radiation Transfer; Rapid Manual Support Methods; Target Acquisition; Electromagnetic Propagation.

20. ABSTRACT *(Continue on reverse side if necessary and identify by block number)*

A foundation for weather support to Precision Guided Munitions operating at visual through microwave wavelengths is established for use by Air Weather Service base weather station forecasters and staff weather officers. Chapter 1 describes the effects of the atmosphere and the earth's surface on electromagnetic energy. Precision Guided Munitions (PGMs) and their sensitivities to the environment are discussed in Chapter 2. The next two chapters discuss weather support concepts and techniques to support PGMs. A glossary of terms, supplemental radiative transfer

(Cont'd)

DD FORM 1 JAN 73 1473

UNCLASSIFIED

SECURITY CLASSIFICATION OF THIS PAGE *(When Data Entered)*

014 670

20. ABSTRACT (Cont'd).

theory, and example worksheets illustrating support techniques to TV, infrared, and laser designator systems are included in the appendixes. (Author)

ELECTRO-OPTICAL HANDBOOK
WEATHER SUPPORT FOR PRECISION GUIDED MUNITIONS

PREFACE

This Electro-Optical (E-O) Handbook, Volume I, Weather Support for Precision Guided Munitions represents over four years of effort in producing a publication suitable for use by Air Weather Service (AWS) personnel. Originally designed for the Advanced Weather Officer at AWS wing level, the draft E-O Handbook was restructured and simplified for use as a text for formal instruction in weather support to E-O systems and as a reference for the base weather station (BWS) forecaster.

The authors wish to express thanks to a number of people who were involved in the development of this Handbook. Members of the AWS Electro-Optical Systems Working Group, the reviewers at Air Force Geophysics Laboratory (Dr. Robert McClatchey), the USAF Environmental Technical Applications Center (USAFETAC) (Dr. Pat Breitling, Maj John Mill, and Mr. John Louer), the Institute for Defense Analysis (Mr. Lucien Biberman), Lt Col Tom Pries (USAF Reserve), and the Headquarters AWS Aerospace Sciences clerical staff (particularly Mrs. Phyllis Eggemeyer) deserve special recognition.

A future volume(s) of the E-O Handbook will be designed for the Advanced Weather Officer.

Comments and criticism are welcomed and should be addressed to HQ AWS/DN, Scott AFB, IL 62225, AUTOVON 638-4781, or Commercial (618) 256-4781.

Kit G. Cottrell, Maj, USAF
Paul D. Try, Lt Col, USAF
Donald B. Hodges, Lt Col, USAF
Ronald F. Wachtmann, Lt Col, USAF

TABLE OF CONTENTS

LIST OF ILLUSTRATIONS

LIST OF TABLES

INTRODUCTION

The Electro-Optical (E-O) Handbook is designed for use by the base weather station (BWS) forecaster and the advanced weather officer. Chapters 1, 2, 3, and 4 contain rudimentary discussions of electromagnetic radiation in the atmosphere (Chapter 1), E-O Precision Guided Munitions (PGMs) (Chapter 2), weather support concepts (Chapter 3), and simple, manual techniques which can be used to quantitatively estimate environmental effects on PGMs (Chapter 4 and Appendixes B, C, and D). The manual techniques should be used as backup methods to computerized products which will originate at the Air Force Global Weather Central (AFGWC) and as preliminary support methods until centralized techniques can be developed and implemented operationally. These simple techniques for support are preliminary due to newness of E-O systems and have not been proven in operational use. Furthermore, these techniques are evolving and will be replaced as better techniques become available. The forecasts derived from the techniques must be reviewed with physical insight before dissemination to the operational user. AWS personnel must familiarize the user with the new forecast parameters.

The advanced weather officer and interested BWS personnel will find Appendix A an extension of the information presented in Chapters 1 and 2. Appendix E contains a graphical method for computing solar elevation angle, and Appendix F references Third Weather Wing (3WW) activities related to support of the TV-GBU-15. The glossary and acronym sections define many electro-optically related terms.

Chapter 1

THE EFFECTS OF THE ATMOSPHERE AND THE EARTH'S SURFACE ON ELECTROMAGNETIC RADIATION

1.1 Introduction. Precision Guided Munitions (PGMs) use guidance systems which respond to electromagnetic radiation as a sensed stimulus. This chapter describes fundamental environmental processes which affect the source of this radiation and its propagation through the atmosphere. Knowledge of these processes should provide greater understanding of the weather sensitivities of PGMs described in Chapter 2, and enhance the ability to support them operationally.

1.2 Electromagnetic (EM) Radiation. Electromagnetic radiation is energy that propagates through space, the atmosphere, and other media in the form of an advancing wave in the ambient electric and magnetic fields. The propagation of radiation is called radiation transfer. Common examples of radiation include light from a searchlight, radio, or television waves, and energy created by a microwave oven.

1.2.1 Since electromagnetic energy travels in wave forms, radiation is often characterized by the associated wavelength or frequency. Usually, wavelength is used for radiation in the visible and infrared spectra; however, frequency is usually used to characterize radio, TV, and radar waves. Figure 1 provides the radiation wavelengths and frequencies of interest, relates wavelength to frequency, and defines common terminology. Subsequent discussion will reference the main categories and subcategories illustrated in Figure 1.

1.3 Examples of Electromagnetic Radiation Interaction within the Atmosphere. Electromagnetic radiation interacts with the atmosphere (and the earth's surface) in different ways. Depending on the atmospheric constituents involved and the radiation wavelength, the effect of this interaction on a PGM ranges from insignificant to devastating. The following examples illustrate the physical processes causing some of these interactions.

1.3.1 Examples of Interaction with Visible Light. The sun is the primary source of EM energy in the atmosphere. Most of this energy arrives in the lower atmosphere at visible and near infrared wavelengths.

1.3.1.1 When sunlight passes through a cloudless, clean atmosphere, the solar disc appears white. This white appearance represents a combination of all the wavelengths of visible light (i.e., there are many colors in white light). The sky is blue because molecules within the atmosphere preferentially redirect more of the incident blue light of the sun than any other color toward an observer on the earth's surface. This redirection of light is called scattering. With a clear, clean atmosphere, the solar disc is distinct in shape and the solar brilliance originates almost exclusively from the disc.

1.3.1.2 On a very hazy, smoky, cloud-free day, a surface observer observes that the sky appears bright white. This results from scattering (redirection) of sunlight by haze and smoke particles. Usually, the solar disc is indistinct; this blurring of the solar image is also caused by scattering. In this case the white sky color results from scattering of all visible wavelengths.

1.3.1.3 Consider a hazeless and smokeless atmosphere with a thin layer of cloud cover. Sunlight passing through the clouds causes them to appear nearly white as a result of the scattering of the multicolored sunlight by the cloud droplets. The white appearance indicates that all visible wavelengths are scattered to approximately the same degree. The image of an airplane flying above this thin cloud cover may be blurred by the cloudiness. The cloud droplets randomly scatter the image light from the airplane out of a surface observer's field of view, while scattering nonimage light into the field of view. Receipt of both image and nonimage light causes blurring.

1.3.1.4 As the cloud cover the solar disc and objects above the clouds are no longer seen. The sunlight is scattered numerous times or absorbed by the cloud droplets; if the solar energy leaving the cloud base is sufficiently reduced, the cloud bases may appear black. The image light from an airplane above the clouds is likewise scattered and absorbed in its interaction with the cloud droplets. Although some of the image light may pass through the cloudiness, the airplane cannot be recognized below the cloud because of this blurring caused by the clouds. When viewing the clouds from above, bright reflection of sunlight is seen.

1.3.2 Example of the Interaction with Infrared Radiation. Consider the effect of cloud cover on the nighttime cooling process in the lower atmosphere near the earth's surface. We know that minimum nighttime surface temperatures associated with clean (i.e., unpolluted), cloudless skies are

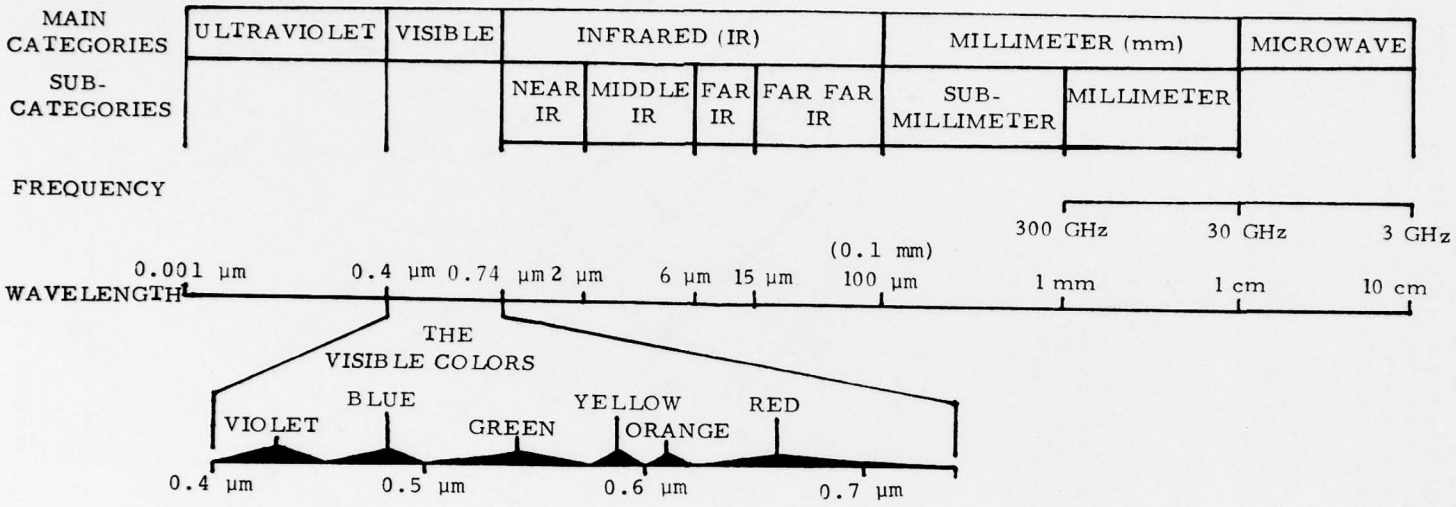

Symbol definition: 1 Hz = 1 Hertz = 1 cycle/sec; 1 GHz = 1 Gigahertz = 10^9 Hz;

1 cm = 1/100 meter = 10^{-2} meter; 1 mm = 1/1000 meter = 10^{-3} meter;

1 μm = 1 micrometer = 1/1,000,000 meter = 10^{-6} meter.

Frequency-Wavelength relationship: $S = f \cdot \lambda$ where

S = speed of light (2.997×10^{10} cm/sec), f = frequency (Hz), λ = wavelength (cm).

Figure 1. Categories of Electromagnetic Radiation and Their Wavelength and Frequency Limits.

colder than those associated with cloudy skies. The degree of cooling achieved at the earth's surface is related to the net loss of surface radiation at infrared wavelengths. Cloud cover will absorb and re-emit the infrared energy received from the earth's surface. Much of this energy is re-emitted by the clouds toward the surface and reduces the degree of surface cooling. With clean, cloudless skies, very little infrared radiation is absorbed by the atmosphere, and very little is, in turn, re-emitted by the atmosphere downward to the surface. Thus, the net loss of surface radiation is usually greater with cloudless skies, the earth's surface cools at a faster rate, and the minimum temperature is lower.

1.3.3 These examples illustrate some of the effects of the physical processes affecting radiation transfer. These physical processes are identified and described in the next section in general terms. Appendix A contains a more detailed discussion of these radiative transfer processes.

1.4 Interaction of Atmospheric Physical Processes with Electromagnetic (EM) Radiation. Four atmospheric processes affect radiation transfer: reflection, scattering, absorption, and emission.

1.4.1 Size Parameter. Atmospheric gaseous molecules and particulates (dusts, hazes, smokes, fogs, other aerosols, cloud droplets, and precipitation) affect the propagation of radiation. The types and sizes of these atmospheric constituents and the wavelengths of the radiation determine their influence. It is convenient to introduce the concept of the size parameter in discussing reflection and scattering. The value of this size parameter determines whether scattering or reflection is the predominant process. The size parameter is defined by the equation

$$X = \frac{2\pi r}{\lambda} \tag{1-1}$$

where r is the particle radius, and λ is the wavelength of incident radiation. Figure 2 illustrates the values of the size parameter as a function of the wavelength of the radiation and the size of the atmospheric particles.

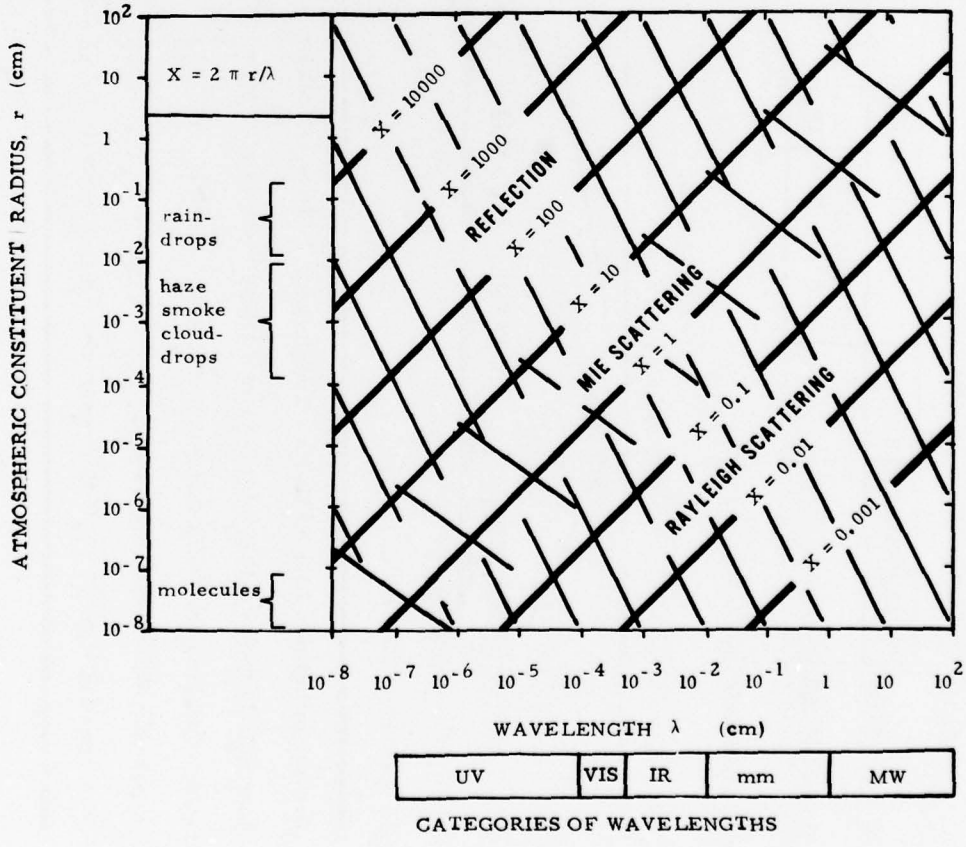

Figure 2. Size Parameter (X) as a Function of Atmospheric Radius (r) and Electromagnetic Radiation Wavelength (λ).

1.4.2 Reflection. Sunlight is reflected from the tops and sides of clouds. Reflection takes place when the wavelength of radiation is much smaller than the size of the atmospheric constituents; that is, the size parameter, X, is greater than approximately ten (as may be seen from Figure 2).

1.4.2.1 Three terms are frequently used in the discussion of reflection. Reflectance (from an object) or reflectivity (property of a material), describes the ratio of the amount of radiation at a specific wavelength that is reflected from a substance (for example, clouds) to the total amount of radiation incident on the substance at a specific wavelength. Values of reflectance (or reflectivity) range from zero to one where a perfect reflector (i.e., all incident energy is reflected) has a reflectance value equal to one. Reflectance varies widely at different wavelengths for a given reflecting surface. The albedo is the average value (averaged over wavelength) of the reflectivity. The averaging interval may be the entire electromagnetic spectrum, or some specified interval such as the visible spectrum.

1.4.3 Scattering. The blue sky on cloud free, clear days and the sunlight brightness from all sky quadrants on hazy days are manifestations of atmospheric scattering. The blue sky results from the preferential scattering of the short wavelengths (blue) of sunlight by molecules in the atmosphere; this type of scattering is called Rayleigh scattering. Larger particles such as cloud droplets, dust, haze, and smoke particles cause the sky to appear white. Because the size parameters for these particles with respect to visible light is near one, the scattering of sunlight by these particles is called Mie scattering. Figure 2 discriminates between regions of Rayleigh and Mie scattering for other wavelengths and particle sizes. Mie scattering occurs when the size parameter is on the order of one. Rayleigh scattering occurs when the size parameter is much less than one (i.e., the particle size is much less than the wavelength of the radiation).

1.4.3.1 Mie scattering by atmospheric particles is directional in nature. Light incident on a particle may be scattered in any direction, but theory and observation have shown that the distribution of the scattered energy follows a well-defined pattern. Figure 3 depicts the basic geometry of the scattering process. The forward scattering direction is defined as the direction of propagation of the incident radiation. Figure 4 describes the directional distribution of scattering by a typical atmospheric aerosol particle. Forward scattering predominates, while a secondary maximum is evident in the backward direction (backscattering). The strong tendency toward forward scatter explains why on a sunny, hazy day, objects may be more easily seen with the sun at our backs than if we look toward the sun when viewing the same object. When looking toward the sun, image quality (i.e., apparent contrast between object and background) is degraded by the sunlight which is "forward scattered" into the line of sight between the observer and the object. Figure 5 shows a typical angular distribution of scattering intensity for spherical atmospheric particles.

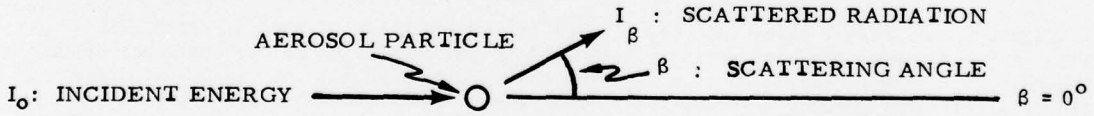

Figure 3. The Geometry of Scattering of Radiation by Spherical Particles.

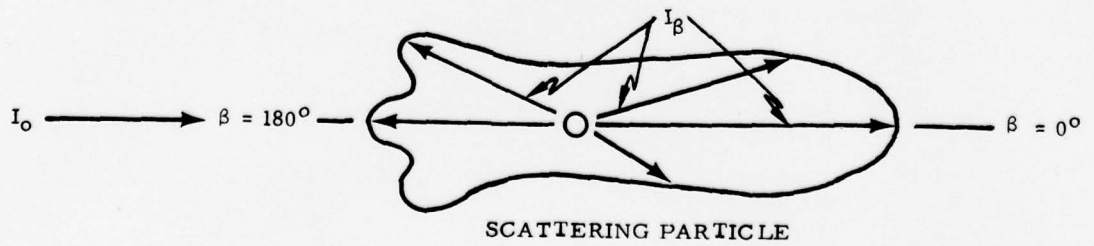

Figure 4. Typical Mie Scattering Pattern for Spherical Particles. The length of the arrows is proportional to the percentage of incident energy scattered in each direction by the scattering particle.

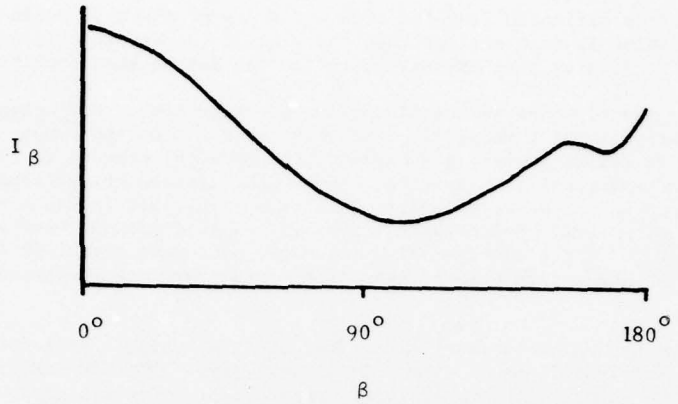

Figure 5. Mie Scattered Radiative Intensity (I_β) as a Function of Scattering Angle (β) for an Atmospheric Particle (assumed spherical).

1.4.3.2 The scattering process in the atmosphere is difficult to quantify and forecast due to the lack of appropriately measured parameters such as the size distributions of aerosols and cloud droplets, their shapes, their refractive indices, and their chemical properties (through which refractive index can be determined). Visibility forecasts are usually "guesstimated", because the characteristics of air pollutants and natural aerosols are not measured, and certainly not forecast. Forecasting visibility in haze, smoke, and dust is really a prediction of the scattering effect.

1.4.3.3 The strong degree of scattering and reflection by cloud particles at visible and infrared wavelengths indicates that clouds of any appreciable thickness will be nearly opaque to visible and and infrared radiation.

1.4.4 Absorption. Many atmospheric constituents (mainly water vapor, carbon dioxide, ozone, and oxygen) absorb radiation propagating through the atmosphere. This absorption takes place on a molecular scale and occurs selectively with respect to wavelength. Each absorbing constituent characteristically absorbs in specific wavelength intervals called absorption bands. Radiation at other wavelengths is not significantly absorbed by that constituent. Because the atmospheric constituents selectively absorb radiation at varying wavelengths, each wavelength or wavelength interval must be examined separately to assess the total effect of all atmospheric absorbing constituents. No attempt will be made in this text to detail the effects of each constituent on each wavelength.

1.4.4.1 Figure 6 and Table 1 illustrate the effects of certain gases on some important wavelength intervals. A few comments are appropriate. Ozone and oxygen absorption in the upper atmosphere prevent harmful ultraviolet radiation from reaching the earth's surface. At visible wavelengths, there are no significant gaseous absorbers of EM radiation. Two atmospheric windows exist in the region from 3.5 μm to 4.2 μm and the region from 8.5 μm to 13 μm; within these windows very little band absorption takes place.

Table 1. Significant Atmospheric Gaseous Absorbers (H_2O, CO_2, O_3, O_2)* at Visible and Infrared Wavelengths.

WAVELENGTH OR WAVELENGTH INTERVAL (μm)	BAND	ABSORBER
1.319-1.498		H_2O
1.762-1.977		H_2O
2.520-2.845		H_2O
2.904-3.571	3.2	H_2O
4.10-4.45	4.3	CO_2
4.876-8.699	6.3	H_2O
9.4-9.9	9.6	O_3
10.591		CO_2
12.9-17.1	14.7	CO_2
18-20		H_2O

* H_2O - water, CO_2 - carbon dioxide, O_3 - ozone, O_2 - oxygen.

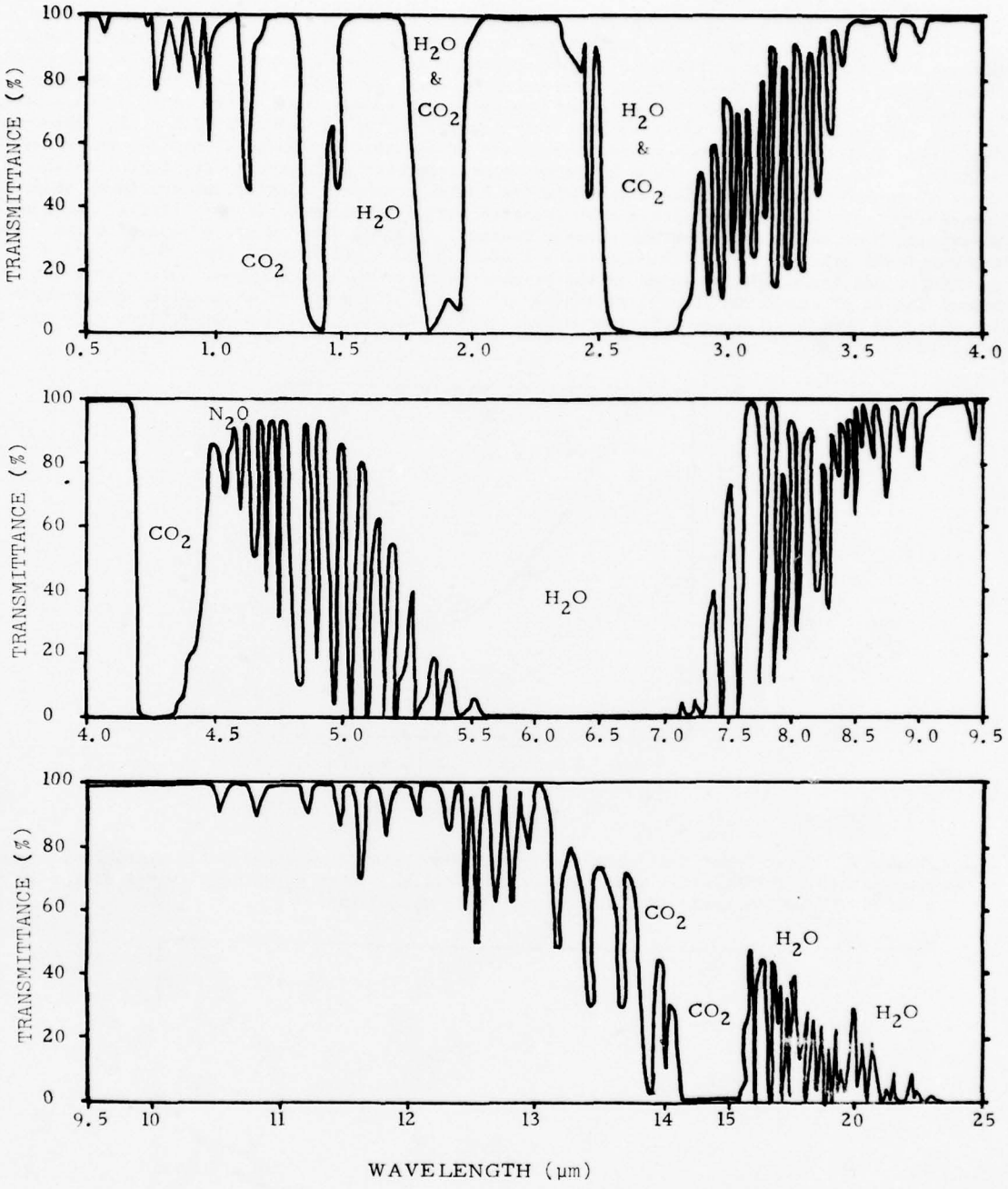

Figure 6. Major Absorption Bands of Atmospheric Gases in the Region from 0.5 to 25 Micrometers. Low transmittance values indicate strong absorption. Note the existence of little or no absorption in the region from 3.5 to 4.2 micrometers and the region from 8.5 to 13 micrometers. These two regions are the so-called atmospheric windows. These transmittances are for a 0.3-km path length at sea level and 79°F containing 5.7 mm of precipitable water. (Drawn on basis of RCA [16], pp. 83-84).

1.4.4.2 In addition to band absorption, certain gases exhibit a characteristic described as continuum absorption. The water vapor continuum is the most important with regard to effects on PGMs. Continuum absorption is characterized by an absorption coefficient which varies slowly with wavelength across broad regions of the spectrum. The value of this coefficient shows a strong dependence on the concentration of water vapor, and a lesser dependence on temperature. The result of this dependence is that absorption by water vapor becomes very significant in atmospheres with a high absolute humidity. Note that the important parameter here is the absolute humidity and not the relative humidity. The continuum absorption by water vapor is most significant in tropical atmospheres. Even tropical desert atmospheres with a low relative humidity exhibit significant continuum absorption. Conversely, cold atmospheres with a high relative humidity will exhibit very little continuum absorption because of their low water vapor content. Figures 7 and 8 are examples of the value of the continuum absorption coefficients for a typical humid atmosphere in the 3.5-4.0 μm and 8.0-13.0 μm regions, respectively. Water vapor is the primary absorber in both regions. Nitrogen exhibits a lesser degree of continuum absorption in the 3.3- to 4.2-μm region. The so-called atmospheric windows described in Para. 1.4.4.1 are not true windows because of the continuum absorption; they are sometimes referred to as "dirty" windows.

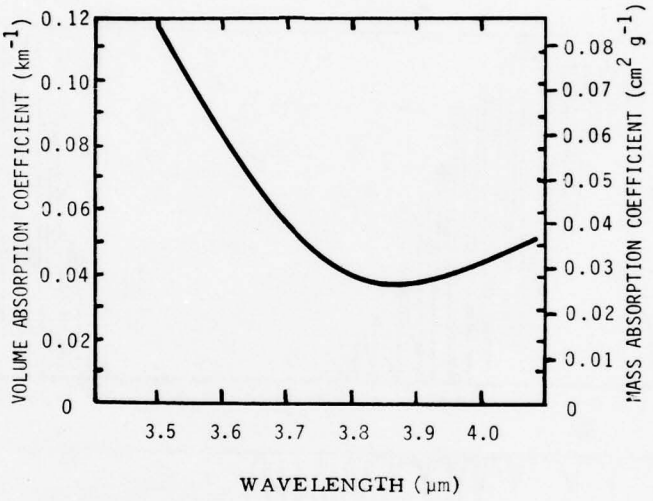

Figure 7. Water Vapor Continuum Absorption Coefficients in the 3.5-4.0 Micrometer Region. Temperature = 296°K, water vapor pressure = 19.1 mb, water vapor density = 1.3982×10^{-5} g cm^{-3}. (Drawn on basis of White et al. [20], pp. 63-78).

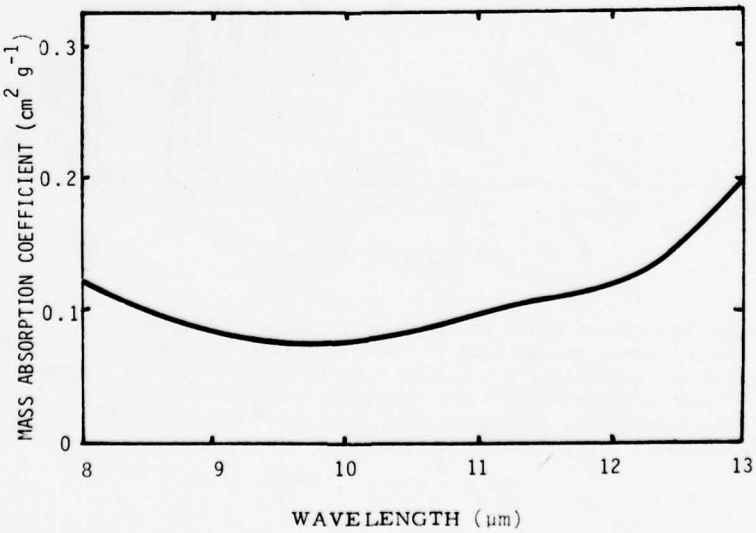

Figure 8. Water Vapor Continuum Mass Absorption Coefficients in the 8-13 Micrometer Region (representative sample). (Drawn on basis of Kondratyev [10], p. 116).

1.4.4.3 Absorption by liquids and solids is also important. Aerosols and cloud droplets remove radiation by absorption in addition to scattering. This absorption is wavelength dependent (as is the case for gaseous absorption).

1.4.4.4 The term absorptivity is often used to describe the ratio of the amount of radiation (at a specific wavelength) absorbed by a substance (for example, ozone, or water vapor) to the total amount of radiation (at the same wavelength) incident on the substance. Absorptivity may have a value of zero to one where a value of one implies that all radiation incident on a substance is absorbed by the substance. Although there is no real substance that has an absorptivity equal to one, certain substances approach the perfect absorptivity of unity. These substances are referred to as "black bodies" at those wavelengths at which they exhibit this characteristic. In mathematical terms the degree of absorptivity for a given atmospheric path containing a mixture of absorbing constituents is described by means of the absorption coefficient (see Section 1.5).

1.4.5 Emission. All electromagnetic radiation must originate at some location (for example, a flashlight or a household radiator). The process operates at the molecular scale and is called emission. Every constituent in the atmosphere emits radiation (gases, clouds and aerosols are included). However, emission occurs selectively with respect to wavelength, and the amount of emitted energy may or may not be significant at a given wavelength. In general, atmospheric constituents emit radiation at the same wavelengths at which they absorb radiation.

1.4.5.1 To describe emission more fully, two terms must be defined: "black body" emission and emissivity. The perfect absorber, known as a black body, is also a perfect emitter. Planck specified the intensity of energy emitted by a black body. Planck's Law relates the energy emitted by a black body at each wavelength to the temperature of the body. "Black body" emission is the maximum energy that any real substance can emit at a given temperature and wavelength. Figure 9 illustrates a plot of this expression for two temperatures. This expression cannot be applied to

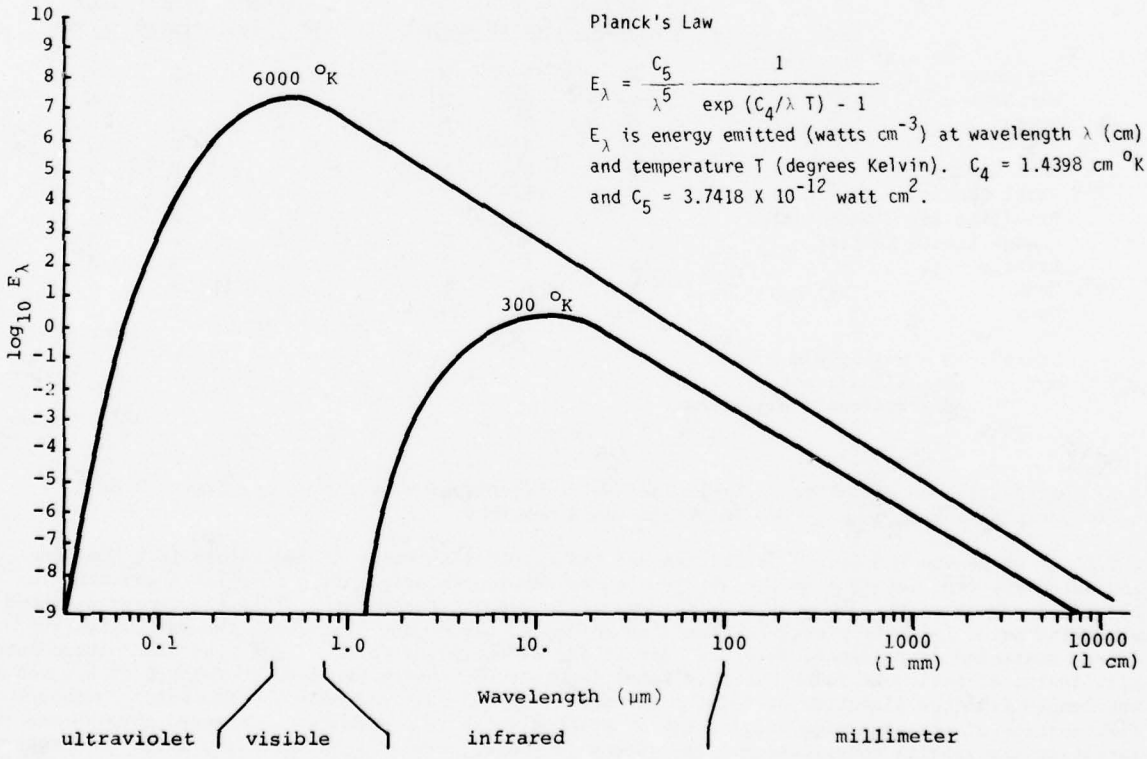

Figure 9. Plot of Planck's Law for 300°K and 6000°K.

real-world emitters without a corrective factor. The term, emissivity, is this factor. It is defined as the ratio of the actual amount of energy emitted at a specific wavelength and temperature to the black body emission at the same wavelength and temperature. Values for emissivity range from zero to one. An emissivity value of one implies that a substance is a "black body" at the specified wavelength. Emissivity accounts for the molecular emissions for specific substances, whereas the black body emission is independent of the type of substance.

1.4.6 Table 2 describes the relative importance of the various extinction (i.e., scattering and absorption) processes as a function of wavelength for various meteorological conditions. The importance of each process cannot be quantified precisely in general terms; the information provided is intended to highlight the importance of various extinction processes at each wavelength interval under different meteorological conditions. The importance of the extinction processes at infrared wavelengths pertain to the two atmospheric windows at 4 micrometers and 10 micrometers. Different values would be assigned in the major absorption bands. Similarly the values in the microwave/millimeter wavelengths apply to windows near 19GHz, 37GHz, and 94GHz.

Table 2. Importance of Various Extinction Processes at each Wavelength Interval under Various Meteorological Conditions. Note that molecular extinction processes apply only to water vapor; aerosol extinction processes apply to aerosols and to hydrometeors which attenuate radiation by scattering processes. Infrared values apply to the two windows centered near 4 and 10 micrometers. Millimeterwave (mm)/microwave (MW) values apply to windows at 19 GHz, 37 GHz, and 94 GHz.

	MOLECULAR ABSORPTION (Visible Infrared mm/MW)			MOLECULAR SCATTERING (Visible Infrared mm/MW)		
Low Absolute Humidity	N	S	N	S	N	N
High Absolute Humidity	N	E	S	S	N	N
	AEROSOL ABSORPTION (Visible Infrared mm/MW)			**AEROSOL SCATTERING (Visible Infrared mm/MW)**		
Dry Haze	N	N	N	S	S	N
Wet Haze	S	S	S	E	S	N
Dust	N	N	N	E	S	N
Fog	E	S	S	E	S	N
Thin Clouds	S	S	N	E	E	N
Thick Clouds	E	E	S	E	E	S
Precipitating Clouds with High Liquid Content	E	E	S	E	E	S
Drizzle	S	S	S	S	S	S
Rain	E	S	S	E	S	S
Snow	S-E	S-E	S-E	E	E	S

Legend: N - negligible
S - significant
E - extremely significant

1.5 Conservation of Radiative Energy. The law of conservation of energy applies to a beam of radiation propagating between two points in the atmosphere.

1.5.1 If we denote the origin as Point A and the receiver as Point B (see Figure 10), then the radiand intensity (EM radiation or energy) as a given wavelength originating at Point A and arriving at Point B is equal to the sum of the energy departing Point A for Point B, less the energy absorbed along the path, less the energy scattered or reflected out of the beam along the path, plus the energy scattered or reflected into the beam in the direction of Point B, and plus the emitted intensity in the direction of Point B. This total intensity of energy received at Point B at a given wavelength from the direction of Point A is made up of two main components. The first component is that portion of the radiation originating at Point A which is transmitted unchanged through the intervening atmospheric constituents. The second component, called path radiance, is in turn made up of two parts. The first part is the radiation emitted toward Point B by atmospheric constituents along the path and transmitted to Point B. The second part is made up of radiant energy scattered or reflected into the path by the particles in the path or surrounding atmosphere arriving at Point B from the direction of Point A.

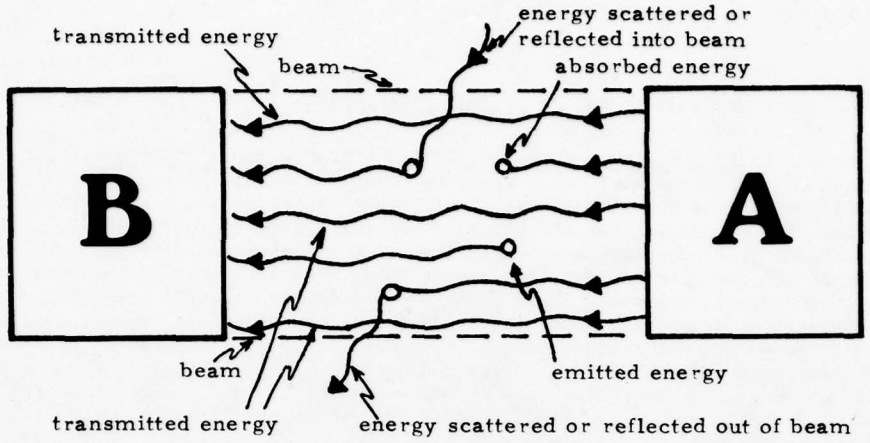

Figure 10. Components of EM Radiation Arriving at Point B from the Direction of Point A.

1.5.2 This section summarizes the atmospheric interactions with electromagnetic radiation in simple mathematical terms. The support methods used in Chapter 4 of this handbook are based on a mathemetical description of the physical processes described thus far. Familiarity with basic terminology and symbology will enhance understanding these methods.

1.5.2.1 The beam transmissivity of an atmospheric path is defined as that fraction of the radiation entering the path at one end which is transmitted to the other end of the path. Mathematically, this is expressed by

$$\tau_\lambda = I_{\lambda,B} / I_{\lambda,A} \tag{1-2}$$

where τ_λ is the monochromatic (i.e., single wavelength) beam transmissivity,

$I_{\lambda,A}$ is the monochromatic beam intensity at Point A, and

$I_{\lambda,B}$ is that portion of $I_{\lambda,A}$ which reaches Point B.

In general, the beam transmission τ_λ for a specific wavelength or a narrow wavelength interval is

$$\tau_\lambda = \exp(-b_\lambda D) \tag{1-3}$$

where b_λ is the total volume monochromatic extinction or attenuation coefficient with dimensions of per unit length, and

D is the geometric length of the path.

The coefficient b_λ is defined as

$$b_\lambda = b_{ma,\lambda} + b_{ms,\lambda} + b_{aa,\lambda} + b_{as,\lambda} \tag{1-4}$$

where $b_{ma,\lambda}$ is the monochromatic molecular volume absorption coefficient,

$b_{ms,\lambda}$ is the monochromatic molecular volume (Rayleigh) scattering coefficient,

$b_{aa,\lambda}$ is the monochromatic aerosol volume absorption coefficient, and

$b_{as,\lambda}$ is the monochromatic aerosol volume scattering coefficient

The logarithm of the beam transmissivity is given by

$$\ln \tau = -bD \qquad (1\text{-}5)$$

This value, $b_\lambda D$ is often referred to as the optical path length.

1.6 Physical Processes Acting on Electromagnetic Radiation at the Earth's Surface. Detection of an object at the earth's surface from aloft is a function of object's size, distance from the object, the object-to-background energy contrast (i.e., the inherent contrast), and the effects of the atmosphere on the transmission of energy from the object to an observer (or other sensor). For the most part, we will assume that for our purposes objects are large enough to be detected. We have discussed the processes that affect the transmission of energy through the atmosphere in previous sections. This section describes the physical processes at the earth's surface which affect the ability of a sensor to see an object against a background. PGMs employed against ground targets are effective only when the target can be detected against its background. The difference between the energy received from the target and the energy received from its background determine how well the target can be detected in the absence of intervening atmosphere (i.e., the inherent contrast). Three processes act to determine how much inherent contrast is established at the surface. Those processes are reflection, absorption, and emission.

1.6.1 Reflection. For visible and near infrared wavelengths, reflection is normally the most important process in seeing an object. Without reflected sunlight or reflection of energy from some artificial source (such as a search light shining on an object), an object cannot be detected unless it emits significant amounts of radiation at visible or near infrared wavelengths (for example, a fire). Reflection is also an important process at other infrared and millimeter/microwave wavelengths. Visible and infrared lasers are used to spotlight targets for sensors that operate at corresponding wavelengths. Similarly, at microwave wavelengths, radar returns from objects on the earth's surface are reflected (as opposed to weather radar backscatter from raindrops and snowflakes) back to an observer.

1.6.1.1 Objects are discriminated from their background due to differences in reflectance (recall Para. 1.4.2.1) and have texture due to the nonuniformity of the reflection process on rough and variable composition surfaces.

1.6.1.1.1 Through use of Figure 11, visualize an object on the ground. Assume that the object has a reflectance equal to 0.2 and the ground (the background) has a reflectance equal to 0.5. Sunlight shining on the object and the ground is reflected toward an observer. Since the same intensity of sunlight falls on all surfaces, the reflectances of the object and ground determine whether a contrast exists, and whether the object can be discriminated against the background. The product of the individual reflectances and the sunlight's intensity yields a measure of the intensity of radiation reflected from the object and from the background. A comparison of the two reflected energies determines whether there is a significant contrast. The contrast must exceed the minimum threshold contrast characteristic of the human eye, for the human eye to see the object against the background. All sensors of EM radiation have minimum energy or contrast thresholds.

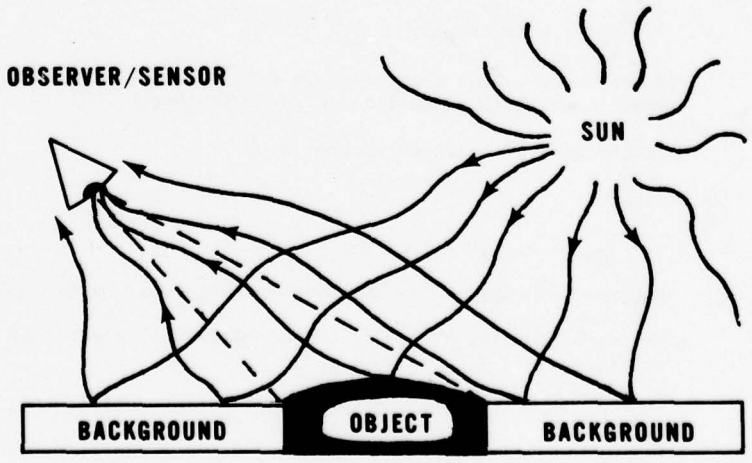

Figure 11. Reflection from an Object and Background.

1.6.1.1.2 The texture and composition of an object and its background affect their reflective properties and may either enhance or degrade the contrast between object and background. Section 2.4 further illustrates reflection effects.

1.6.2 Absorption. Incident electromagnetic radiation that is not reflected from an object or its background must be absorbed or transmitted. Absorption is dependent on the wavelength of the incident radiation. Most terrestrial objects and backgrounds transmit little or no radiation at visible or infrared wavelengths, but transmission may be significant at millimeter wavelengths for certain surfaces such as snow.

1.6.3 Emission. The emission of radiation at the earth's surface is similar to the emission by atmospheric constituents. The concepts of "black body" emission and emissivity apply. The amounts of energy emitted by an object and its background at a specific wavelength are directly related to the composition and the physical temperature of the object and its background. Emissivity (see Para. 1.4.5.1) is an important control on the intensity of radiation from an object or background and should not be discounted as a secondary influence in comparison to physical temperature.

1.6.3.1 Emission at visible wavelengths by surface objects and their background is practically zero in most cases. Fires and other illuminators (such as search lights) which may be of interest (i.e., targets) are exceptions. Terrestrial emission is about 10 times more intense than reflected solar radiation in the 3-5 micrometer wavelength region, and about 100 times more intense than reflected solar radiation in the 8-12 micrometer region. Hence, the transfer of thermal/terrestrial radiation at infrared wavelengths is of primary importance to the temperatures and temperature changes of terrestrial objects. Furthermore, sensors viewing target/background scenes at middle and far infrared wavelengths rely almost solely on emitted radiation for their operation. The reflected solar radiation at these wavelengths is negligible.

1.6.3.2 Radiative temperature, equivalent radiative temperature, and brightness temperature are frequently used to describe a property related to the emission of EM radiation from an object or its background. All three terms are effectively the same term but none equate to physical temperature (except for perfect emitters). Physical temperature refers to the temperature that is measured with a thermometer. Radiative temperature or brightness temperature is the physical temperature an object would have, if it had an emissivity equal to one (inferring a black body) and an emission energy for a specific wavelength equal to that calculated from Planck's law at that physical temperature. (Appendix A describes this concept more fully.) For example, an object at 293^{o} K (20^{o} C) and an emissivity of 0.5 emits at 10 micrometers with an intensity of 0.832 units. A perfect emitter (emissivity = 1) at a temperature of about 271^{o} K (-2^{o} C) emits at 10 micrometers with an intensity of 0.832 units. Hence, the radiative or brightness temperature of the first object is about 271^{o} K. A sensor viewing the first object with a temperature of 293^{o} K would receive equal amounts of energy from that object and a perfect emitter next to it with a temperature of 271^{o} K. The concept of radiative temperature is important in describing thermal contrast between objects and their background at infrared and millimeter/microwave wavelengths and will be used in the next three chapters to describe the performance of precision guided munitions.

1.6.4 Influence of Atmospheric Radiation Processes on the Heat Balance at the Earth's Surface. Many factors influence the rate of net loss or gain of heat, and hence temperature change, at the earth's surface. A very important factor is the net flux (actually, flux divergence) of electromagnetic radiation. When incoming radiation exceeds outgoing radiation, then radiative flux contributes to a temperature increase; a net outgoing radiative flux contributes to temperature decrease. Under certain meteorological conditions (especially with calm winds) radiative processes dominate temperature changes at the earth's surface. The net flux of radiation at the earth's surface is, in turn, strongly influenced by emission and absorption processes occurring in the atmosphere.

1.6.4.1 Effects of atmospheric radiation processes on net solar radiation at the surface. Under clear sunny conditions, a large portion of the incoming solar radiation reaches the earth's surface. The effect of this radiation on temperature change at the surface depends to a large extent on the physical properties of the surface. Because these properties can vary greatly over short distances, hot spots occur. Under cloudy conditions, on the other hand, much less solar radiation reaches the surface and much of the radiation arrives as diffuse radiation after interaction with clouds. As a result, the tendency toward formation of hot spots is much less. The effect of solar radiation on local temperature change is diluted by other meteorological phenomena, such as wind and precipitation. For example, asphalt pavement is much hotter than an adjacent field on a sunny day; less difference will exist on a cloudy day; almost no difference will exist on a rainy, windy day.

1.6.4.2 Effects of atmospheric radiation processes on terrestrial radiation at the surface. Just as net flux of solar radiation affects surface temperature change, similar effects result from the flux of terrestrial radiation at infrared wavelengths. Figure 9 shows that the peak intensity of radiation for bodies at terrestrial temperatures occurs at about 10 micrometers. Clouds at a temperature of -60^{o} C have their peak emission at about 13-14 micrometers. Thus, we see that almost

all of the terrestrial heat flux occurs at wavelengths in the region from 2 micrometers to about 100 micrometers. Atmospheric extinction and emission processes occuring at these wavelengths will strongly influence the net flux of radiation at the earth's surface.

1.6.4.2.1 Effects of surface emission on surface temperature change. We noted in Para. 1.6.3 that terrestrial objects emit radiation at an intensity determined by their emissivity and physical temperature. Terrestrial objects vary considerably in their emissivity at infrared wavelengths; they emit, and hence, lose heat at varying rates depending on their emissivity. Other factors, such as soil type and moisture of the underlying surface, control the object's ability to replace radiative heat loss by conduction. Consequently, strong local temperature variations can result. For example, on a calm clear night, frost may form on an automobile windshield when the surrounding air and ground temperatures are well above freezing.

1.6.4.2.2 Effects of atmospheric absorption and emission on surface temperature change. We noted in Para. 1.4.4 that clouds, aerosols, and gaseous constituents absorb at infrared wavelengths. Consequently, only a portion of the infrared radiation emitted at the earth's surface escapes to space. Under clear dry conditions only a portion of the radiation emitted in the windows escapes to space; the remainder is absorbed by the atmosphere. Under conditions of high absolute humidity and/or cloud/fog cover, little or no surface radiation escapes. Just as the atmospheric constituents absorb strongly at infrared wavelengths, so also they emit radiation at the same wavelengths. A portion of this radiation is directed toward the earth's surface. Consequently, the radiative heat loss at the surface is counterbalanced by radiation returned by the atmosphere. Under a clear dry atmosphere, this effect is relatively small; under a clear humid atmosphere, this effect is somewhat stronger; under dense clouds, the return radiation is quite strong. The result affects surface temperature changes and hence affects thermal contrast at the earth's surface. Localized cooling and local temperature differences can become quite strong under a clear dry night sky; such differences will be reduced by a cloudy sky. While frost may form on the windshield on a clear dry night, frost formation on a cloudy night with the same air temperature is unlikely.

1.7 Summary. The four examples presented in Figure 12 illustrate the physical processes discussed in this chapter. Each case represents a ray (photons of energy) of visible radiation which originates at the sun. Many other cases are possible.

1.7.1 Example Case I. A visible light ray originating at the sun is reflected by a cloud droplet at Point A and returned to space. This reflection may occur because of the exceptionally large value of the size parameter (see Para. 1.4.1).

1.7.2 Example Case II. A light ray with the same energy as in Case I enters a haze environment and is scattered (Mie) by aerosols at Points A, B and C. At the ground (Point D), the light ray is absorbed by a molecule of the ground. The energy level of the molecule is raised and emission at infrared wavelengths subsequently occurs. Within a molecule of a cloud droplet (Point E), the infrared radiation is absorbed and emission at infrared wavelengths again occurs (but maximum energy - see Figure 9 - will not be at the same wavelengths as that of the incident radiation).

1.7.3 Example Case III. Another light ray is scattered by a molecule (Rayleigh) at Point A; hence, the size parameter is very much less than unity. Within the haze layer (Points B & C), Mie scattering (size parameter of about 1) redirects the ray toward the ground. The visible ray is reflected from the ground (Point D), scattered (Mie) by a haze particle at Point E, and absorbed by a cloud droplet at Point F. Following this absorption, emission at infrared wavelengths occurs. Many subsequent interactions are possible.

1.7.4 Example Case IV. The visible ray is absorbed by a molecule in a cloud droplet (Point A). Subsequently, emission at an infrared wavelength occurs.

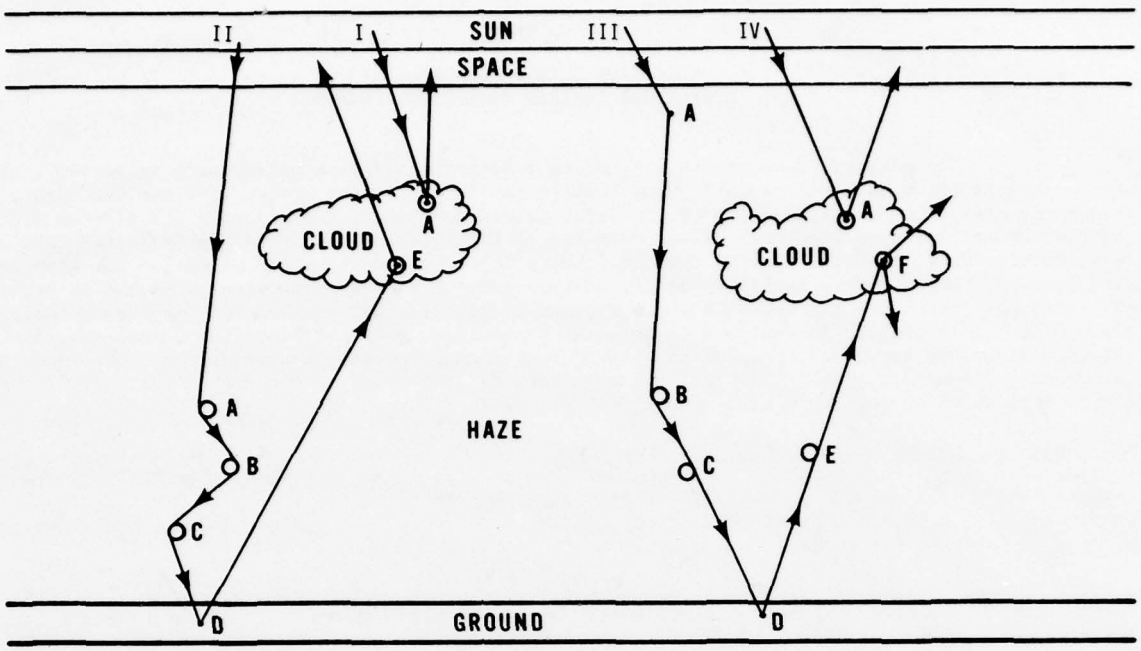

Figure 12. Examples of Electromagnetic Radiation Interacting with Constituents in the Atmosphere and at the Earth's Surface.

Chapter 2

PRECISION GUIDED MUNITIONS AND THEIR SENSITIVITIES TO THE ENVIRONMENT

2.1 General. The history of conventional warfare illustrates a perpetual problem in aerial bombardment -- how to hit a specific target? Many bombs were dropped in the target area but the target was frequently missed. The introduction of Precision Guided Munitions (PGMs) during the Vietnam era greatly increased weapon accuracy. Newer PGMs are in the inventory and more sophisticated PGMs are being developed by Air Force Systems Command. While these systems have the potential for high precision bombing, they are very sensitive to the environment. Air Weather Service is tasked to provide environmental support to the users of these systems to minimize adverse weather impacts on their employment. This chapter is designed to acquaint forecasters with the Precision Guided Munition (PGM). The text describes types of PGMs, PGM tactics of employment, the target acquisition cycle, and PGM environmental sensitivities. The text also describes certain types of electro-optical target acquisition devices which perform a vital function during PGM employment.

2.2 Precision Guided Munition (PGM) Description. A PGM is a missile, bomb, or artillery shell equipped with a terminal guidance system to enhance the PGM's ability to hit a target. For the purposes of this text, a PGM is an air-to-ground missile or bomb equipped with a terminal guidance unit designed to sense the difference in electromagnetic radiation emitted or reflected by a target and its background and to guide the weapon to the target.

2.2.1 PGM Components. Two components of a PGM are the seeker (guidance unit) and the tracker (control unit). The environment can degrade the effectiveness of these components in achieving their function. Overall, the seeker is the most environmentally sensitive.

2.2.1.1 Seeker. The seeker or guidance unit contains a sensor. The human eye and a TV camera are familiar examples of electro-optical sensors. These sensors "see" electromagnetic energy at visible wavelengths. Sensors used in PGMs can operate at visible wavelengths or at infrared and millimeter/microwave wavelengths. The energy received by a PGM seeker is converted to electrical voltages which drive electronic logic circuits. The seeker discriminates between differences in the received energy levels from different points within its field of view (FOV). This ability to detect contrast between energy levels is basic to the PGM's operation. Two characteristics of PGM seekers are important from the viewpoint of environmental support. First, each seeker has a minimum energy contrast threshold. Below this threshold, energy differences are insufficient to activate the logic circuits. Second, seekers can work only in limited energy ranges. Too little energy cannot be detected, and too much energy will saturate, or perhaps damage, the sensor (for example, looking directly into the sun).

2.2.1.2 Tracker. While the sensor in the seeker sees the energy within its field of view (FOV), the tracker activates the PGM's aerodynamic control surfaces to keep the pattern of energy differences within the sensor's FOV and guides the weapon to the target. Trackers have different levels of sophistication which improve the ability of a PGM to continue on course to the target. The term lock on is used to describe the activation of the tracker. There are two fundamental sensor-tracker systems: edge and centroid. The edge tracker locks on and guides the PGM toward the area of the most intense energy contrast within the sensor's field of view (FOV). The Electro-Optical Guided Bomb has an edge-tracker. The centroid tracker locks on and guides the PGM toward the center (centroid) of the most intense radiation (maximum reflected or emitted energy) or least intense radiation (minimum reflected or emitted energy). This capability to select a centroid with a maximum or minimum radiative intensity is called dual polarity. The pilot selects this option from the cockpit by means of a polarity switch. The TV Maverick Missile (AGM-65A and AGM-65B) has a centroid tracker.

2.2.2 PGM Advantages versus Disadvantages. The PGM's advantage is accuracy. However, there are three significant disadvantages.

2.2.2.1 Weapon Cost. The cost per weapon is high. The TV Maverick (AGM-65A) costs $21,700 per unit and the Imaging Infrared Maverick (AGM-65D) will cost approximately $31,000 (1977 dollars) per unit.

2.2.2.2 Environmental Sensitivity. Precision Guided Munitions are sensitive to the weather and other environmental factors. A "mix" of PGMs and other weapons is essential to achieving an optimum PGM employment capability; however, this does not guarantee success since PGMs, collectively, do not have a truly "all weather" capability (e.g., heavy rain affects all PGMs).

2.2.2.3 Exposure Time to Enemy Defenses. A deterrent to employing PGMs is exposure time to enemy defenses. This exposure time can be more significant than with conventional bombs and rockets due to increased crew member busy-time during the preparation for launch of a PGM. In unfavorable weather, a single seat fighter pilot may be extremely busy and vulnerable.

2.3 Guidance System Types. PGM guidance systems are categorized as active, semiactive, or passive.

2.3.1 Active. An active guidance system responds to reflected energy. The PGM emits radiation in the direction of the target, the target reflects the energy back to the PGM, the PGM senses the reflected radiation, and the PGM "homes in" on the beam of reflected energy.

2.3.2 Semiactive. A semiactive guidance system functions in much the same manner as an active system. The difference is that the energy is radiated by an external source such as a radar or a laser designator on another aircraft or the ground. Figure 13 illustrates an airborne laser designator in action. The emitted EM radiation from the laser is reflected by the target, and the PGM "homes in" on the reflected energy.

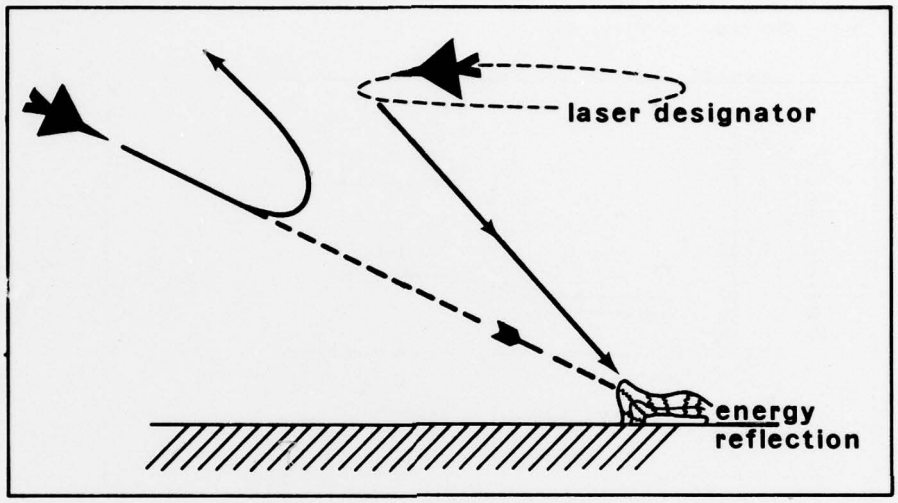

Figure 13. Laser Designator as an Example of a Semiactive Guidance System.

2.3.3 Passive. Passive guidance systems "home in" on the naturally emitted or reflected energy contrast between a target and its background. The TV and Infrared Mavericks and the TV-GBU-15 are passive PGMs.

2.4 E-O Sensors and Their Operating Characteristics. The E-O sensors currently in the Air Force inventory or under research and development are/will be operating at visible, infrared, and millimeterwave/microwave wavelengths.

2.4.1 E-O Sensors Operating at Visible Wavelengths. Visible radiation from a target and its background is reflected natural or artificial visible radiation. The human eye and the TV camera (with peak response near 0.55 μm) are examples of E-O sensors operating at visible wavelengths. In general, sensors which operate at visible wavelengths have the best spatial resolution when compared to sensors operating at longer wavelengths. (There are inherent physical reasons for a reduction in resolution with increasing wavelength. Although high-resolution systems at infrared and microwave wavelengths are feasible, their cost and size generally prohibit their use.)

2.4.1.1 Contrast. The contrast between the reflected energies from the target and the background are viewed by the sensor. The target/background contrast received at the detector must exceed the minimum contrast threshold of the sensor in order to activate the tracker. By virtue of the dual polarity capability, the contrast can either be a dark target against a light background or vice versa (Note: Dark and light refer to shades on a black and white TV).

2.4.1.2 Illumination and Shadows. Television systems also require a minimum illumination (visible energy) level for successful operation. Sensors operating at visible wavelengths are usually limited to daylight use. The reduction in illumination by clouds near dawn and dusk may be significant. TV systems used to support "first light" operations or operations during hours with long shadows may be adversely affected by the contrast formed by shadows on a light background; these contrasts can be significant and PGMs may track on them rather than the target-to-background contrast.

2.4.2 E-O Sensors Operating at Infrared Wavelengths. As noted in Para. 1.6.3, the sun is the primary energy source in the near infrared region of the spectrum. Natural emissions from the target and its background emit significant amounts of radiation in the far infrared.

2.4.2.1 Near Infrared Passive Systems. The effectiveness of TV sensors can be enhanced by extending the wavelength interval sensed by the sensor into the near infrared wavelengths. Such a detector is the silicon vidicon which senses radiation between 0.5 and 1.2 μm with a peak response near 0.75 μm. This enhancement of image quality at the sensor occurs because, for many atmospheric hazes, the size parameter (see Para. 1.4.1) is reduced at the longer wavelength. Figure 14 illustrates another reason for enhanced effectiveness. The differences in reflectances between the natural objects and painted objects are often significantly enhanced over visible reflectances in the near-infrared. A dark green tank against a dark green hedgerow becomes a dark tank against a light hedgerow in the near-infrared. This effect can be enhanced by a deep red filter (which filters out the blue and green wavelengths) on a silicon vidicon TV. Usually, camouflaging paint will stand out against the terrain when viewed in the near-infrared.

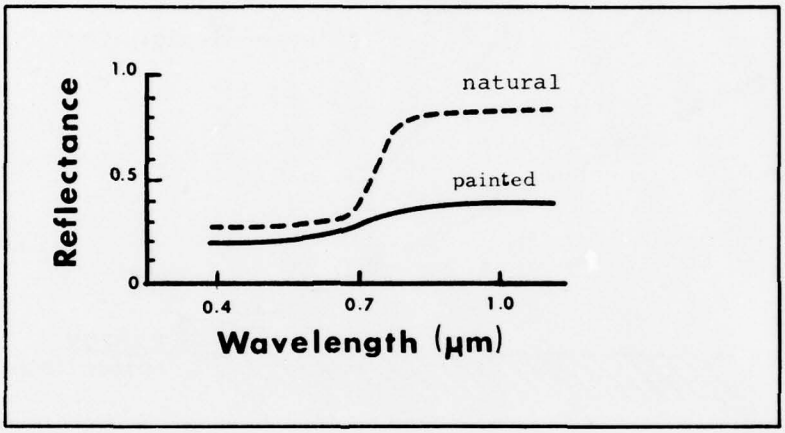

Figure 14. Sample Reflectances for Natural Objects and Painted Surfaces in the Visible and Near IR Wavelengths.

2.4.2.2 Infrared Semiactive Systems. Semiactive PGM systems employ lasers which operate at infrared wavelengths (at present, most of them operate at 1.06 μm) and are used as designators. The laser acts like a searchlight and is shined (irradiated) from the ground or an airborne platform onto or near an object on the ground. The reflected laser energy from the object or its near surroundings dominates solar reflection and terrestrial emission at the laser wavelength. Although the laser beam is collimated (i.e., straight line, parallel beams) light, the target reflects in all directions, usually unequally (i.e., nonisotropically). The maximum reflectance from a target surface is along the reflected beam (see Figure 15). The direction of reflected radiation follows the "angle of incidence equals the angle of reflection" law. Target orientation and size are significant factors. A flat bunker wall may reflect much better than an antiaircraft site with many small surfaces at all angles to the designator. The PGM sensor receives the energy reflected in its direction and homes in on the peak intensity of the reflected energy using a centroid tracker system. The laser can be employed in daytime or at night.

2.4.2.3 Middle and Far Infrared Passive Systems. The thermal emission contrast (i.e., radiative temperature difference) between the target and background drives the operation of passive infrared sensors operating at the middle and far infrared wavelengths. As with visible sensors, the target/background thermal contrast received at the detector must exceed a minimum operating threshold for successful system operation. The passive thermal contrast sensor can be used during the day or night.

2.4.3 E-O Sensors Operating at Millimeterwave/Microwave Wavelengths. Air-to-ground PGMs operating at millimeterwave/microwave wavelengths detect energy contrast in a manner similar to visible and infrared sensors. These sensors can be used at day or night. Emission of radiation from the target and background is the prominent energy process. Reflection is important only for active and semiactive systems when energy is supplied by an external source such as an airborne radar.

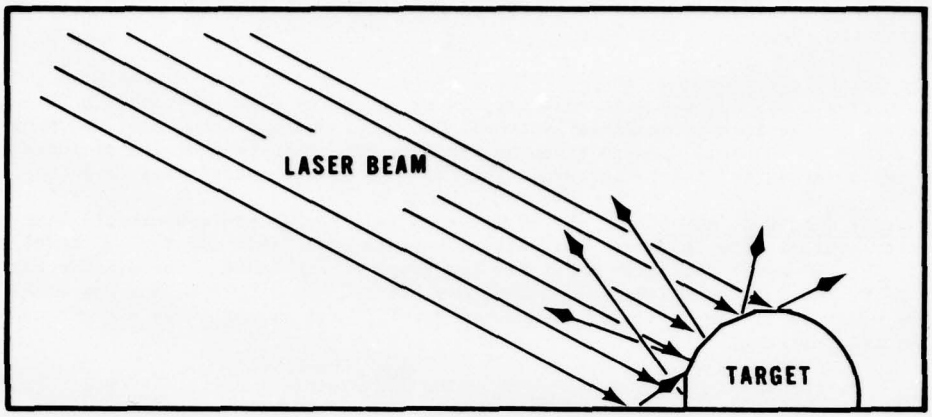

Figure 15. Illustration of Laser Designation of Targets and Nonisotropic Reflection.

Table 3. Precision Guided Munitions, Their Operating Wavelengths and Guidance Systems Types [1].

	ACTIVE	SEMIACTIVE	PASSIVE
Visible			Modular Guided Glide Bomb (GBU-15)
			TV Maverick (AGM-65A, AGM-65B)
			Electro-Optical Guided Bomb (GBU-8)
			Bullpup* (AGM-12B, AGM-12C)
Infrared		Laser Guided Bomb (GBU-10, GBU-12, GBU-16)	I^2R Maverick (AGM-65D)
		Laser Maverick (AGM-65C)	Modular Guided Glide Bomb (GBU-15)
		Bulldog** (AGM-83A)	
Millimeterwave/ Microwave	Harpoon* (AGM-84A)		Anti Radiation Missile (AGM-78)
			Shrike (AGM-45A)
			HARM*

* USN weapon
** USMC weapon

2.5 Precision Guided Munitions (PGMs) in the DOD Inventory and in Advanced Research and Development. Table 3 identifies specific PGMs, their operating wavelengths bands and guidance system types. The following describes some of the Air Force and other DOD PGMs currently in the inventory or about to enter the inventory.

2.5.1 Laser Guided Bomb (GBU-10, GBU-12, GBU-16). The tactical Laser Guided Bomb (LGB), called Paveway during the Southeast Asia conflict, has a semiactive guidance system. The LGB is an unpowered bomb with a sensor-tracker at the front end and aerodynamic control section at the rear. A target is designated by a laser flown on an airborne platform (see Figure 13) or by a ground-located laser designator (GLLD). The LGB is released from the airborne platform after the tracker system

locks on to the target. The LGB homes in on the centroid of the reflected energy from the target. The LGB's are in the operational inventory.

2.5.2 Electro-Optical Guided Bomb (GBU-8). The tactical Electro-Optical Guided Bomb (EOGB), also known as HOBO during the Southeast Asia conflict, is an unpowered 2,000 lb bomb (MK 84) with a passive TV sensor - edge tracker guidance system at the front end and aerodynamic control section at the rear. The EOGB is released from an airborne platform after the tracker system locks on to the contrast between a target and its background. The GBU-8 is in the operational inventory.

2.5.3 TV Maverick (AGM-65A, AGM-65B). The TV Maverick is a rocket powered missile with a passive TV sensor - tracker system. The "A" model was initially produced in 1971 and the "B" model was delivered in late 1975. The "B" model optically magnifies the image of the scene. The missile can be launched from an A-7, A-10, F-4 and the Teledyne Ryan Remotely Piloted Vehicle (RPV, BGM-34) after the tracker locks onto the centroid of the reflected visible energy from the target. The AGM-65A and AGM-65B are in the operational inventory.

2.5.4 Imaging Infrared (I^2R) Maverick (AGM-65D). The I^2R Maverick, currently under AFSC development and testing, is a rocket powered missile with a passive infrared sensor-tracker system. The tracker locks onto the thermal contrast between target and its background. The AGM-65D entered advanced engineering development in May 1978.

2.5.5 Laser Guided Maverick (AGM-65C). The laser guided Maverick uses a semiactive sensor-tracker system designed for use in the close air support role. Employment of this missile is similar to the laser guided bomb (Para. 2.5.1). The AGM-65C is in advanced engineering development.

2.5.6 Modular Guided Glide Bomb (GBU-15). The GBU-15 is another version of the EOGB (Para. 2.5.2). This passive sensor-tracker system currently operates at visible wavelengths; planned later models will use a passive infrared or laser sensor. This weapon has two aerodynamic versions. With the cruciform wing configuration, low-altitude attack is achievable, and a high-altitude standoff attack capability is obtained with the planar (flip-out) wing configuration. Another unique feature of the GBU-15 is that the tracker does not have to be locked onto the target prior to release from the airborne platform. The GBU-15 can be guided after launch by radar and data link with the launching aircraft to a position where the TV sensor-tracker system can be locked onto the target. The image seen by the GBU-15 is displayed continuously in the cockpit of the launching aircraft.

2.6 Target Acquisition (TA), Lock On, and Tactics. This section describes a classical target acquisition cycle and its variations, and addresses the general tactics of PGM employment.

2.6.1 Target Acquisition (TA) Cycle. The classical TA cycle discussed here is an adaptation of the discrimination level classification that is described by Johnson (Biberman [2]). In practice, the cycle will be modified to fit the mission, the tactics of the delivery system, the enemy threat, and the type of PGM sensor-tracker system. However, the classical TA cycle is instructive to the understanding of the mental sequence of events used in attacking a target. Figure 16 illustrates the modified classical cycle. The first stage of the cycle is locating (detecting) the area in which the

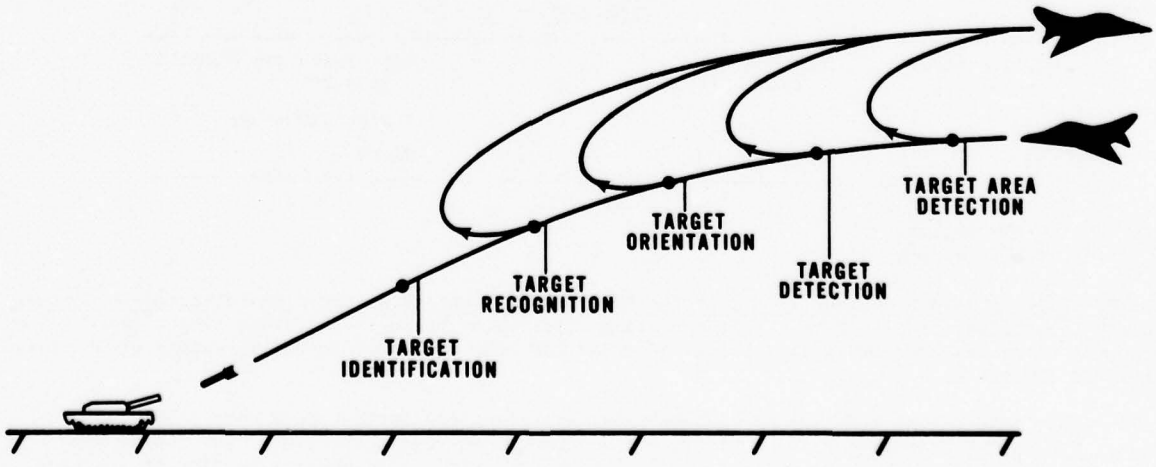

Figure 16. Illustration of Classical Target Acquisition Cycle and Possible Launch Points for the Interdiction Role.

target is located. The launching platform may be directed to this target area by a Forward Air Controller or by navigational aids. The second stage is target detection; an object is detected although no further target information can be determined. The next stage is target orientation; target symmetry and orientation are noted. Target recognition is the fourth stage; the class in which the target can be placed (e.g., the target is a house, or truck) is noted. Target identification occurs when the target can be described to the limit of the observer's knowledge (e.g., the target is a motel, or a pickup truck). Classically, weapon release follows target identification.

2.6.2 Variations of the Target Acquisition (TA) Cycle. The pilot will frequently deviate from the sequence of stages of the classical TA cycle, through elimination of some of the stages to accommodate the mission, the enemy threat, the tactics of weapons delivery system, and the capabilities of a particular PGM.

2.6.2.1 The close air support role (when friendly forces are close to enemy forces) may require considerable adherence to the classical TA cycle. However, TA may occur so rapidly that the individual stages appear to occur simultaneously. From target detection to target identification, only a few seconds of time may elapse. For visible sensors, adherence to the classical TA cycle is feasible, but sensors operating at other wavelengths where sensor resolution is not as good, positive target identification may not be possible. Furthermore, target identification may be established by a FAC who may then cue the attacking aircraft to the target. Thus, all TA stages need not be accomplished by the attacking pilot.

2.6.2.2 The nature of the interdiction role can allow considerable deviation from the conventional cycle (see Figure 16). Under the assumption that no friendly forces are present in the target area, only target detection may be necessary prior to lock on and launch of the PGM.

2.6.2.3 Weapon release (without lock on) could occur immediately following the detection of the target area. For example, the weapon could be launched upon detecting the target area. Then, the weapon would detect, while in flight, a sufficient contrast within its field of view, and lock onto the contrast. This process is classified as a "launch (or release the PGM) - leave (the target area) - lock-on (to the target)" tactic. Under the evolving concept of wide area antiarmor munitions, PGMs are launched in the direction of the target area.

2.6.3 Target Acquisition (TA) Systems. A target acquisition system must be used to employ a PGM. The pilots eye, a TV sensor/display system, a Forward Looking Infrared (FLIR) sensor/display system, or millimeterwave/microwave sensor/display system are used for this purpose.

2.6.3.1 Human Eye. The most common target acquisition sensor is the human eye. The overall eye capability to resolve target-to-background contrast under various conditions is generally unexcelled by other sensor types. Specific sensors can outperform the human eye in some instances. For example, a low light level TV outperforms the human eye in viewing under starlight skies; or a microwave system can see through clouds, but cannot resolve a target against a background as well as the eye.

2.6.3.2 Radar. Target acquisition by radar is feasible. However, all parts of the target acquisition cycle may not be achievable. Radar can aid in the data link command of the GBU-15.

2.6.3.3 Pave Tack. Pave Tack (see Stein [19]) is a FLIR sensor/display system which is used for TA and contains a laser rangefinder/designator which is boresighted with the FLIR to enable the system to designate targets for laser-guided weapons or to obtain slant range information. The sensor is in a pod attached to the aircraft/airborne platform. The sensor feeds the cockpit's display unit.

2.6.3.4 Pave Spike. Pave Spike is a TV sensor/display system combined with a laser designator and range finder.

2.6.3.5 Pave Penny. Pave Penny is a day/night laser seeker/tracker system that is designed to search, acquire, and track a target illuminated by an airborne or ground-located laser designator.

2.6.4 Tactics. The general tactics implied in this section are dictated by PGM characteristics and the solar-atmospheric-terrestrial environment. Specific tactics are designed by the appropriate major command based on the combat role, the delivery system's capabilities, the PGM's characteristics, the target, and the environment.

2.6.4.1 Regardless of whether the weapon is a bomb or a missile, the type of sensor-tracker guidance system is the primary tactic determinant. The imaging systems (either TV or FLIR) are either lock on (LO), launch (LA), and leave (LV) (see Figure 17), or launch, leave, and lock on (LA-LV-LO). The Maverick and EOGB are of the LO-LA-LV type. The LA-LV-LO type of systems are not in the operational inventory.

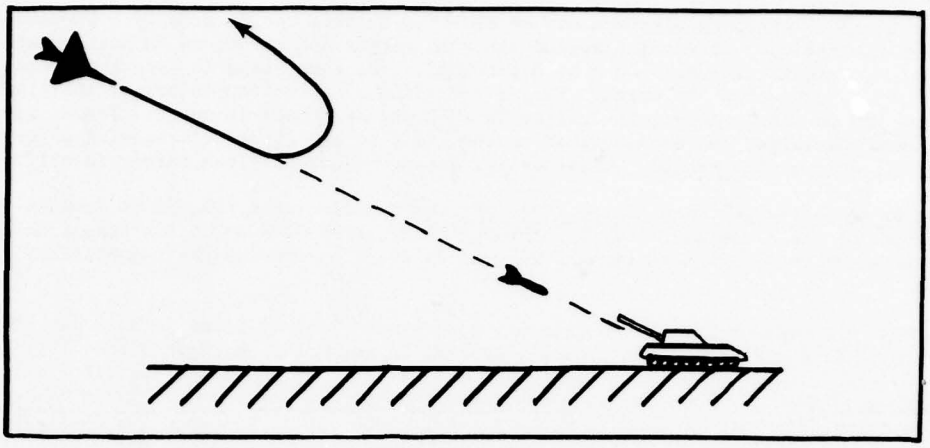

Figure 17. TV or IR Lock On, Launch, and Leave Tactic.

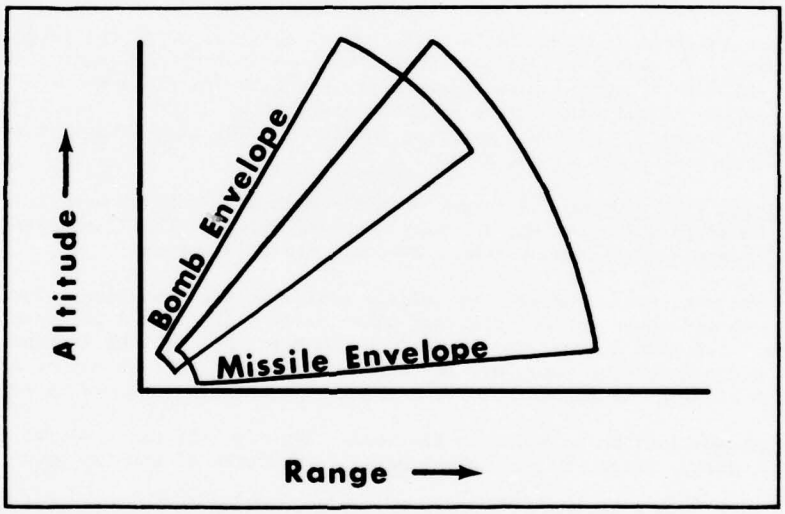

Figure 18. Aerodynamic Launch Envelopes of Guided Bombs and Missiles.

2.6.4.2 The launch envelopes (see Figure 18) of guided bombs and missiles are constrained by basic aerodynamic factors which are modified by wind profiles and aircraft speeds. Because of its internal power, a missile has a longer stand-off range and a wider range of possible altitude/dive angle combinations (e.g., it can be launched from a lower altitude) than a bomb.

2.6.4.3 In determining tactics, the pilot considers the size of the target and the approach altitude and speed optimum for target detection, the enemy defenses (e.g., SAM or small arms), and his aerodynamic launch envelope. Weather can force him to low altitudes where speed and shallow attack angles make target acquisition difficult and may also increase the attrition rate. Figure 19 shows how clouds, visibility, and enemy defenses shrink the safe launch zone.

2.6.4.4 For TV systems, careful mission planning with respect to sun-aircraft-target angle is necessary because of the shadow and up-sun sensing effects. As discussed in Para. 1.4.3, the directional nature of aerosol scattering (predominately forward scatter) produces a "blinding" effect for visible and near IR sensors just as it does for the human eye. The degree of blinding is dependent on the

aerosol size distribution. Target shape and size are also important since shape can govern the sensor's ability to acquire and lock on to a target, and size governs the acquisition and lock-on ranges.

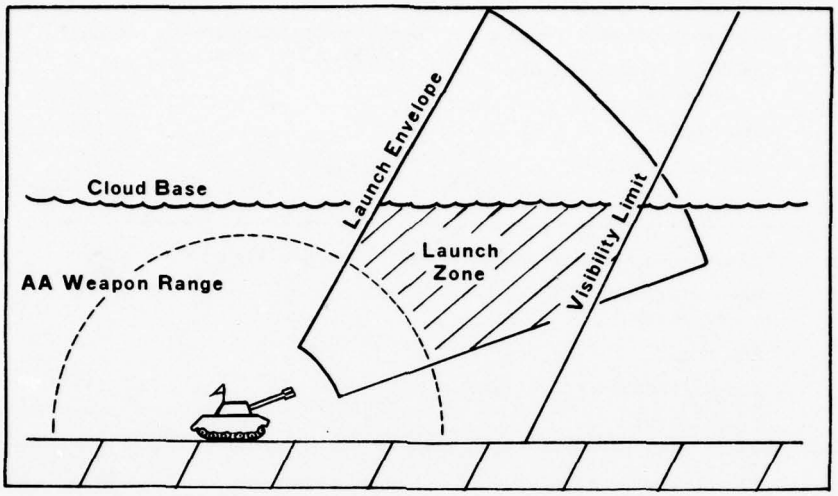

Figure 19. Launch Zone in a Visual Acquisition, Air-to-Ground Scenario.

2.6.4.5 For laser designator/target acquisition systems after the target image is acquired by the aircraft target acquisition sensor, the designator aircraft lases the target and holds the laser beam on target until all weapons impact (see Figure 13). Multiple weapon launches at a single designated target may be undesirable since the explosion from the first impact may disrupt the guidance of subsequent weapons (*i.e., disrupt the pattern of reflected energy*).

2.7 Environmental Sensitivities of Precision Guided Munitions (PGMs). The environment influences the effectiveness of PGMs in a highly complex manner. Chapter 1 describes the effects of the atmosphere and earth's surface on the propagation of EM radiation. The atmosphere affects PGMs in other ways; Para. 2.7.1 describes these effects. Para. 2.7.2 summarizes the sensitivities to atmospheric parameters of the generic classes of PGMs (i.e., TV, silicon vidicon TV, laser-guided, infrared, and millimeterwave/microwave), and Para. 2.7.3 describes the environmental effects on the target and its background.

2.7.1 Nonelectromagnetic Sensitivities. Icing, turbulence, lightning, ablation (erosion), and electrical charge buildup (triboelectrification) have the potential for adversely affecting the employment of a PGM. The degree of PGM system degradation caused by these parameters is not known in detail. Severe or greater turbulence may be sufficient to "break lock." Icing can disturb aerodynamic flight, but it can also coat the sensor cover to such an extent that the sensor is no longer useful. The term ablation (or erosion) describes the deterioration, through pitting, of the sensor cover by passage through large aerosols, hail and the like. This deterioration and the icing over of the sensor cover are probably most significant to shorter wavelength systems (i.e., visible wavelengths). Lightning and electrical charge buildup have the potential for creating transient currents in the PGM's electronics which may affect system performance.

2.7.2 Electromagnetic Propagation and PGMs. The basic problems in selecting a sensor which can see through weather with enough resolution to recognize a target are illustrated in Figure 20. Table 4 illustrates these problems in terms of specific types of guidance and target acquisition systems.

2.7.2.1 Visual Systems. A cloud-free line-of-sight (CFLOS) between the target and a sensor (e.g., a television camera or the human eye) is essential since visible systems cannot see very far through clouds or dense fogs. Furthermore, reduced visibility due to scattering and absorption by haze, fog, and precipitation limit the capabilities of visual systems. These systems require a clear line-of-sight (CLOS) to the target; that is, a line-of-sight (LOS) clear of clouds and sufficient visibility so the target can be seen. Within the context of this report, a CLOS exists if there is a CFLOS within the maximum target acquisition range/lock-on range of the sensor. Also, each visible system requires a minimum level of illumination.

Table 4. Major Atmospheric and Solar Effects on Precision Guided Munitions (PGMs) and Target Acquisition (TA) Systems (electromagnetic only).

PGM/TA SYSTEMS	ENVIRONMENTAL LIMITATIONS	TIME OF EMPLOYMENT	SYSTEM RESOLUTION
Eye/TV (Visible)	Clouds (includes fogs) Haze (includes all dry aerosols) Sun angle Precipitation Light levels	Day (avoid dawn and dusk)	High
Silicon Vidicon TV (Visible and near IR	Clouds (includes fogs) Haze (includes all dry aerosols) Sun angle Precipitation Light levels	Day (and moonlight)	High
Laser (Infrared)	Clouds (other than very thin) Haze (Near IR only) Absolute humidity (Far and Far Far IR only)	Day or night	NOT APPLICABLE
Infrared	Clouds (other than very thin) Haze (Near IR only) Absolute humidity (Far and Far Far IR only)	Day or night	Medium
Millimeterwave/ Microwave	Heavy clouds (high liquid water content) Precipitation	Day or night	Low

2.7.2.2 Infrared Systems. In general, laser sensor systems operating at various infrared wavelengths and passive infrared systems require a cloud-free line-of-sight to the target. However, a laser beam can sometimes penetrate thin cloudiness with enough energy to be detected, and passive infrared systems may detect hot targets (e.g., a rocket exhaust) through thin clouds. As with visual systems, the transmission of energy at near infrared wavelengths will be degraded by haze, fog, and precipitation. In addition, systems operating at longer infrared wavelengths are degraded by the absorption of infrared energy by atmospheric water vapor. These systems will generally require a clear line-of-sight to the target. They can operate during the daytime or at night.

2.7.2.3 Millimeterwave/Microwave Systems. Millimeterwave/microwave system performance may be degraded by two main atmospheric factors: heavy cloudiness (thick cloudiness which contains large droplet distributions of near-precipitation-sized particles), and precipitation. These systems can be employed during the day or night.

2.7.3 Target/Background Contrast. Fundamental to the detection capability and hence the effectiveness of passive PGM sensors is sufficient inherent contrast between the target and background. The inherent contrast between the target and background are influenced by the environment in numerous ways. This environmental effect is not nearly as important at visible and near infrared wavelengths as it is for passive systems or infrared and millimeter/microwave wavelengths. Our understanding of the environmental effects at infrared and micrometer/microwave is limited by lack of a comprehensive data base and by limited experimence in using contrast-dependent systems. We can describe many of the effects from our knowledge of physical processes alone. However, we don't know the importance of each in the operational world. This section describes some of them on the basis of physical principles and experience to date.

WAVELENGTH CATEGORIES	MICROWAVE	MILLIMETER	INFRARED				VISIBLE
			FAR FAR	FAR	MIDDLE	NEAR	
WAVELENGTH/ FREQUENCIES	10cm - 1cm 3GHz - 30GHz	1cm-0.1mm	0.1mm-15μm	15μm-6μm	6μm-2μm	2μm-0.74μm	0.74μm-0.4μm
RESOLUTION	USUALLY INCREASES WITH DECREASING WAVELENGTH						
WEATHER SENSITIVITY	GENERALLY INCREASES WITH DECREASING WAVELENGTH						
CLOUDS & FOGS	SIGNIFICANT		EXTREMELY SIGNIFICANT				
DRY AEROSOLS	INSIGNIFICANT			SIGNIFICANT	EXTREMELY SIGNIFICANT		
PRECIPITA-TION	SIGNIFICANT		EXTREMELY SIGNIFICANT				
ABSORPTION	SIGNIFICANT		CAN BE EXTREMELY SIGNIFICANT		EXTREMELY SIGNIFICANT		
SCATTERING	SIGNIFICANT			EXTREMELY SIGNIFICANT			

Figure 20. Significance of Adverse Weather Elements and Sensor Resolution as a Function of Sensor Wavelength Categories.

2.7.3.1 Important Parameters. Three fundamental quantities describe the inherent target to background contrast. For visible systems and passive systems operating at near infrared wavelengths, reflectivities or reflectances of the target and background are sufficient to determine the inherent target-to-background contrast (contrast measured in situ). For passive infrared (i.e., middle infrared and beyond) and millimeterwave/microwave systems, the emissivities and physical temperatures are sufficient to determine contrast. The reflectance and emissivity are dependent on the type of materials which comprise the target and background, surface orientation and structure, and the wavelength interval of interest.

2.7.3.2 Visible Contrast. Values of target reflectance (R_t) and background reflectance (R_b) are sufficient to determine the inherent target to background contrast when target and background are equally illuminated. In this case, inherent target-to-background contrast is defined as

$$C_o = (R_t - R_b)/R_b \qquad (2.1)$$

Weather effects on visible contrast are fairly predictable and easily understood. Snow cover has a strong influence. Soil moisture and precipitation influence soil color and hence the contrast. Level of illumination can affect the apparent brightness of certain objects. In general, except for snow cover effects, weather phenomena have only a secondary influence on visual contrast.

2.7.3.3 Thermal Contrast. Target emissivity ($\varepsilon_{t,\lambda}$) and background emissivity ($\varepsilon_{b,\lambda}$) at the wavelength of interest and the physical temperatures of the target (T_t) and the background (T_b) are required to determine inherent target-to-background contrast. Contrast based on emissivity and physical temperature is usually expressed in terms of a radiative temperature difference. The radiative temperature (see Para. 1.6.3.2) difference (ΔT^*) between a target and a background is a function of wavelength $\lambda, \varepsilon_{t,\lambda}, \varepsilon_{b,\lambda}, T_t$, and T_b. Section A-7 contains an explicit expression of this functional relationship.

2.7.3.4 Crossover. In the remaining infrared and millimeterwave/microwave wavelengths where thermal emission is important, a problem can occur which is a function of the diurnal temperature cycle. This problem, known as radiative temperature "crossover," occurs when the target and background achieve the same radiative temperature (i.e., the target against its background is invisible to the sensor). Figure 21 illustrates the concept of crossover for a typical inactive target (e.g., a bunker, or a tank that has not been recently running). As the atmospheric temperature increases after sunrise or decreases near sunset, a radiative temperature difference can be achieved that is near zero. Although

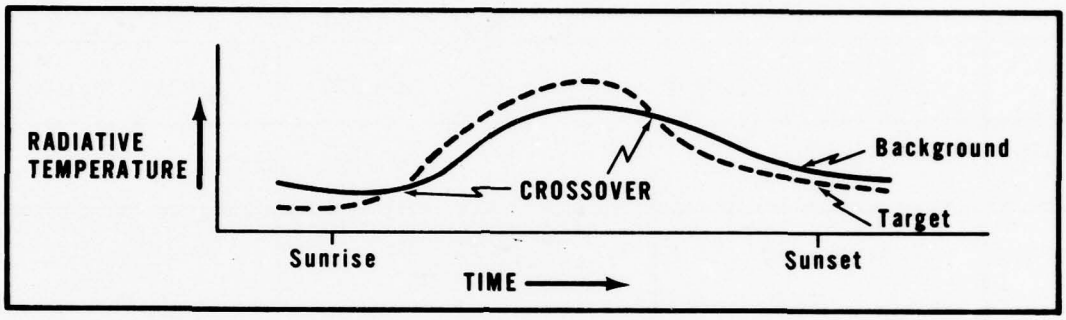

Figure 21. Example of Radiative Temperature "Crossover."

this figure illustrates the basic pattern, numerous variations from the basic pattern occur. It is most important to note that trees, road surfaces, water puddles, snow thrown up from below the surface layer by a moving vehicle, etc., may not have the same emissivity and/or physical temperature as the general background. For active targets (e.g., a moving tank), the crossover time is even more difficult to estimate because different portions of an active target are at different physical temperatures (e.g., a tank engine versus a tank turret). Crossover may occur on one portion of the target and not another during the same time period. Thus, a significant ΔT^* contrast can exist between the different parts of the target. Hence, crossover for different parts may occur at different times.

2.7.3.5 Weather Effects. A number of meteorological phenomena have a direct effect on the target/background thermal contrast.

2.7.3.5.1 Under clear night sky conditions, particularly with low atmospheric humidity and light or calm winds, strong thermal contrast can develop by radiational cooling. If high absolute humidity exists, this radiation cooling effect is reduced by return infrared radiation emitted by the atmospheric water vapor. The reduction in radiational cooling is even more pronounced with broken or overcast cloud cover. Infrared emissions from the cloud layers are received by the target and background and counteract the cooling by infrared emission from the target and background. This usually reduces the thermal contrast. This effect is most pronounced with low clouds and with thick clouds. Similarly, clouds tend to inhibit through the extinction of incoming solar radiation the effect of differential solar heating in creating strong thermal contrast during the daytime.

2.7.3.5.2 Wind speed also will have the effect of reducing the temperature difference by equalizing the physical temperature difference between target and background. The higher the speed, the smaller the difference. Rainfall or snowfall will completely change the infrared scene. Standing water, the percolation of rainfall into the ground and the coverings of the target and background by snow alter the emissivities and radiative temperatures of the target and/or background.

2.7.3.6 Thermal Clutter. The likelihood of successful operation of passive infrared guidance systems increases directly with increasing thermal contrast between target and background. However, other characteristics of the target/background scene can adversely affect their operation. A typical target/background scene may contain in addition to a hot (cold) target other "hot (or cold) spots" surrounding the target within the field of view of the guidance sensor. These "hot (or cold)" spots are called thermal clutter. Since the sensor will lock on to the centroid of the hottest (or coldest)

area within its field of view, the weapon may lock on to one of these "hot (or cold) spots" instead of the target. Such hot (or cold) spots can result from a variety of causes. Burning objects, hot pavement surfaces or muzzle flashes are obvious examples. However, other less obvious (and sometimes very obscure) phenomena can produce similar effects. For example, infrared imagery taken at Ft Polk, LA in February 1977 showed that tanks operating in a wooded area had a lower radiative temperature than the surrounding trees. Subsequent analysis revealed that the radiative temperatures of the trees were high because of a below-normal precipitation during the preceding winter season and below-normal cooling by evapotranspiration from the leaf surfaces. During tests of the same system at Camp Grayling, MI in December 1977, the system guidance unit locked onto the tracks behind the moving tank instead of the tank. The "hot snow" in this case resulted from thermal conduction through the packed snow from the underlying warm ground surface and emissivity change in the snow due to compaction. These examples serve to illustrate the complexity of the influences (both natural and artificial) on target-to-background thermal signatures.

Chapter 3

WEATHER SUPPORT TO PRECISION GUIDED MUNITIONS

3.1 Support Concept. Air Weather Service will support PGMs using two concepts: cloud-free line-of-sight (CFLOS), and clear line-of-sight (CLOS). Simple techniques for computing the probabilities of cloud-free line-of-sight (CFLOS) and clear line-of-sight (CLOS) for visible, laser, and infrared systems are presented in Chapter 4. These concepts incorporate many of the environmental limitations on PGMs discussed in the previous chapter.

3.1.1 CFLOS. Figure 22 illustrates the concept of cloud-free line-of-sight probability. Visualize an attacking aircraft approaching a target. The cloud structure in Figure 22 suggests that the pilot would be less likely to see the target, because of cloud cover, at Point 1 than at Point 5. CFLOS probability describes this likelihood. Based on a cloud forecast and aircraft elevation angle, a probability of a cloud-free line-of-sight can be assigned to each point along the flight path. For example, probability values of 0.1, 0.2, 0.4, 0.7, and 1.0 might be appropriate for the five points along the flight path beginning at Point 1. A probability of 1.0 implies no cloud will be along the flight path between Point 5 and the target. The 0.2 value at Point 2 implies a 20% probability of not having cloud along the path between Point 2 and the target. For every point in the atmosphere surrounding the target, a CFLOS probability can be specified as illustrated in Figure 23a. Note the horizontal variation of the CFLOS for a specific altitude. These variations result from different elevation angles and differing effects of cloud thickness on the slant view of the target. Different cloud types yield some differences in CFLOS values for the same amount of total cloud cover, although a good estimate of CFLOS probability is possible from a forecast of cloud amount and height and elevation angle.

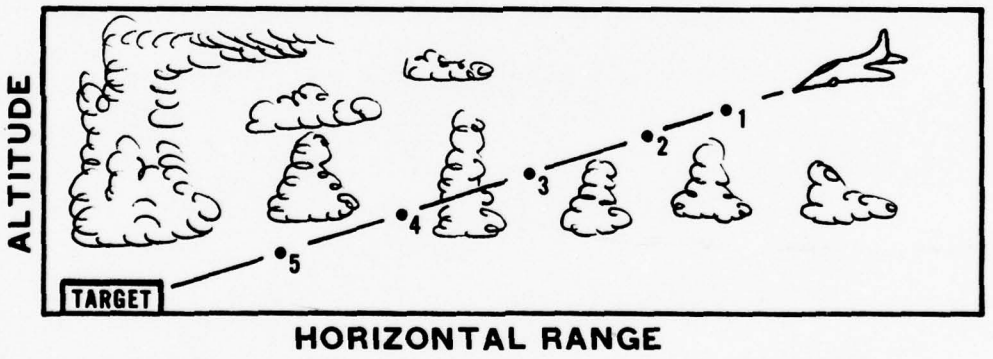

Figure 22. Illustration of the Cloud-Free Line-of-Sight Concept.

3.1.2 CLOS. A CLOS probability is made up of two components: the CFLOS probabilities, and the maximum target acquisition/maximum lock-on range. The maximum target acquisition and maximum lock-on ranges are computed from an estimate of the atmospheric effects on the transmission of the inherent target to background contrast and the threshold contrast of the sensor. With the determination of the maximum ranges for various aircraft attack angles, an envelope can be specified which represents a zone in which target acquisition or lock on can be achieved. Figure 23b is a modified version of Figure 23a and illustrates the envelope defined by the maximum ranges. Note that outside the envelope, the probabilities have been changed to zero, while within the envelope the values are unchanged. These resulting values are termed CLOS probabilities.

3.2 Procedures.

3.2.1 Field Support. In the absence of centralized support from the AFGWC, forecasters supporting the using commands will prepare CLOS forecasts using manual techniques. Chapter 4 provides methods to make these forecasts from observed and forecast meteorological parameters.

3.2.2 Centralized Support. The local forecaster will receive, from AFGWC, a weather forecast that will be a matrix of CFLOS probabilities as a function of range and altitude. Using forecasts of contrast transmission and illumination level for the target area provided by AFGWC, the forecaster

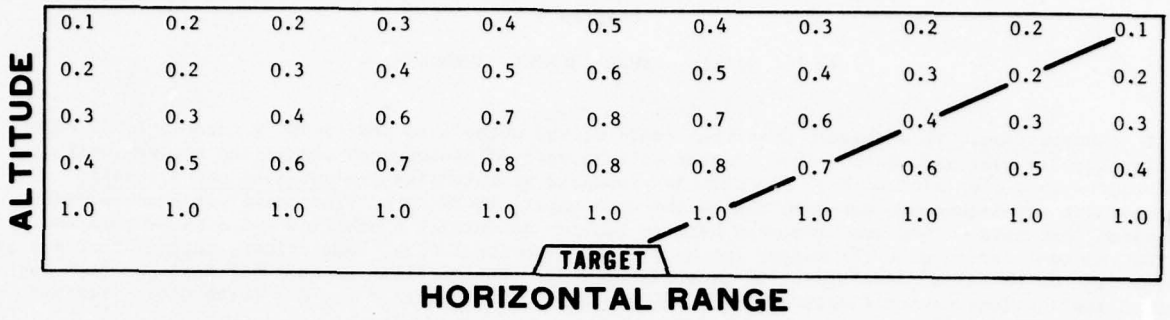

Figure 23a. Example Matrix of CFLOS Probabilities.

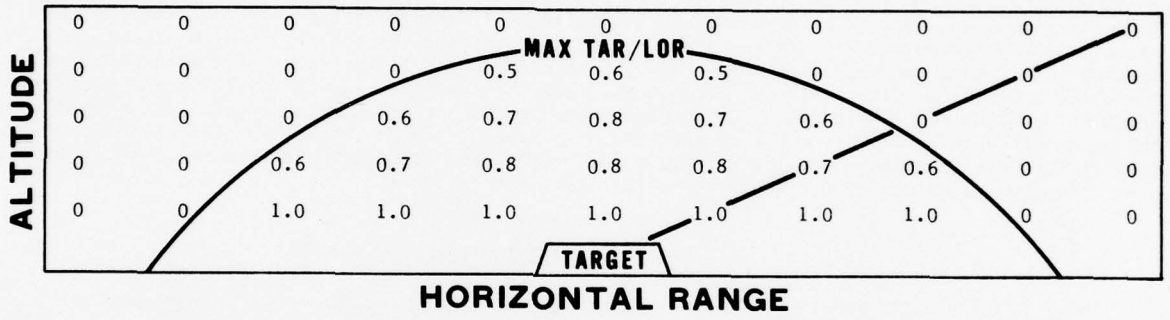

Figure 23b. Example Matrix of *Clear Line-of-Sight (CLOS) Probabilities with Envelope Defined* by the Maximum Target Acquisition Range (TAR)/Lock-On Range (LOR).

determines the maximum detection/lock-on range value for a cloudless situation and combines them with the CFLOS probabilities to prepare a CLOS matrix. AFGWC will provide forecast information for mission planning and execution forecasts. Field unit forecasters may modify these forecasts as necessary based on Forward Air Controller (FAC) observations or other late data. Lead times for mission planning and execution forecasts cannot be stated here specifically since they are not general enough for all missions.

3.3 AWS Capabilities to Support PGMs. Support to PGMs requires techniques which AWS has not had in the past.

3.3.1 Centralized Support. AWS must acquire a centralized capability to provide target detection and lock-on forecasts for specific weapon systems to the operational user. AFGWC, USAFETAC, system staff meteorologists, and AWS wing staff weather officers will develop the need capabilities. AFGWC does not now have the capability to produce CLOS forecasts or forecasts necessary to support PGMs, and must perform technique development to acquire the needed techniques. Technique development required for specific weapon systems will be outlined in annexes to the Weather Support Plan for Precision Guided Munitions.

3.3.2 Field Support. Manual techniques for production of CLOS forecasts are contained in Chapter 4. These methods are based on state-of-the-art methods, many of which are untested. Experience and feedback from verification of forecasts will be the basis for continual refinement of Handbook methods. These and other methods (see Appendix F) will be used in support to systems in the acquisition cycle, to deployed systems until centralized support is available, and as a backup for centralized support thereafter. Experience in use of these methods should be crossfed to the other AWS wings and to AWS headquarters.

Chapter 4

RAPID MANUAL SUPPORT METHODS

4.1 Introduction. This chapter describes rapid manual methods to provide CLOS forecasts for PGMs using locally available data. This chapter will be revised as improved techniques become available. Customers should be advised that the methods presented at this time are untested operationally. The individual techniques are based on theory and some experimental data. They have not been validated against test data. They are presented here to provide an initial capability and a back-up method to AFGWC centralized support for supporting currently operational PGMs. Our primary support concepts are dependent on technique development in progress or under consideration at the USAF Environmental Technical Applications Center (USAFETAC) and will employ the resources of the Air Force Global Weather Central (AFGWC).

4.2 Rapid TV Method.

4.2.1 General. In Step 1 of the procedure outlined below, the forecaster determines the illumination at a given time of day and multiplies the illumination value by the value of the approximate background or target reflectance (whichever is larger) to obtain a value for the approximate brightness (luminance) of the target or background. If the value of illumination (for clear or cloudy skies) when multiplied by the value of reflectance (yielding brightness) is smaller than the threshold illumination value, then the TV sensor cannot operate successfully. If the value of threshold illumination is smaller than the computed value of brightness, then the maximum target acquisition and lock-on ranges may be computed (Steps 2-4). Threshold contrasts for both the target acquisition sensor and the lock-on sensor must be known for the computation. In Step 5, the probabilities of a cloud-free line-of-sight (CFLOS) at maximum target acquisition range (TAR) and at maximum lock-on range (LOR) are computed. Input data needed in the rapid TV method are given in Table 5.

Table 5. Input Data Required for Rapid TV Method.

DATA REQUIRED	PROBABLE SOURCE	SYMBOL
Solar Angle	Appendix E	SA
Surface Visibility	Observation/Forecast	V
Inversion Height (base) (or haze layer top)	Observation/Forecast	H
Cloud Amount in Tenths	Observation/Forecast	N
Type		t_c
Height		b
Target Reflectance	Wing Targeting Shop or Table 8	R_t
Background Reflectance	Wing Targeting Shop or Table 8	R_b
Target Dimension	Wing Targeting Shop	L
Sensor Altitude	Customer	h
Threshold Illumination of Target Acquisition Sensor	Wing Targeting Shop	I_T
Threshold Contrast of Acquisition Sensor	Wing Targeting Shop	C_{TA}
Threshold Contrast of Lock-On Sensor	Wing Targeting Shop	C_{LO}
Acquisition Sensor Modification (if any)	Wing Targeting Shop	M_{TA}
Lock-On Sensor Magnification (if any)	Wing Targeting Shop	M_{LO}
Minimum Resolvable Subtense Angle for Acquisition Sensor	Wing Targeting Shop	α_{TA}
Minimum Resolvable Subtense Angle for Lock-On Sensor	Wing Targeting Shop	α_{LO}

4.2.2 Procedures (see Appendix B for TV method illustration and worksheet and Appendix E for computation of solar elevation angle).

STEP 1: Insure that the target scene brightness B is greater than the threshold illumination I_T. [NOTE: This step may be skipped if the solar elevation angle (SA) is sufficiently high enough to cause an illumination level (see Table 6) that is two orders of magnitude (i.e., approximately 100 times) or more larger than the threshold illumination I_T.]

a. Determine solar angle (SA) based on location (latitude and longitude), Greenwich mean time and date. Follow procedure in Appendix E to find solar angle (SA). Using Table 6 and SA, find the illumination level (I) with cloud-free skies.

Table 6. Horizontal Luminous Incidence (illumination level, I) for Various Solar Angles (SA) (Brown [3]).

SA (degrees)	I (fc)	SA (degrees)	I (fc)	SA (degrees)	I (fc)
-20	0.00005	17	2045	54	8580
-19	0.00005	18	2210	55	8740
-18*	0.00006	19	2375	56	8890
-17	0.00007	20	2540	57	9040
-16	0.00010	21	2705	58	9180
-15	0.00014	22	2875	59	9320
-14	0.00022	23	3050	60	9450
-13	0.00039	24	3230	61	9570
-12*	0.00077#	25	3410	62	9690
-11	0.00174	26	3600	63	9800
-10	0.0043#	27	3790	64	9900
-9	0.0116#	28	3980	65	10000
-8	0.0325#	29	4180	66	10100
-7	0.1	30	4370	67	10200
-6*	0.316	31	4560	68	10300
-5	1.00	32	4750	69	10400
-4	2.92	33	4940	70	10480
-3	7.80	34	5120	71	10570
-2	18	35	5300	72	10650
-1*	37	36	5480	73	10720
0	68	37	5660	74	10800
1	116	38	5840	75	10870
2	183	39	6020	76	10930
3	263	40	6200	77	11000
4	350	41	6370	78	11060
5	442	42	6540	79	11110
6	543	43	6710	80	11180
7	653	44	6880	81	11220
8	763	45	7050	82	11280
9	882	46	7220	83	11310
10	1015	47	7390	84	11350
11	1150	48	7560	85	11380
12	1290	49	7730	86	11420
13	1430	50	7900	87	11450
14	1575	51	8070	88	11470
15	1725	52	8240	89	11490
16	1885	53	8410	90	11500

* Lower limit of astronomical twilight is -18°; lower limit of nautical twilight is -12°; lower limit of civil twilight is -6°; sunrise, sunset, moonrise, and moonset at -0.8°.

At zenith (SA = 90°), the full moon produces a maximum illuminance of 0.0345 fc while a quarter moon (apparent half moon) produces a maximum illuminance of 0.004 fc. At SA = 20°, these values are approximately 0.009 fc and 0.0009 fc, respectively.

b. Determine illumination level with/without clouds (I_c):

(1) For clear and partly cloudy skies, set $I_c = I$ and go to Step 1c.

(2) For mostly cloudy and cloudy skies, use Table 7 to determine the ratio (R_c) of illumination with overcast clouds to the illumination level with cloudless sky (I). Then $I_c = I \cdot R_c$.

c. Multiply I_c by the target (R_t) or background (R_b) reflectance (whichever is larger) from Table 8 to obtain an approximate brightness value (B).

d. Determine whether brightness is adequate: Is $B > I_T$? If no, do not continue. Target cannot be seen.

Table 7. Ratio (R_c) of Illumination with Overcast Sky to Illumination with Cloudless Sky (I) as a Function of Cloud Type (t_c). Values in decimal. Based on approximations from Table 152 of Smithsonian Meteorological Tables (List [11]).

CLOUD TYPE (t_c)	Ci	Cs	Ac	As	Sc	St	Ns	FOG
Sun Near Zenith (SA = 90°)	0.85	0.84	0.52	0.41	0.35	0.25	0.15	0.17
Sun Near Horizon (SA = 0°)	0.80	0.65	0.45	0.41	0.29	0.24	0.25	0.19

Table 8. Estimated Reflectance (for visible wavelengths) Values for Selected Targets and Backgrounds. Values in Decimal.

OBJECT	REFLECTANCE	OBJECT	REFLECTANCE
Pond Water	0.01	Sandy Ground	0.11
Black	0.03	Sea Gray	0.11
Black Asphalt Runway	0.03	Slate Gray	0.11
Tar Paper Roof	0.04	Plant Leaves	0.12
Brown Field	0.04	Vegetation (Mean)	0.12
Water	0.04	Olive Drab Canvas (Truck)	0.12
Water w/Suspended Material	0.04	Olive Drab Burlap	0.13
Mud Covered w/Water	0.05	Weathered Wood	0.14
Ground (Dark)	0.05	Ocean Gray	0.15
Dark Volcanic Rock	0.05	Field Drab	0.15
Olive Drab Paint (Tank)	0.05-0.15	Black Top Road	0.15
Weathered Steel	0.05	Dry Loam	0.16
Grass Field	0.06	Light Sand	0.17
Green Field/Vegetation	0.07-0.15	Weathered Asphalt (Road)	0.19
Wet Mud	0.08	Wet Sand	0.20
Dark Green	0.08	Ground (Light)	0.20
Sea Blue	0.08	Haze Gray	0.25
Forest Green	0.09	Concrete	0.25
Wet Loam	0.09	Blue Gray	0.26
Ground w/a Little Vegetation	0.09	Dry Vegetation	0.26
Yellow-Green Vegetation	0.09	Sand (Mean)	0.27
Asphalt	0.10	Desert Sand	0.35
Earth Brown	0.10	Dry Sand	0.37-0.40
Earth Works	0.10	Concrete	0.37
Dead Vegetation	0.10	Earth Yellow	0.43
Dirt Road	0.10	Sky Gray	0.50
Wood	0.10	Tan Painted Steel	0.50
Red	0.10	Cloud (Dense)	0.60
Red Soil/Earth Red	0.10-0.15	Snow	0.80
Olive Drab	0.11		

STEP 2: Determine slant range visibility (V_s):

a. Enter Figure 24 with the inversion height H and sensor altitude h to find the ratio of visibilities R_v (for surface visibilities less than 2 statute miles, caution should be exercised in using Figure 24 since only aerosol - no clouds - extinction is considered).

b. Then use the surface visibility V to determine slant range visibility V_s, where $V_s = V/R_v$.

STEP 3: Determine the maximum target acquisition range (TAR) for the detection sensor (e.g., the eye):

a. Use target (R_t) and background (R_b) reflectances to determine inherent contrast (C_o) from Figure 25 or through the use of the equation $(R_t - R_b)/R_b$.

b. Use C_o and V_s found in Step 2 to determine TAR from either Figure 26 (for the eye; threshold contrast equal to 0.02) or Figure 27 (for a TV sensor; threshold contrast equal to 0.2).

c. Determine effective target dimension (L_{TA}) by using actual target dimension (L) and system magnification factor (M_{TA}), if any. Set M_{TA} equal to one if M_{TA} is already accounted for in the minimum resolvable subtense angle (α_{LO}). $L_{TA} = M_{TA} \cdot L$

d. Enter Figure 28 with effective target dimension (L_{TA}) and determine the maximum TAR on the basis of effective target size (L_{TA}) and sensor type.

e. Compare the TAR of Step 3b and 3d above, and use the smaller value as the maximum TAR.

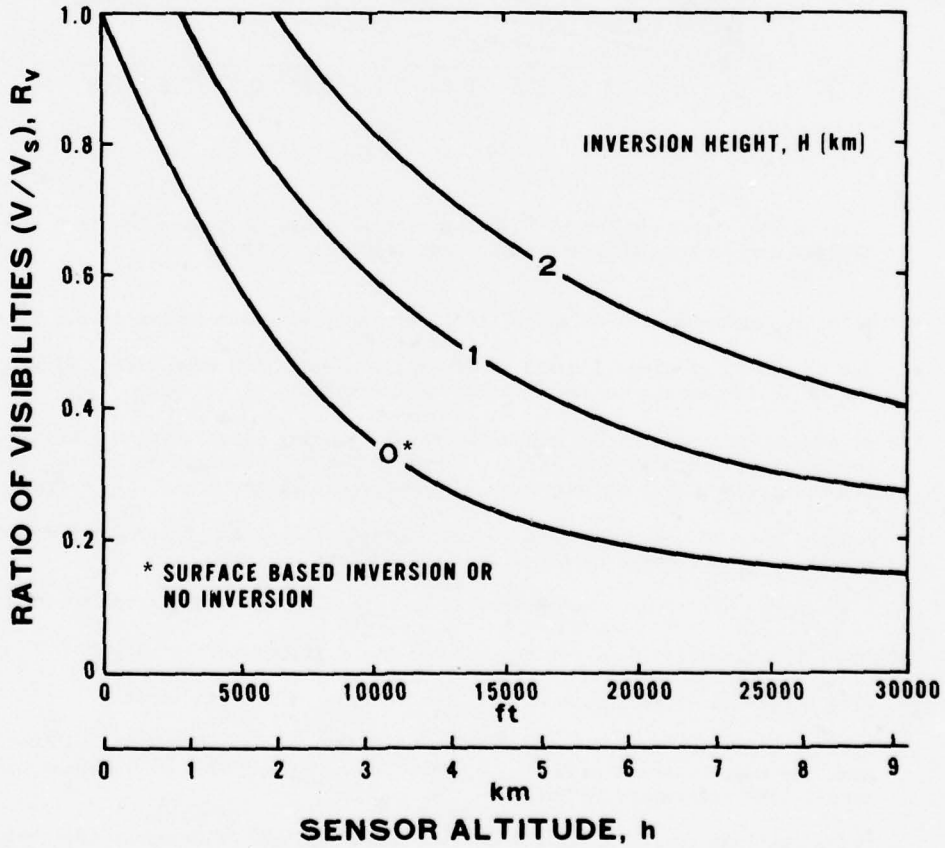

Figure 24. Relationship Between Ground Visibility V, Slant Range Visibility V_s, Sensor Altitude h, and Inversion Height H. (Surface based inversion: Jones et al. ([9], pp. 3-48); 1- and 2-km inversions: modeled based on aerosol extinction - Figure 14 of McClatchey et al. [13], constant aerosol extinction coefficient below inversion, exponential decrease of aerosol extinction coefficient above inversion.)

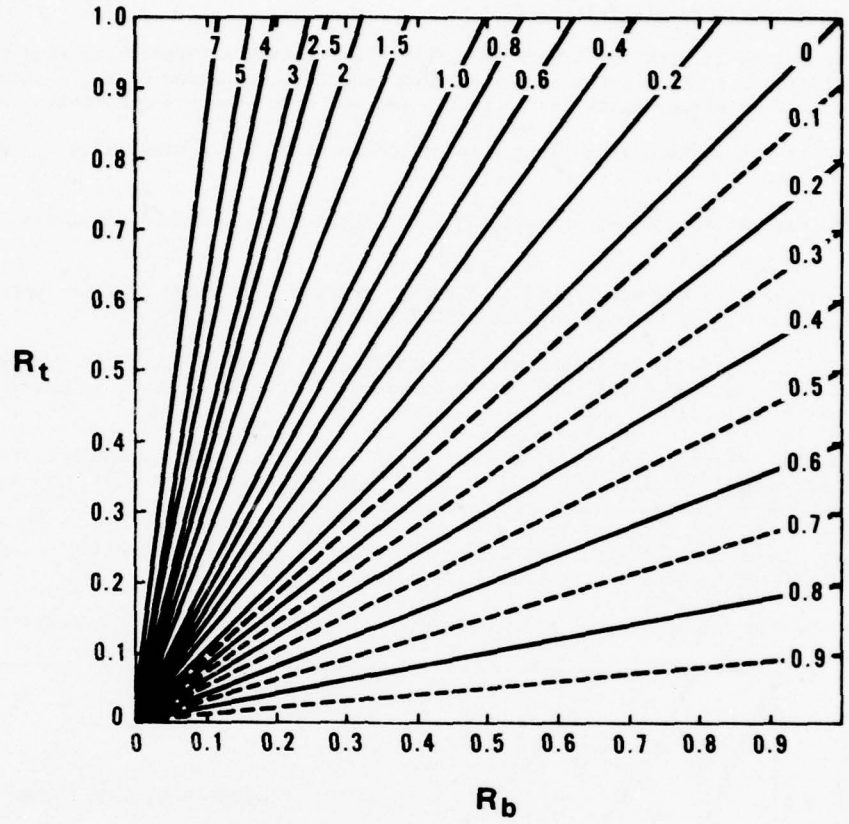

Figure 25. Inherent Target-to-Background Contrast (C_o) as a Function of Target Reflectance (R_t) and Background Reflectance (R_b).

STEP 4: Determine the maximum lock-on range (LOR) for the PGM sensor system (e.g., TV Maverick):

a. Use C_o and V_s of Steps 2 and 3 to determine maximum LOR from either Figure 26 or Figure 27 (depending on sensor contrast threshold).

b. Determine effective target dimension (L_{LO}) by using actual target dimension (L) and sensor magnification factor (M_{LO}), if any. Set M_{TA} equal to one if M_{TA} is already accounted for in the minimum resolvable subtense angle (α_{LO}). $L_{LO} = M_{LO} \cdot L$

c. Enter Figure 28 with effective target dimension (L_{LO}) and determine the maximum LOR on the basis of effective target size (L_{LO}) and sensor type.

d. Compare the LOR of Step 4a above, and use the smaller value as the maximum LOR.

STEP 5: Determine the probability of a clear line-of-sight (CLOS) to the target.

a. Find summation of cloud amount (N_T) below sensor altitude (tenths).

b. Using the maximum target acquisition range (TAR) of Step 3 and the altitude (h), determine the approximate look angle, θ (dive angle) from Figure 29. Repeat using the lock-on range (LOR) determined in Step 4.

c. Using the look (dive) angle (θ) and the summation of cloud amount (N_T) below the sensor altitude (h), determine the probability of a cloud-free line-of-sight (CFLOS) for target acquisition and for lock on from Table 9. Since Steps 2-4 determined that within this range the target could be seen, this value is also the CLOS probability.

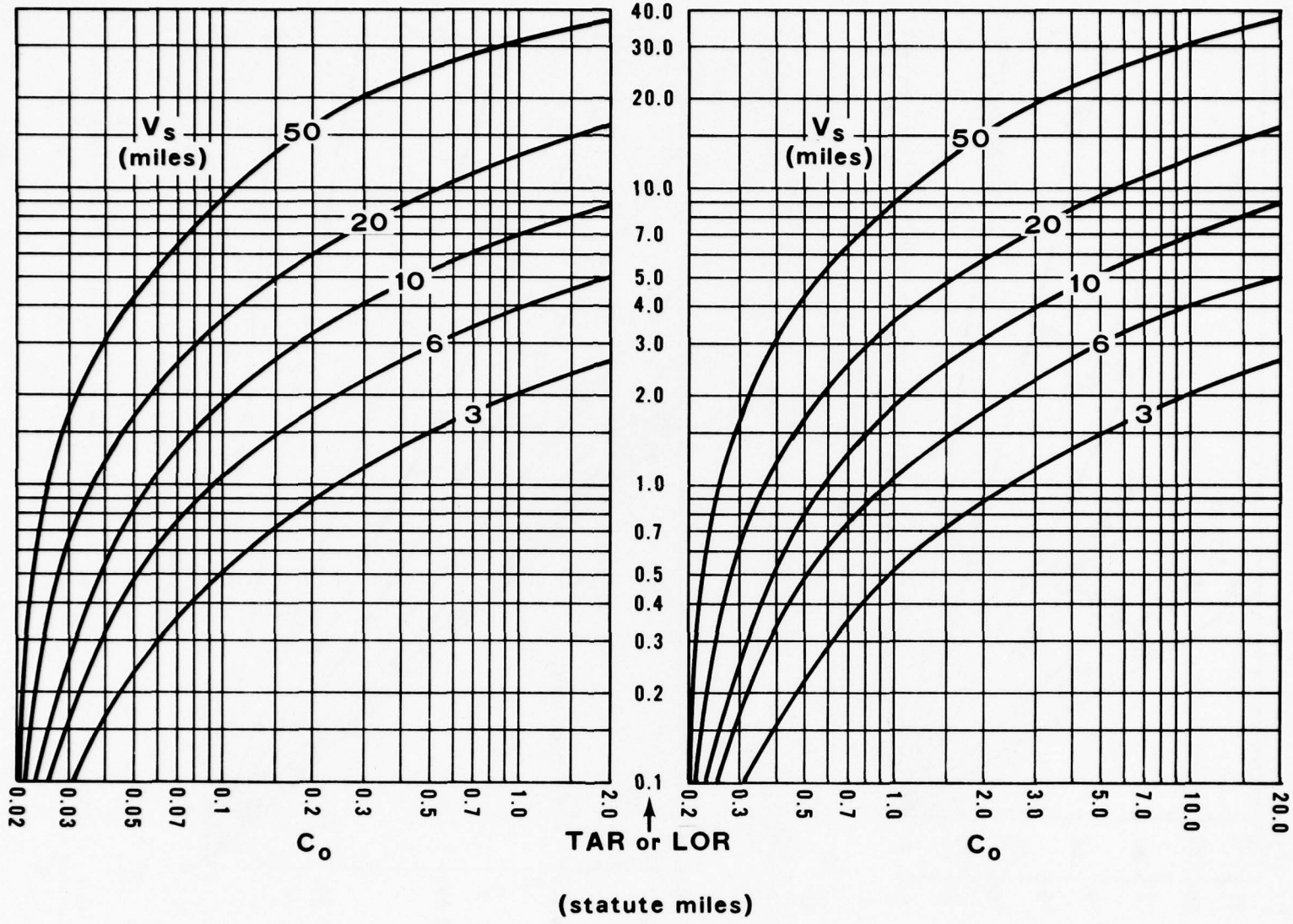

Figure 26. Maximum TAR or LOR as a Function of Slant Range Visibility (V_S) and Inherent Contrast (C_o) Where Contrast Threshold (C_{TA} or C_{LO}) is 0.02.

Figure 27. Maximum TAR or LOR as a Function of Slant Range Visibility (V_S) and Inherent Contrast (C_o) Where Contrast Threshold (C_{TA} or C_{LO}) is 0.2.

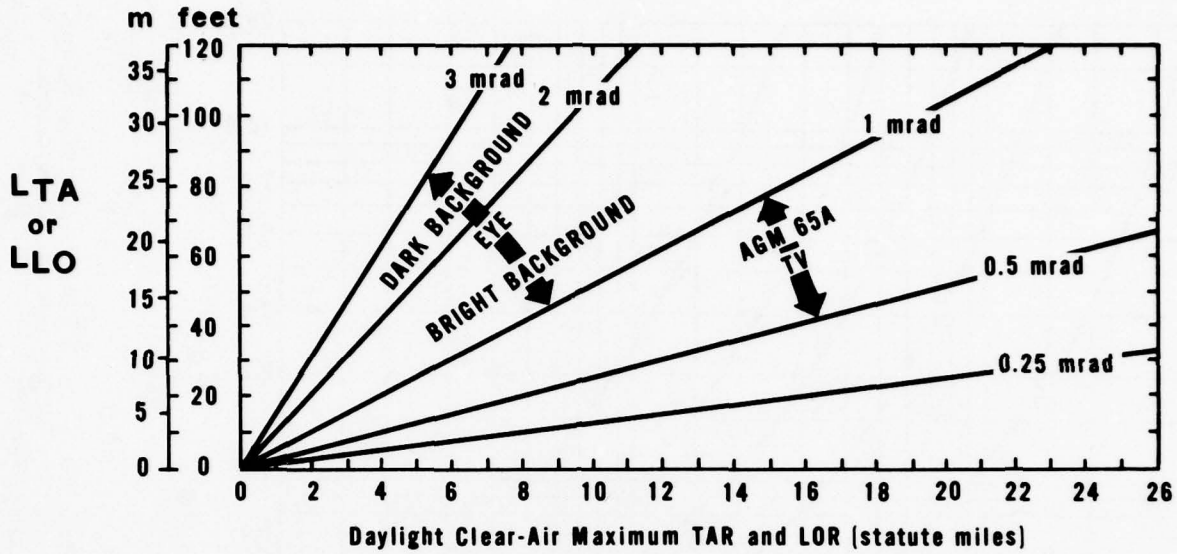

Figure 28. Maximum Acquisition Range (TAR) and Lock-On Range (LOR) as a Function of Effective Target Size (L_{TA} or L_{LO}) and Sensor's Minimum Resolvable Subtense Angle (α_{TA} or α_{LO}) (in milliradians).

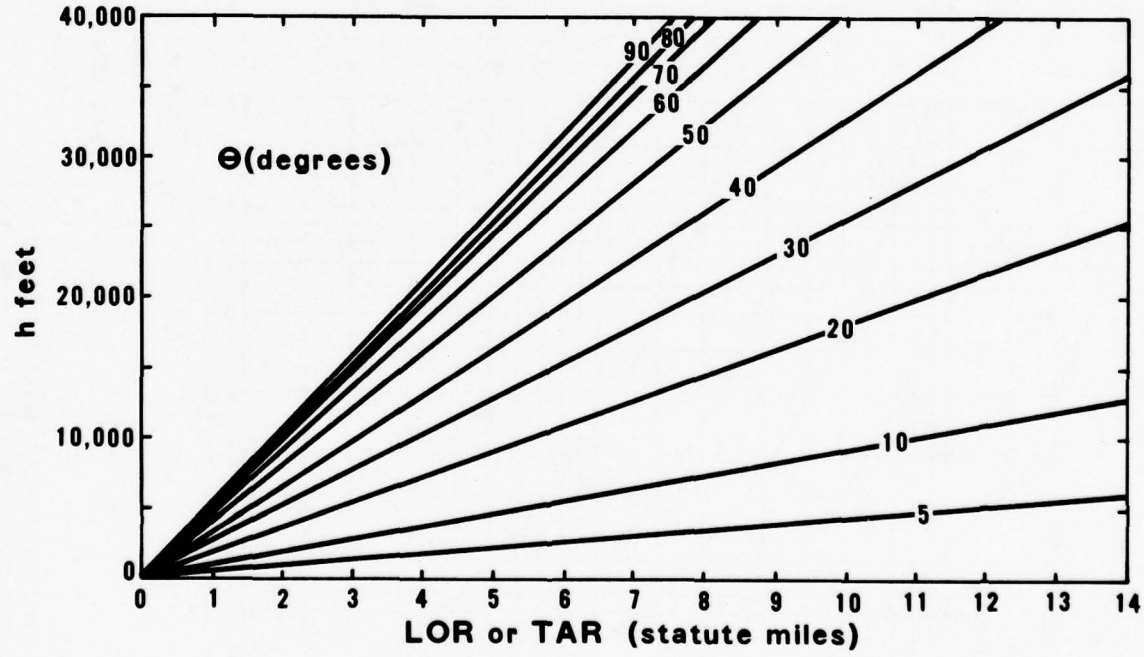

Figure 29. Look (dive) Angle (θ) as a Function of Sensor Altitude (h) and Maximum Lock-On Range (LOR) or Target Acquisition Range (TAR).

Table 9. Probabilities of Cloud-Free Line-of-Sight (CFLOS) as a Function of Look (dive) Angle (θ) and Total Sky Cover Below Sensor Altitude (N_t) (Lund and Shanklin [12]).

Look (dive) Angle (deg)	N_T (tenths) 0	1	2	3	4	5	6	7	8	9	10
90	1.00	0.97	0.92	0.87	0.81	0.77	0.70	0.62	0.48	0.31	0.08
80	0.99	0.97	0.92	0.87	0.81	0.77	0.69	0.61	0.47	0.31	0.08
70	0.99	0.97	0.91	0.86	0.80	0.76	0.68	0.61	0.47	0.30	0.08
60	0.99	0.96	0.90	0.85	0.80	0.75	0.66	0.60	0.46	0.29	0.08
50	0.99	0.96	0.90	0.85	0.78	0.73	0.64	0.58	0.45	0.29	0.08
40	0.99	0.95	0.88	0.83	0.76	0.71	0.62	0.55	0.42	0.27	0.07
30	0.98	0.93	0.86	0.80	0.73	0.66	0.57	0.50	9.38	0.24	0.06
20	0.98	0.90	0.83	0.75	0.67	0.59	0.50	0.42	0.33	0.21	0.05
10	0.97	0.86	0.76	0.65	0.55	0.47	0.39	0.32	0.24	0.16	0.03
8*	0.96	0.84	0.74	0.60	0.51	0.42	0.35	0.28	0.22	0.13	0.02
5*	0.93	0.80	0.66	0.50	0.42	0.35	0.26	0.22	0.17	0.10	0.01
2*	0.85	0.65	0.45	0.39	0.33	0.21	0.11	0.10	0.09	0.05	0.00

* Values based on extrapolation of data.

4.3 Rapid Laser Method.

4.3.1 General. While detailed and accurate lock-on ranges for laser systems will vary with the particular system characteristics (e.g., power, wavelength, detection sensitivity, etc.), Coolidge [4] and Hedin [6] have calculated some helpful results for a system using a 1.06 micrometer wavelength and reasonable target reflectance. A method of calculating lock-on ranges (LLOR) for a 1.06-μm laser based on their results is presented below (Steps 1-3).

4.3.1.1 In Step 1 of the procedure the forecaster must determine which of the three cases presented (all based on continental aerosol models) is the applicable to the current situation. The determination is based on both prevailing weather conditions (surface visibility, visibility restriction, etc.) and system characteristics (designator and receiver collocated, etc.). He must then find the horizontal component of the LLOR from the nomogram applicable to the chosen case (Figures 30, 31, and 32), and the LLOR from Figure 33.

4.3.1.2 However, the lock-on range for laser guided systems is generally limited by the target acquisition system which must identify the target before it can be designated by the laser. Therefore, in Step 2, both the maximum target acquisition range (TAR) and the maximum lock-on range (LOR) for the laser designator-seeker system need to be determined. If the acquisition device operates at visual wavelengths (i.e., human eye or TV), compute the visual TAR (see Appendix B for computation procedures) and compare it with the laser lock-on range (computation procedures below). Use the minimum value as the maximum practical LLOR. If a FLIR target acquisition (TA) device is used, compute the maximum visual TAR and the infrared lock-on range (IR_{LOR}) (see Appendix D for rapid IR computational method) and compare it with the LLOR. Use the minimum value of the three chosen as the maximum practical LLOR.

4.3.1.3 In Step 3, determine the probability of a clear line-of-sight (CLOS) to the target as in Step 5 of Para. 4.2.2. Use the maximum practical LLOR to determine the CLOS probability instead of the maximum TAR. Table 10 shows the parameters needed to make worksheet computations and their anticipated sources.

4.3.2 Procedures (see Appendix C for laser method illustration and worksheet).

STEP 1: Determine laser lock-on range (LLOR):

a. Determine atmospheric case that applies from the three cases below from the following criteria: If the designator and receiver are approximately collocated, then chose Case (1) or (2). If the ground designator and airborne receiver are employed, choose Case (3).

(1) Homogeoeous mixing depth is 1.5 km. Choose if there is a low-level inversion present and/or visibility is restricted (Figure 30).

(2) Exponential mixing depth is 5.0 km. Choose if visibility is unlimited (Figure 31).

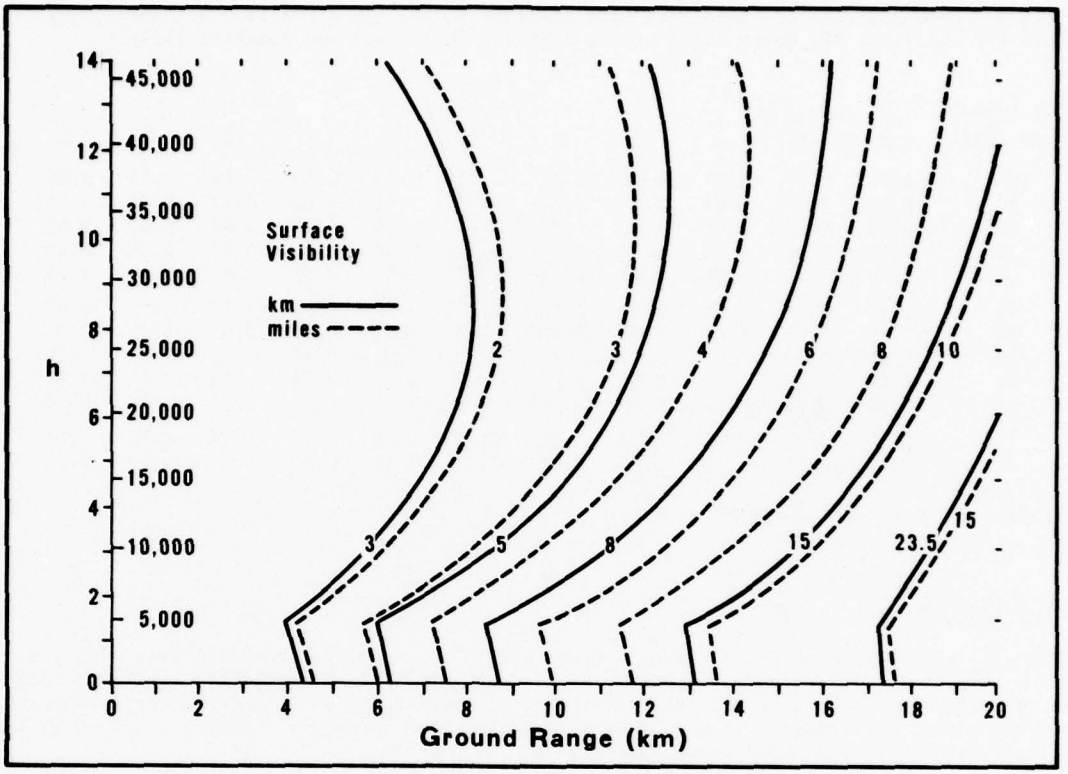

Figure 30. Horizontal Component (ground range) of Lock-On Range for a 1.06-μm Laser as a Function of Sensor Altitude (h) and Surface Visibility (V). (Continental aerosols; homogeneous mixing layer depth is 1.5 km; designator and receiver collocated) (Hedin [6]).

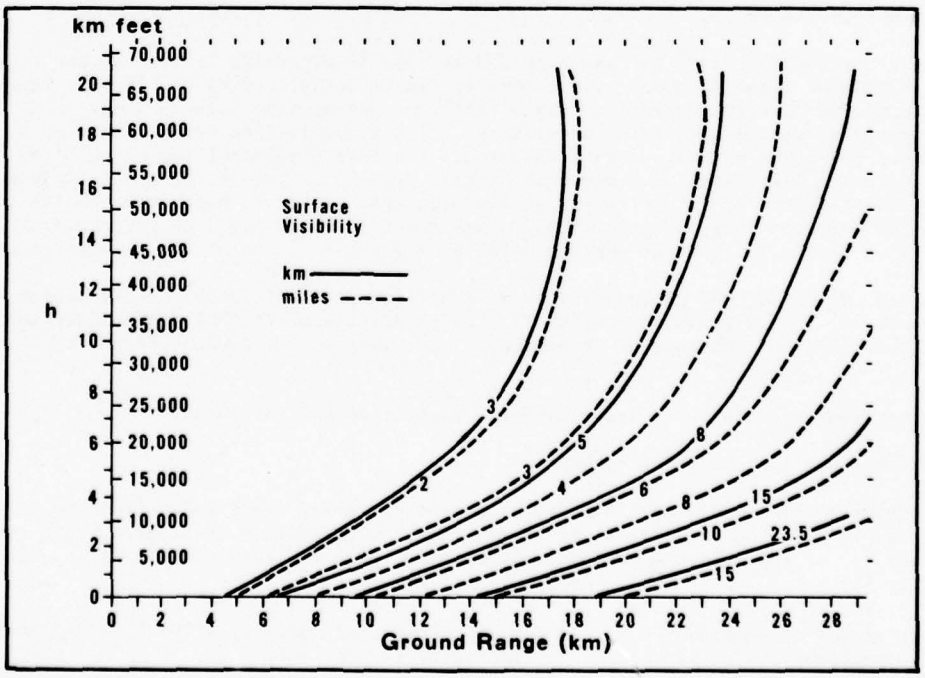

Figure 31. Horizontal Component (ground range) of Lock-On Range for a 1.06-μm Laser as a Function of Sensor Altitude (h) and Surface Visibility (V). (Continental aerosols; exponential mixing layer depth is 5.0 km; designator and receiver collocated) (Hedin [6]).

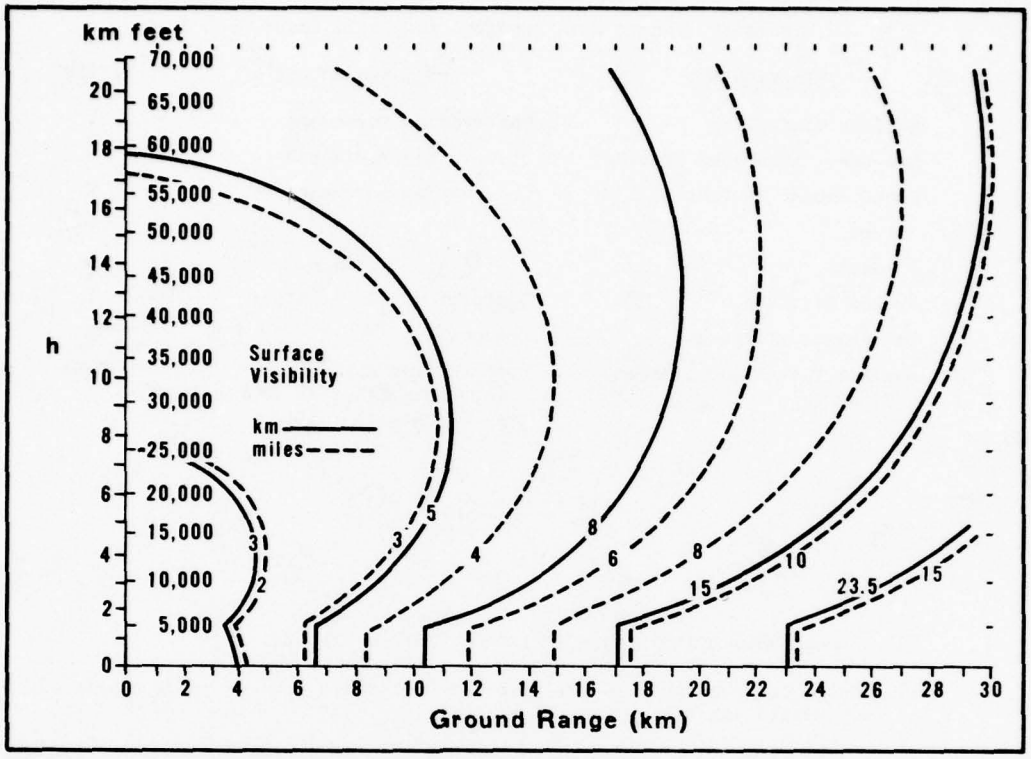

Figure 32. Horizontal Component (ground range) of Lock-On Range for a 1.06-μm Laser as a Function of Sensor Altitude (h) and Surface Visibility (V). (Continental aerosols; homogeneous mixing layer depth is 1.5 km; ground designator at 5-km range; airborne receiver) (Hedin [6]).

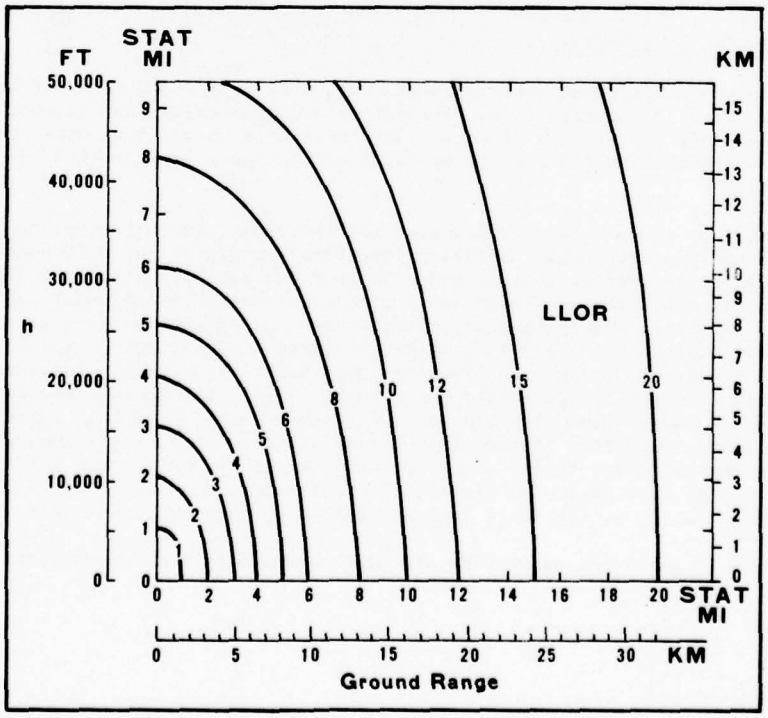

Figure 33. Laser Lock-On Range (LLOR) as a Function of Sensor Altitude (h) and Horizontal Component (ground range) of the Laser Lock-On Range.

Table 10. Input Data Required for Rapid Laser Method.

DATA REQUIRED	PROBABLE SOURCE	SYMBOL
Surface Visibility	Observation/Forecast	V
Low-Level Inversion (Yes/No)	Skew-T, Log-P Diagram	H
Cloud Amount in Tenths,	Observation/Forecast	N
Type		t_c
Height		b
Sensor Altitude	Customer	h
Designator Altitude	Customer	h_d
Maximum Target Acquisition Range	Compute from Rapid Visual (Appendix B) or IR (Appendix D) Techniques	TAR

(3) Homogeneous mixing depth is 1.5 km (Figure 32).

b. Find laser lock-on range (LLOR) from the applicable figures using sensor altitude (h) and surface visibility (V).

STEP 2: Compare LLOR with TAR and choose minimum as maximum practical LLOR. If a FLIR target acquisition device is used, compare the LOR_{IR} with the LLOR also.

STEP 3: Determine clear line-of-sight (CLOS) as in Step 5 of Para. 4.2.2. Use the maximum practical LLOR (result of comparisons in Step 2) to determine CLOS probability instead of the maximum visual LOR.

4.4 Rapid IR (8-12 μm) Method.

4.4.1 General. The infrared lock-on range LOR_{IR} will be reduced from its environmentally-free value by both water vapor extinction (i.e., absorption and scattering) and aerosol extinction. The method below includes only the effects of water vapor molecular absorption, water vapor continuum absorption and aerosol extinction in the 8-12 μm band. A discussion of this method is presented in Appendix A (Section A-8).

4.4.1.1 Step 1 of the procedure calculates the threshold transmittance, T_{IRT}. This is the ratio of the sensor's minimum detectable radiative temperature contrast (or difference) to the inherent radiative temperature contrast (or difference) between the target and background. In Step 2, the infrared lock-on range is calculated. Figure 34 is used to calculate water vapor absorption; the derived parameter is the water vapor absorption coefficient b_w. Figure 35 is used to calculate the aerosol extinction coefficient b_a. The water vapor absorption coefficient b_w and the aerosol extinction coefficient b_a are added to produce the lock-on range LOR_{IR} due strictly to atmospheric extinction. Because the target must be sufficiently large to be seen by the sensor, the maximum detection range (MDR) due to the target dimension and any sensor magnification is then calculated using Figure 28 (as in the TV method). However, if the minimum resolvable subtense angle includes sensor magnification, consider the magnification factor equal to one. The LOR_{IR} and the MDR are compared, and the minimum value is chosen as the LOR_{IR}. In Step 3, the probability of a clear line-of-sight is calculated as in Step 5 of Para. 4.2.2, except LOR_{IR} is used instead of maximum visual LOR.

4.4.1.2 Table 11 shows the parameters needed to make worksheet computations and their anticipated sources.

Figure 34a* produces an average** dew-point temperature ($\overline{T}_d$) from an average** relative humidity ($\overline{RH}$) and an average** temperature ($\overline{T}$).

Figure 34b* produces a representative absolute humidity given sensor altitude (h) and average** dew-point temperature ($\overline{T}_d$).

Figure 34c* produces the water vapor molecular absorption coefficient using the absolute humidity derived from Figure 34b.

Figure 34d* produces the water vapor absorption coefficient for 8-12 μm (b_w) using the average** temperature ($\overline{T}$) and the water vapor molecular absorption coefficient derived from Figure 34c.

* See Appendix A-8 for discussion of origin of graphs.

** Average within layer capped by low-level inversion.

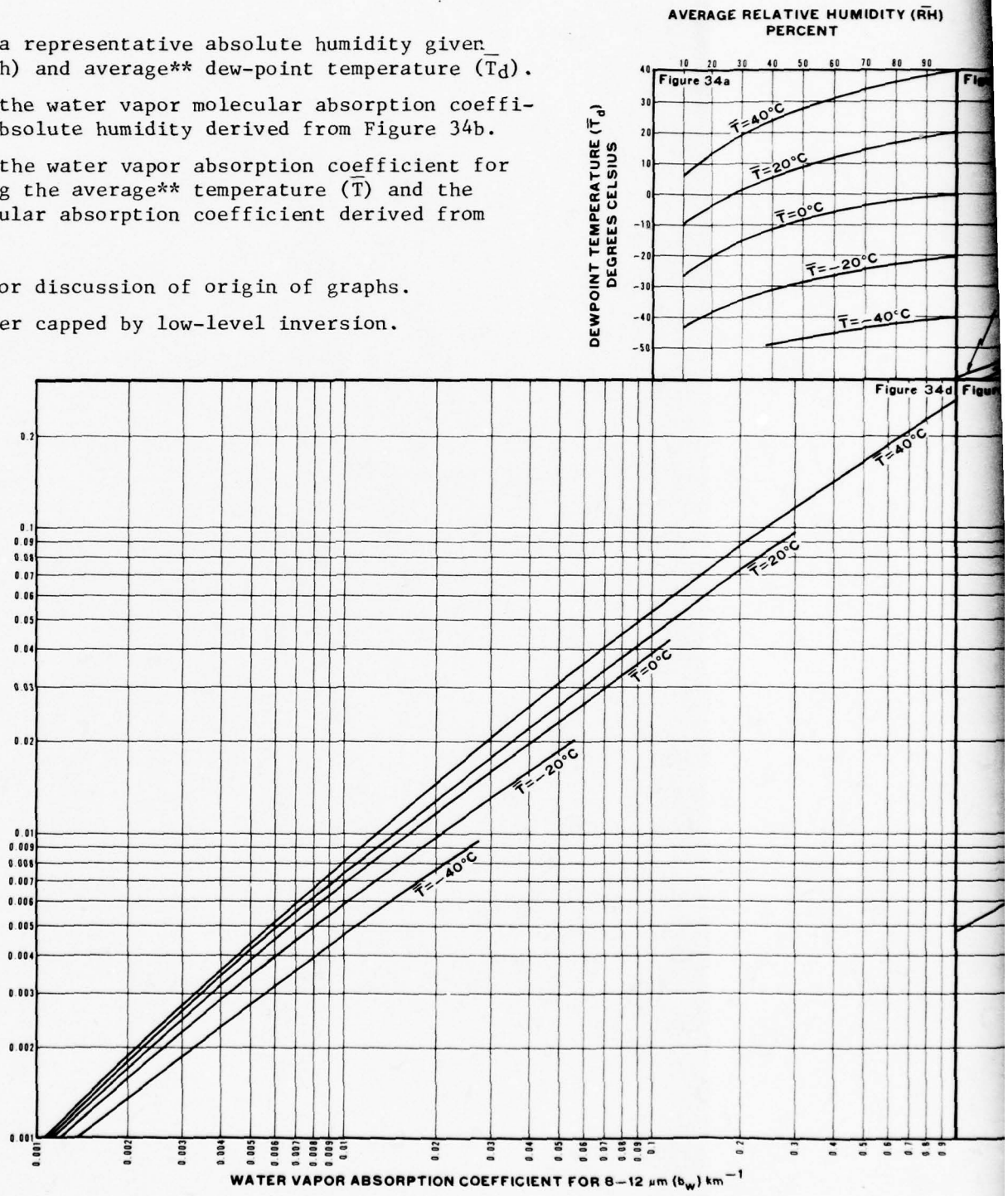

Figure 34. Water Vapor Absorption C
($\overline{T}$), and Sensor Altitude (h).

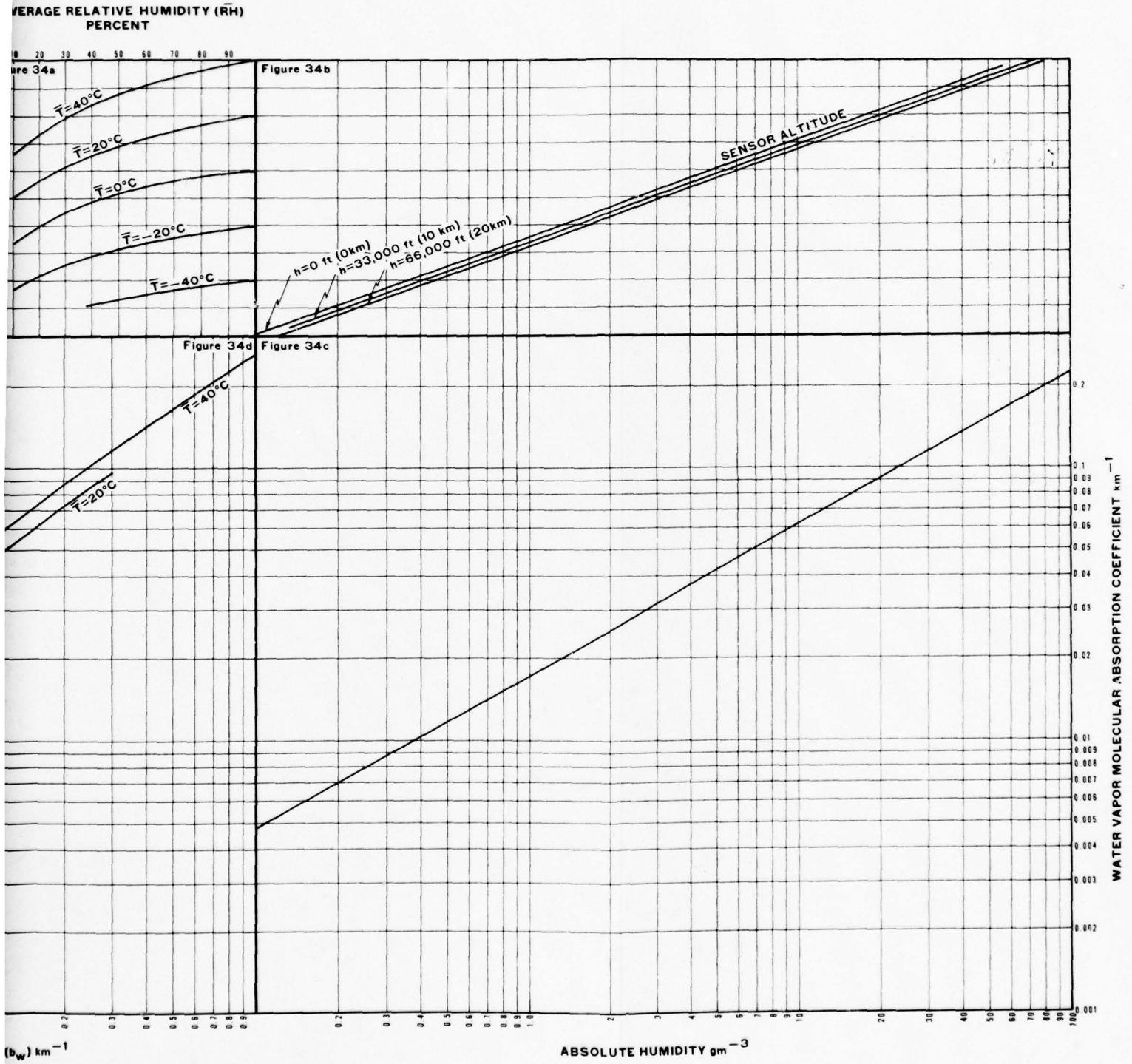

gure 34. Water Vapor Absorption Coefficient for 8-12 μm (b_w) as a Function of Average Relative Humidity ($\overline{RH}$), Average Temperature), and Sensor Altitude (h).

Figure 35a* relates the surface visibility (V) to slant range visibility (V_S) through a ratio (R_V). Based on a model which assumes an exponential decrease in the extinction coefficient above the inversion height (H) and a constant extinction coefficient below the inversion height.

Figure 35b* takes the determined ratio R_V and the given surface visibility (V) to produce the slant range visibility (V_S). $V_S = V/R_V$.

Figure 35c* produces the aerosol extinction coefficient for visible wavelengths.

Figure 35d* yields the aerosol extinction coefficient for 8-12 μm.

* See Appendix A-8 for origin of graphs.

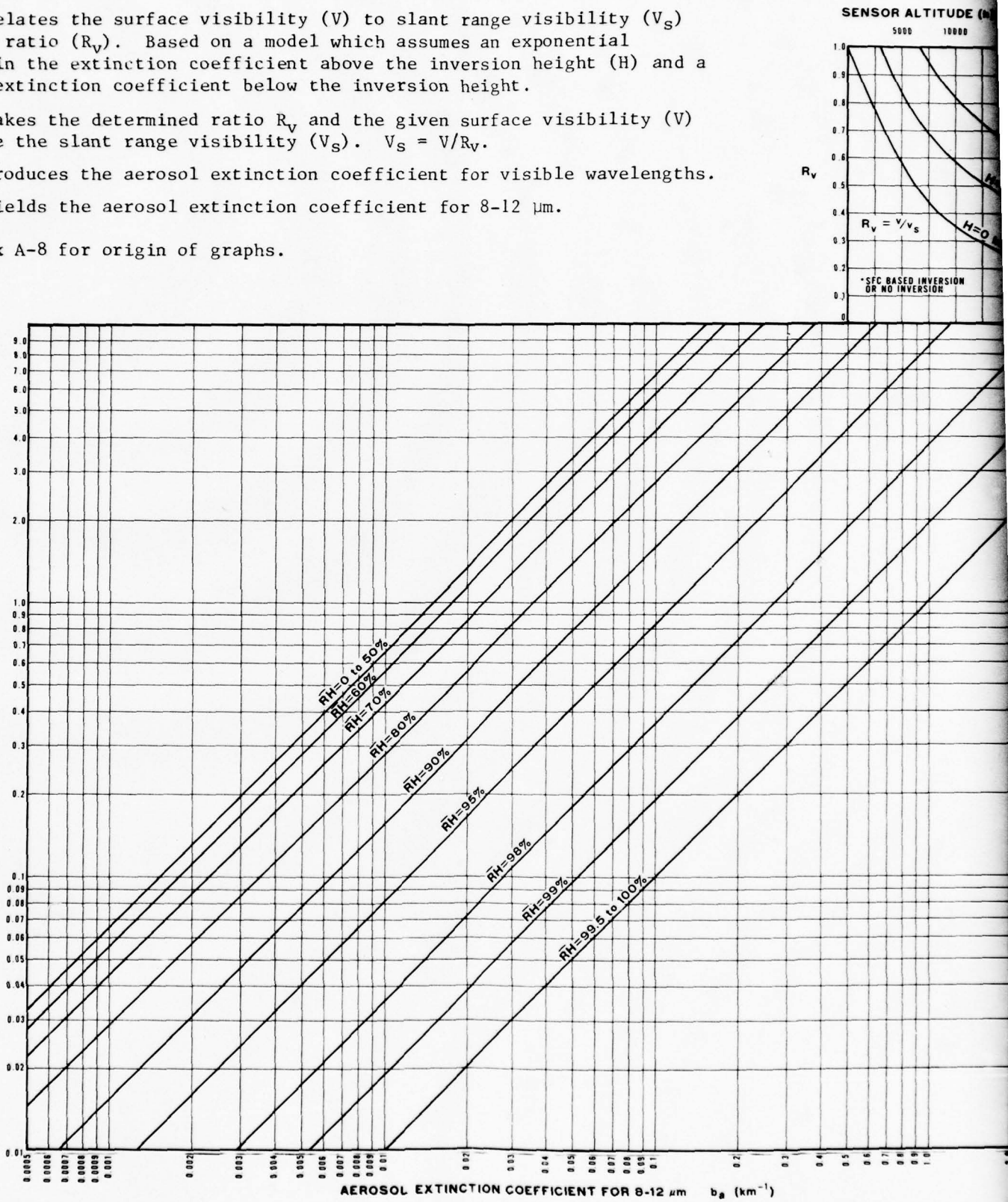

Figure 35. Aerosol Extinction Coefficient (b_a) for 8-12 μm as
Visibility (V), and Average Relative Humidity Below Inversion

slant range visibility (V_S)
assumes an exponential
he inversion height (H) and a
rsion height.

given surface visibility (V)
$_S = V/R_V$.

cient for visible wavelengths.

nt for 8-12 μm.

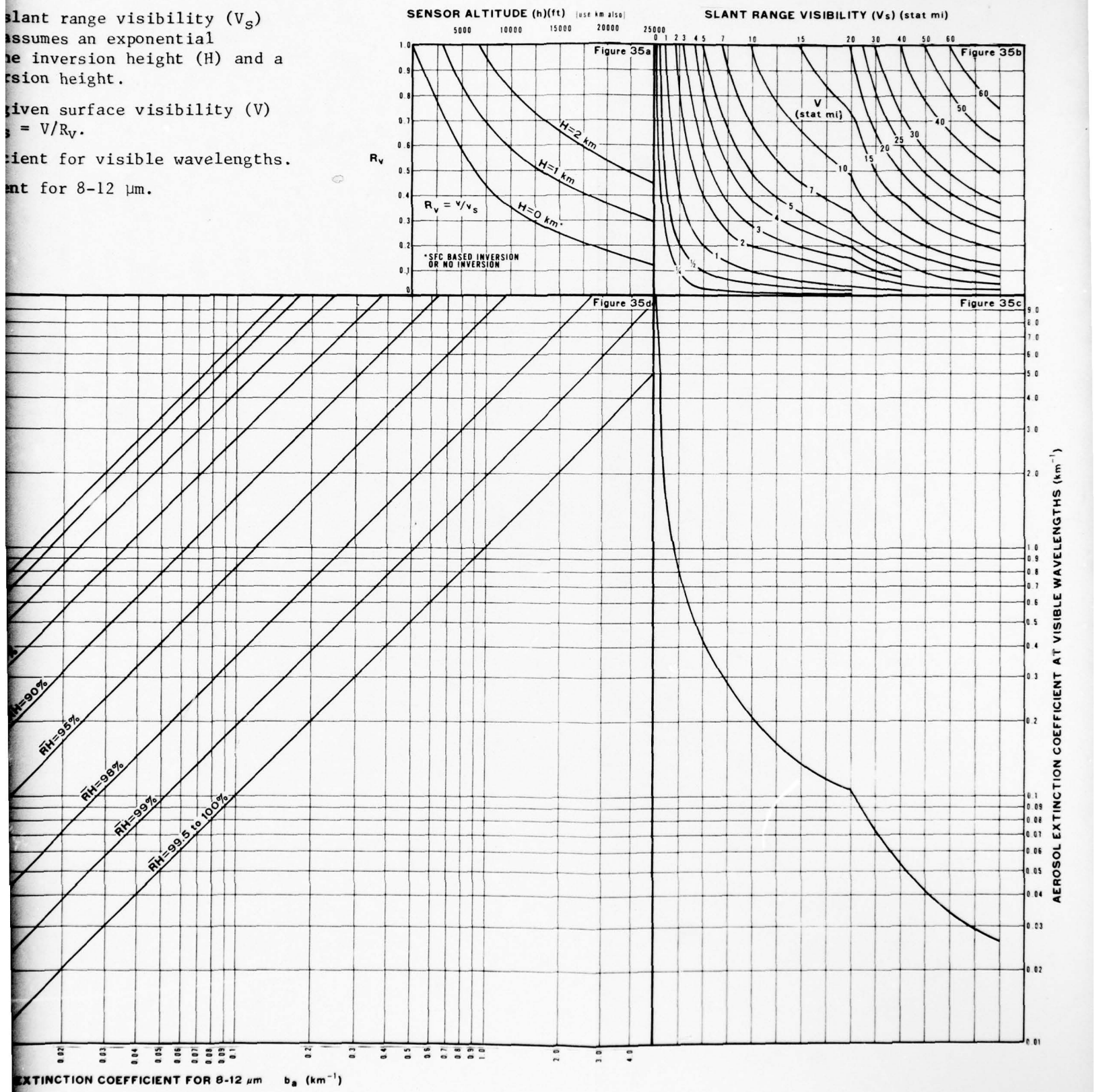

Figure 35. Aerosol Extinction Coefficient (b_a) for 8-12 μm as a Function of Sensor Altitude (h), Inversion Height (H), Surface Visibility (V), and Average Relative Humidity Below Inversion ($\overline{RH}$).

Table 11. Input Date Required for Rapid IR Method.

LOCAL DATA REQUIRED	PROBABLE SOURCE	SYMBOL
Minimum Detectable Radiative Temperature Contrast	Wing Targeting Shop	ΔT^*_{RT}
Inherent Difference between Target and Background Radiative Temperature	*Customer and or Observation/Experience	ΔT^*_o
Vertically Averaged Temperature (below inversion)	Observation/Forecast	$\overline{T}$
Vertically Averaged Dew-Point Temperature (below inversion) (or vertically averaged relative humidity)	Observation/Forecast	$\overline{T}_d$ $(\overline{RH})$
Cloud Amount in Tenths,	Observation/Forecast	N
Type		t_c
Height		b
Inversion Height (base) (or top of haze layer)	Observation/Forecast	H
Surface Visibility	Observation/Forecast	V
Sensor Altitude	Customer	h
Target Dimension (significantly sized hot spot)	Wing Targeting Shop	L
Lock-On Sensor Magnification	Wing Targeting Shop	M_{LO}
Minimum Resolvable Subtense Angle	Wing Targeting Shop	α_{LO}

* Initially, may have to use range of estimates to encompass high (approximately 10^δ), average (approximately 3^oC), and low (1^oC contrast) so customers can at least see possible variance in acquisition/lock-on range and forecasters can learn the method. With increased customer feedback and results of research now underway, better inherent contrast information can be forecast.

4.4.2 Procedures (see Appendix D for IR method illustration and worksheet).

STEP 1: Find threshold transmittance $T_{IRT} = \Delta T^*_{RT}/\Delta T^*_o$ using ΔT^*_{RT} and ΔT^*_o (e.g., assume ΔT^*_o for a passive tank equals 3^oC, and ΔT^*_o for an active tank equals 10^oC).

STEP 2: Determine maximum IR lock-on range LOR_{IR}.

a. Find the water vapor absorption coefficient b_w from Figure 34. Enter Figure 34b directly if $\overline{T}_d$ is known, or enter Figure 34a with a representative relative humidity and $\overline{T}$ to find $\overline{T}_d$. In Figure 34b, follow the $\overline{T}_d$ value to the right until intersection with the curve labeled sensor altitude h. This intersection produces a value of absolute humidity (read at bottom of Figure 34c) representative of the atmospheric layer bounded by the sensor's altitude and the ground. Using this value, move down the graph into Figure 34c and intersect the curve. The determined value (read at right of graph) is the water vapor molecular absorption coefficient. Move left from the intersection with the curve into Figure 34d. Intersect the appropriate $\overline{T}$ curve. This intersection determines b_w (read at bottom of graph), the sum of the water vapor molecular absorption coefficient and the water vapor continuum absorption coefficient for the 8-12 μm region.

b. Find the aerosol extinction coefficient b_a from Figure 35. Enter Figure 35a with H and h to determine the approximate ratio (R_V) of the surface visibility V to the slant range visibility V_S. With the value of R_V, move to the right into Figure 35b until the appropriately labeled V curve is intersected. This intersection provides an estimate of V_S. Using V_S, move down the graph until the curve in Figure 35c is intersected. This intersection provides an estimate of the aerosol extinction coefficient at visible wavelengths.

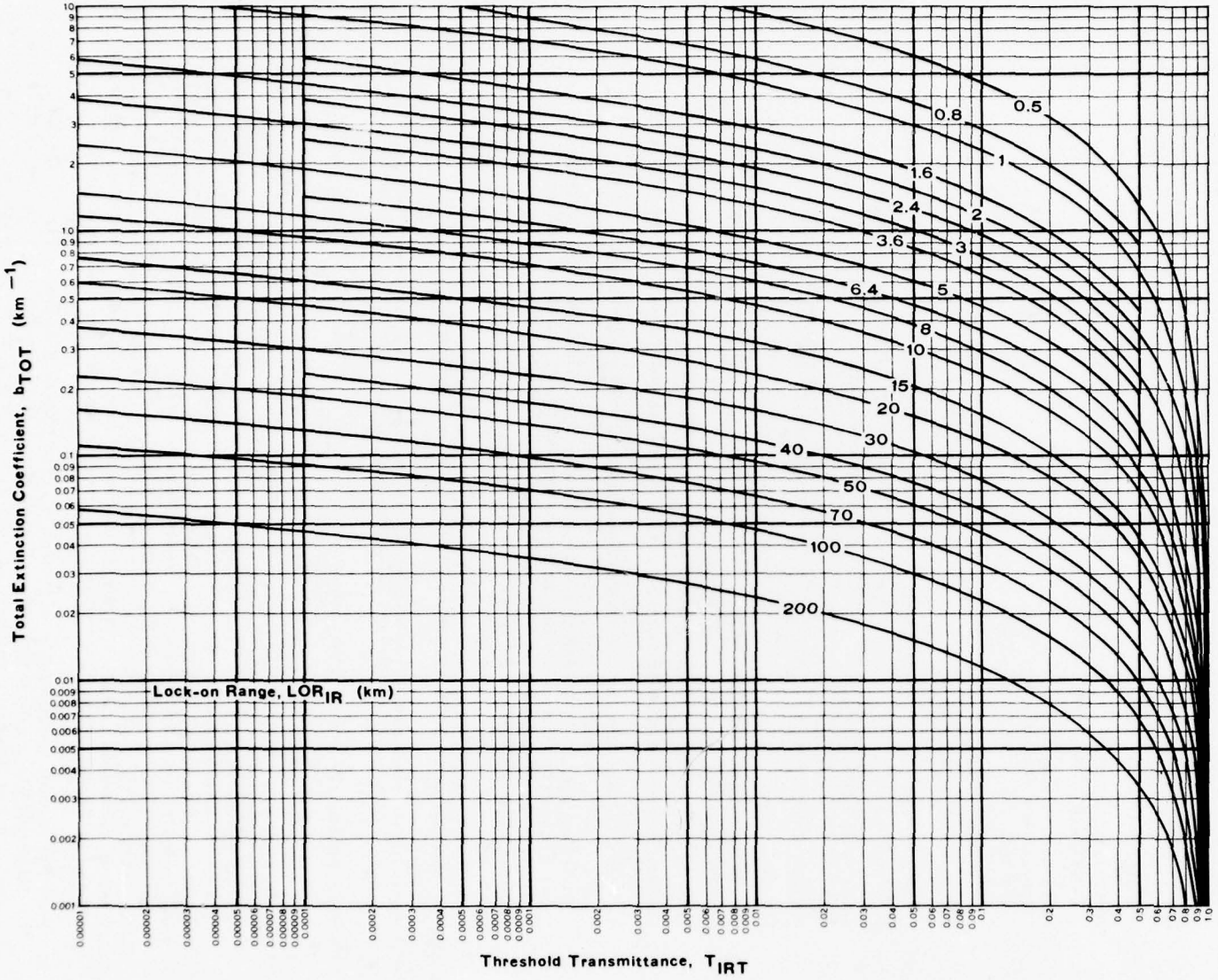

Figure 36. Lock-On Range for 8-12 μm as a Function of Threshold Transmittance and Total Extinction Coefficient.

From this intersection, move to the left in the graph into Figure 35d. Intersect the curve representing the relative humidity associated with $\overline{T}$ and $\overline{T}_d$ (note the importance of aerosol growth due to high relative humidity in Figure A-2 of Appendix A). Relative humidity can be obtained from Figure 34a. From the intersection, move down to the bottom of the graph and read the value of the aerosol extinction coefficient for the 8-12 μm region.

c. Add the water vapor absorption coefficient (b_w) and the aerosol extinction coefficient (b_a) together to find a representative total extinction coefficient b_{TOT} for the 8-12 μm region.

d. Find the infrared lock-on range (LOR_{IR}) based strictly on environmental parameters. Enter Figure 36 with b_{TOT} and T_{IRT} (from Step 1) to find the first estimate of LOR_{IR}.

e. Using target dimension L and the sensor's minimum resolvable subtense angle α_{LO}, find the maximum detection range (MDR) due to target size from Figure 28. Use the magnification M_{LO} of detector, if necessary, to calculate the effect target size L_{LO} through use of the equation L_{LO} (ft) = $L \cdot M_{LO}$ before entering Figure 28. The magnification factor may be very important in detecting or locking on to a target with an infrared device as active areas of the target can be significantly smaller in size than the target itself (e.g., a passive target dimension of 20-30 ft may have an active area size of only 8-12 ft).

f. Determine the best LOR_{IR} by choosing the minimum value of the LOR_{IR} of Step 2d and the MDR of Step 2e.

STEP 3: Determine the CLOS by combining the infrared LOR with the CFLOS data in the rapid TV methods (see Appendix B).

REFERENCES

[1] "Airborne Tactical and Defense Missiles," Air Force Magazine, 60, 5, 1977, pp. 127-129.

[2] Biberman, LM.: Effect of Weather at Hannover, Federal Republic of Germany, on Performance of Electrooptical Imaging Systems. Part I. Theory, Methodology and Data Base. Institute of Defense Analysis Paper P-1123, Arlington, VA, Aug 1976.

[3] Brown, D.R.E.: Natural Illumination Charts, Report No. 374-1, Department of the Navy, Bureau of Ships, Washington, DC, 1952.

[4] Coolidge, C.H.: Atmospheric Transmission of 1.06 Micron Laser Radiation: Application to Stand-off Missile Performance, M.S. Thesis GEO/PH/74-4, AFIT School of Engineering, Wright-Patterson AFB, OH, March 1974, 167 pp.

[5] Flowers, E.C., R.A. McCormick, and K.R. Kurfis: "Atmospheric Turbidity over the United States, 1961-1966." Journal of Applied Meteorology, 8, 1969, pp. 955-962.

[6] Hedin, V.A.: Atmospheric Effects on 1.06 Micron Laser Guided Weapons, M.S. Thesis GEO/PH/75-5, AFIT School of Engineering, Wright-Patterson AFB, OH, March 1975, 105 pp.

[7] Huschke, R.E., ed: Glossary of Meteorology, American Meteorological Society, Boston, MA, 1959, 638 pp.

[8] Huschke, R.E.: Atmospheric Visual and Infrared Transmission Deduced from Surface Weather Observations: Weather and Warplanes VI, Rand Report, R-2016-PR, Oct 1976, 38 pp.

[9] Jones, D.B., M. Freitag, S.C. Collyer, D.C. Middlekauff (editor): Air-to-Ground Target Acquisition Source Book: A Review of the Literature, prepared for Engineering Psychology Branch, Office of Naval Research, Arlington, VA, under Contract Number N00014-72-C-0389, Work Unit Number 196-121, by Martin Marietta Corp, Orlando, FL 32805, Sep 1974, ADB 000-260L.

[10] Kondratyev, K.Y.: Radiation in the Atmosphere. Academic Press, New York and London, 1969, 912 pp.

[11] List, Robert J., ed: Smithsonian Meteorological Tables, Sixth Revised Edition, Smithsonian Institution, Washington, D.C., 1966, 527 pp.

[12] Lund, I.A. and M.D. Shanklin: "Universal Methods for Estimating Probabilities of Cloud-Free Lines-of-Sight through the Atmosphere," Journal of Applied Meteorology, 12, February 1973, pp. 28-35.

[13] McClatchey, R.A., R.W. Fenn, J.E.A. Selby, F.E. Volz, and J.S. Garing: Optical Properties of the Atmosphere (Revised), AFCRL-71-0279, Air Force Cambridge Research Laboratories, L.G. Hanscom, MA, May 1971.

[14] Middleton, W.E.K.: Vision Through the Atmosphere. University of Toronto Press, USA, 1968, 250 pp.

[15] Poliakova, E.A. and K.S. Shifrin: "The Microstructure and Transparency of Rains." Proc. Main Geophys. Obs. No. 42 (104), 1953.

[16] RCA, Electro-Optics Handbook, EOH-11, Harrison, NJ, 1974.

[17] Shifrin, K.S.: Scattering of Light in a Turbid Medium, Gostekhizdat, Moscow, 1951.

[18] Sivkov, S.I.: Computation of Solar Radiation Characteristics. Israel Program for Scientific Translations Ltd, TT 70-50055, 1971. Available from U.S. Dept of Commerce, NTIS, Springfield, VA 22151

[19] Stein, Kenneth J.: "Pave Tack Pods Enhance Target Tracking Capacity," Aviation Week & Space Technology, 108, 9, Feb 27, 1978, pp. 57-59.

[20] White, K.O., W.R. Watkins and C.W. Bruce: "Water Vapor Line and Continuum Absorption Measurements in the Infrared Region," Proceedings of the Optical-Submillimeter Atmospheric Propagation Conference, 6-9 Dec 76, Vol I, Office of the Director of Defense Research and Engineering, Washington, D.C.

Appendix A

ADDITIONAL RADIATION TRANSFER THEORY

A-1 Introduction. This appendix is designed to cover briefly some of the basics of the radiative transfer processes related to PGM operations.

A-2 Attenuation. The attenuation or extinction of electromagnetic radiation (e.g., visible, infrared, etc.) is described by the Lambert-Beer-Bouquer Law

$$I_\lambda = I_{\lambda,o} \exp(-b_\lambda D) \tag{A-1}$$

where $I_{\lambda,o}$ is the intensity of the incident monochromatic (i.e., single wavelength) radiation, b_λ is the monochromatic volume attenuation (or extinction) coefficient, D is the distance (path length) over which the attenuation occurs, and I_λ is the intensity of the monochromatic transmitted radiation. Equation (A-1) is the combined representation of Equations (1-2) and (1-3).

Attenuation is caused by absorption and scattering due to molecules and aerosols (dry or liquid). The monochromatic volume attenuation coefficient b_λ is given as

$$b_\lambda = b_{ma,\lambda} + b_{ms,\lambda} + b_{aa,\lambda} + b_{as,\lambda} \tag{A-2}$$

where $b_{ma,\lambda}$ is monochromatic molecular volume absorption coefficient (e.g., water vapor, ozone, etc.),

$b_{ms,\lambda}$ is monochromatic molecular volume (Rayleigh) scattering coefficient,

$b_{aa,\lambda}$ is monochromatic molecular volume absorption (wet or dry particles) coefficient, and

$b_{as,\lambda}$ is monochromatic aerosol volume (Mie) scattering coefficient.

Table A-1 illustrates the usual importance of these attenuation processes for selected wavelength regions.

Table A-1. Important Volume Absorption and Scattering Processes in Selected Wavelength Regions.

WAVELENGTH REGION	IMPORTANT VOLUME ABSORPTION AND SCATTERING COEFFICIENTS (in order of importance)
0.4 - 0.74 μm	$b_{as,\lambda}$ $b_{ms,\lambda}$ $b_{aa,\lambda}$
0.74 - 2 μm	$b_{as,\lambda}$ $b_{aa,\lambda}$ $b_{ms,\lambda}$
3 - 5 μm	$b_{ma,\lambda}$ $b_{as,\lambda}$ $b_{aa,\lambda}$ $b_{ms,\lambda}$
8 - 12 μm	$b_{ma,\lambda}$ $b_{aa,\lambda}$ $b_{as,\lambda}$

A-3 Scattering. The topic of scattering was introduced in Para. 1.4.3 and the volume scattering coefficients were introduced in Sections 1.5 and A-2. The monochromatic volume scattering coefficients for molecules ($b_{ms,\lambda}$) and aerosols ($b_{as,\lambda}$) are described in this section.

A-3.1 Monochromatic Volume Scattering Coefficient for Molecules. The monochromatic volume scattering coefficient for molecules (Rayleigh scattering), $b_{ms,\lambda}$, is approximately proportional to the inverse of the wavelength λ raised to the fourth power (Kondratyev [10], p. 177).

Specifically, Kondratyev [10] shows this equation as

$$b_{ms,\lambda} = 17.35\ \rho^2/\tilde{N}\ \lambda^4 \tag{A-3}$$

where ρ is the air density (g cm^{-3}), $\tilde{N}$ is the number of molecules per unit volume (molecules cm^{-3}) and λ is wavelength (cm).

The value of $\tilde{N}$ can be approximated by use of the equation

$$\tilde{N} = \tilde{P}/kT \tag{A-4}$$

where $\tilde{P}$ is the air pressure (dyne cm^{-2}), k is the Boltzmann constant (1.38×10^{-16} erg $molecule^{-1}$ deg^{-1}), and T is temperature (^oK).

The density can be approximated by use of the equation of state for dry air

$$\rho = \tilde{P}/R_d T \tag{A-5}$$

where R_d is the gas constant for dry air (0.278×10^7 erg g^{-1} $^oK^{-1}$).

Combining (A-3), (A-4), and (A-5) results in an approximate relationship for $b_{ms,\lambda}$ (in cm^{-1}) as a function of pressure, temperature, and wavelength

$$b_{ms,\lambda} = (3.0981 \times 10^{-28}) \tilde{P}/T \lambda^4 \tag{A-6}$$

Thus, the monochromatic volume scattering coefficient for molecules can be approximated for a homogeneous region within the atmosphere.

A-3.2 Monochromatic Volume Scattering Coefficient for Aerosols.

A-3.2.1 For a monodispersed (i.e., same size) collection of aerosols, Middleton [14, p. 27] and Kondratyev [10, p. 195] give the monochromatic volume scattering coefficient for aerosols ($b_{as,\lambda}$) as

$$b_{as,\lambda} = N' \pi r^2 Q(X) \tag{A-7}$$

where N' is the number of aerosols per unit volume (number of aerosols cm^{-3}), r is the aerosol radius (cm), and Q(X) is the scattering area ratio (or scattering efficiency) which is function of the size parameter X and the refractive index (Kondratyev, [10, pp. 182-184]).

A-3.2.2 The scattering area ratio, Q(X), represents the dimensionless ratio of the cross-sectional area of a spherical scatterer which would scatter the same amount of radiation as the actual amount of incident radiation to the geometric cross section of a scattering particle.

Figure A-1 illustrates a plot of the Q(X) as a function of X for absolutely reflecting aerosols (i.e., aerosols with refractive indexes approaching infinity). Plots for water droplets (with real refractive indexes between 1.33 and 1.5) have a form similar to Figure A-1 but with more oscillation.

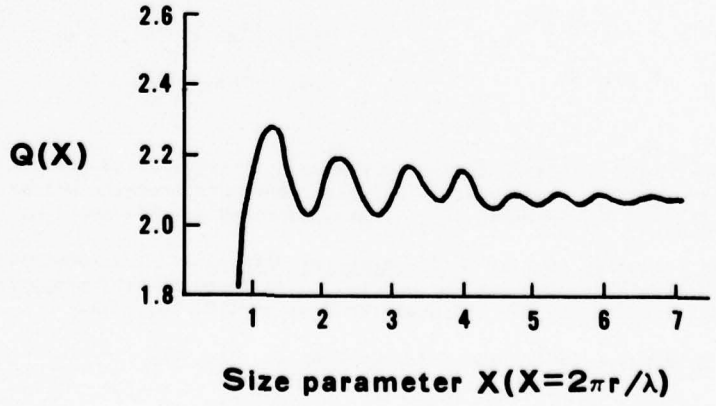

Figure A-1. Scattering Area Ratio Q(X) for Absolutely Reflecting Aerosols (Shifrin [17], see Kondratyev [10], p. 183).

A-3.2.3 For a polydispersed aerosol collection, Kondratyev [10, p. 196] gives this scattering coefficient as

$$b_{as,\lambda} = \int_{r_o}^{r_1} \pi r^2 Q(X) \frac{dN'}{dr} dr \qquad \text{(A-8)}$$

where r_o and r_1 are the minimum and maximum aerosol radii (cm), and dN'/dr is the aerosol size distribution (number aerosols cm^{-3} cm^{-1}).

Junge's power law representation of dN'/dr is frequently used in the study of dry aerosols (dust) in the radius interval $5x10^{-6}$ to 10^{-3} cm. This size distribution is given as

$$dN'/dr = C_1 r^{-4} \qquad \text{(A-9)}$$

where C_1 is a constant.

Poliakova and Shifrin [15] (see Kondratyev [10, p. 197]) have used the raindrop distribution

$$dN'/dr = C_2 r^2 e^{-C_3 r} \qquad \text{(A-10)}$$

when the size parameter (X) lies within the range 600 to 3000. C_2 and C_3 are constants. Other empirical representations for dN'/dr are available elsewhere in the literature.

A-3.2.4 Scattering is also a function of relative humidity (RH). As the RH increases, water molecules will collect on a dry particle, frequently causing it to go into solution. This is called deliquescence. Since a solution droplet can grow much faster in size than the particle, the scattering increases rapidly with RH as the droplet grows. Typical scattering coefficient variations as a function of RH are shown in Figure A-2. This phenomenon explains why visibility in a dry hazy atmosphere is frequently much better than that in a humid (relative) atmosphere. Variations in relative humidity can be as important as variations in dry aerosol content.

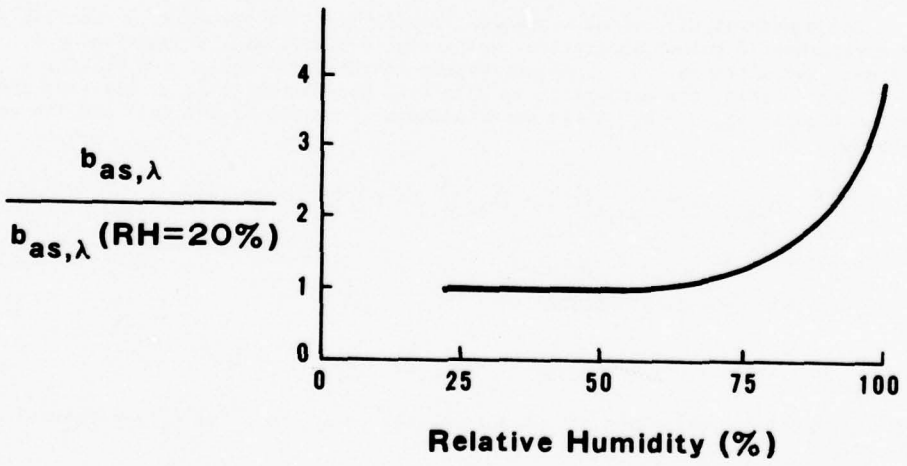

Figure A-2. Example of Ratio of the Scattering Coefficient for Aerosols to the Scattering Coefficient for Aerosols at 20% Relative Humidity as a Function of Relative Humidity.

A-4 Sunphotometry. The purpose of sunphotometry is the measurement of atmospheric turbidity through the determination of the turbidity coefficient. Turbidity is any atmospheric condition which reduces the transmission of radiation, particularly visible radiation (Huschke [7]).

A-4.1 Foundation. Equation (A-1) may be written as

$$I_\lambda = I_{\lambda,o}\ 10^{-b'_\lambda M} \tag{A-11}$$

where b'_λ is the monochromatic decadic extinction coefficient (dimensionless) given as

$$b'_\lambda = \tilde{b}_\lambda\ z'/\ln 10 \tag{A-12}$$

(see Sivkov [18], p. 41), M is the optical air mass (dimensionless), z' is the aerosol scale height (approximately 8 km) representative of an optical air mass M = 1, and $\tilde{b}_\lambda$ is a representative monochromatic volume extinction coefficient (length^{-1}). The intensity of the sunlight at wavelength λ at the top of the atmosphere is $I_{\lambda,o}$ and a sunphotometer measures the intensity at the bottom of the atmosphere as I_λ. Equation (A-11) may be expanded (Flowers et al. [5]) into the form

$$I_\lambda = I_{\lambda,o}\ 10^{-(b'_{ms,\lambda} + b'_{ma,\lambda}(O_3) + B_\lambda) M} \tag{A-13}$$

where $b'_{ms,\lambda}$ is the monochromatic decadic scattering coefficient for air molecules (usually considered a constant), $b'_{ma,\lambda}(O_3)$ is the monochromatic decadic absorption coefficient for ozone (usually considered a constant), and B_λ is the monochromatic decadic turbidity coefficient (a variable). All coefficients are prescribed for a path length equivalent to an air mass equal to one (that is, from the earth's surface to a point directly overhead at the extreme outer edge of the atmosphere). The optical air mass M adjusts the path length for an air mass equal to one to the actual air mass based on the solar elevation angle Ω such that M = cosecant (Ω), $\Omega \geq 10^o$.

A-4.2 Turbidity Coefficient. The monochromatic decadic turbidity coefficient B_λ is directly related to the vertically-integrated monochromatic aerosol volume extinction (i.e., absorption and scattering) coefficient from the earth's surface to the top of the atmosphere and can be defined as

$$B_\lambda = \int_o^\infty [b_{as,\lambda}(z) + b_{aa,\lambda}(z)]\ dz/\ln 10 - C_6 \tag{A-14}$$

where $b'_{as,\lambda}$ is the monochromatic volume scattering coefficient for aerosols (a function of z), $b'_{aa,\lambda}$ is the monochromatic volume absorption coefficient for aerosols (a function of z), and z is the vertical coordinate for altitude. C_6 is approximately constant and equal to 0.0674 (i.e., the sum of $b'_{ms,\lambda} + b'_{ma,\lambda}(O_3)$). Often, the assumption is made (see Kondratyev [10], p. 29) that the extinction coefficient for aerosols ($b_{as,\lambda} + b_{aa,\lambda}$) is an exponential function of altitude and its value at the earth's surface such that

$$[b_{as,\lambda}(z) + b_{aa,\lambda}(z)] = [b_{as,o,\lambda} + b_{aa,o,\lambda}]\ \exp(-z/z') \tag{A-15}$$

where the surface value is $[b_{as,o,\lambda} + b_{aa,o,\lambda}]$.

Substituting (A-15) into (A-14) yields

$$B_\lambda = [b_{as,o,\lambda} + b_{aa,o,\lambda}]\ z'/\ln 10 - C_6 \tag{A-16}$$

The volume extinction coefficient at the surface can be approximated by Koschmieder's theory for visible wavelengths (see Section A-5)

$$(b_{as,o} + b_{aa,o}) = 3.912/V_R \tag{A-17}$$

where V_R is the meteorological visual range.

A-4.3 Comments. A few comments can be made concerning the above discussion.

A-4.3.1 Using a sunphotometer to measure I_λ for a specific solar elevation angle Ω (implying an M), and assuming constant values for $I_{\lambda,o}$, $b'_{ms,\lambda}$ and $b'_{ma,\lambda}(O_3)$, A-13) can be solved for the turbidity coefficient B_λ.

A-4.3.2 Known values of the visual range V_R imply values of $(b_{as,o} + b_{aa,o})$ through (A-17). For an aerosol scale height z', (A-16) can be used to approximate B_λ at visual wavelengths.

A-5 Meteorological Visual Range and Visibility. A target against a background is seen only if the transmission of the contrast between a target and its background is sufficient to be detected by an observer.

A-5.1 Meteorological Visual Range. For detection of a target against a horizon sky background, visual contrast transmission is given by

$$C_R/C_o = e^{-b_\lambda R} \tag{A-18}$$

where C_o is the inherent contrast, C_R is the apparent contrast at range R, and b_λ is the monochromatic volume attenuation (extinction) coefficient. The inherent contrast C_o is the ratio of the difference in the reflectances of the target and the background to the background reflectance evaluated in close proximity to the target. Solving (A-18) for R yield

$$R = \ln (C_o/C_R)/b_\lambda \tag{A-19a}$$

The detection threshold of the eye has been found to be approximately equal to 0.02 (i.e,, 2% apparent contrast*) and the inherent contrast of a black target against the horizon sky is approximately one or 100% inherent contrast. Thus, for the average eye, (A-19a) becomes

$$V_R = R = 3.912/b_\lambda \tag{A19b}$$

The meteorological visual range V_R is defined by (A-19b).

A-5.2 Visibility. Visibility is a more general, less restrictive term than meteorological visual range. Visibility is the greatest distance at which an observer can just see and identify a dark object (not necessarily "black") against the horizon sky during daytime or a moderately intense (preferably unfocused) light source at night (Huschke [7]). On the other hand, meteorological visual range is normally measured by an instrument or calculated from a measured quantity. Although the two terms are not the same, meteorological visual range is frequently used as an approximation to visibility.

A-6 Contrast Transmission. The transmission of energy from a source (i.e., a target and its background) to a sensor is the underlying problem in assessing whether a sensor can be used.

A-6.1 Contrast Transmission for Visible and Near Infrared Sensors. The brightness, B(R), originating from a target or background at range R is

$$B(R) = B(0)\ \tau + P_r \tag{A-20}$$

where B(0) is the brightness at range equal to zero, P_r is the path radiance (i.e., the brightness of light scattered along the path into the sensor), and τ is the atmospheric beam transmission over the homogeneous path between the target/background and the sensor. The beam transmission is given as

$$\tau = e^{-\tilde{b}r} \tag{A-21}$$

where $\tilde{b}$ is the volume extinction (fundamentally scattering) coefficient for the visible wavelength band.

A-6.1.1 The contrast transmission τ_c is defined as

$$\tau_c = C_R/C_o \tag{A-22}$$

where C_R is the target-to-background contrast at range R, and C_o is the inherent target-to-background contrast. Using the definition of contrast with (A-20) and substituting the results into (A-22) yields

---

* NOTE: For natural objects, a detection threshold C_R closer to 0.035 (Huschke [8], p. 8) is used.

$$\tau_c = [1 + P_r/B_b(0)\tau]^{-1} \quad \text{(A-23)}$$

where $B_b(0)$ is the background brightness at range equal to zero.

$$B_b(0) = H_o R_b/\pi \quad \text{(A-24)}$$

where H_o is the surface illuminance (a flux), R_b is the background reflectance or albedo, and the value of π is a conversion factor (approximate since isotropy is assumed by its use) for flux to radiance notation [see Figure A-3 for an illustration of the components of (A-20) and (A-24)]. Considering (A-23) under the same atmospheric conditions, the contrast transmittance can be significantly different depending on whether the target is on a white concrete surface or a muddy field. This difference results from the strong role played by the background brightness in the contrast transmission. Figure A-4 illustrates this concept.

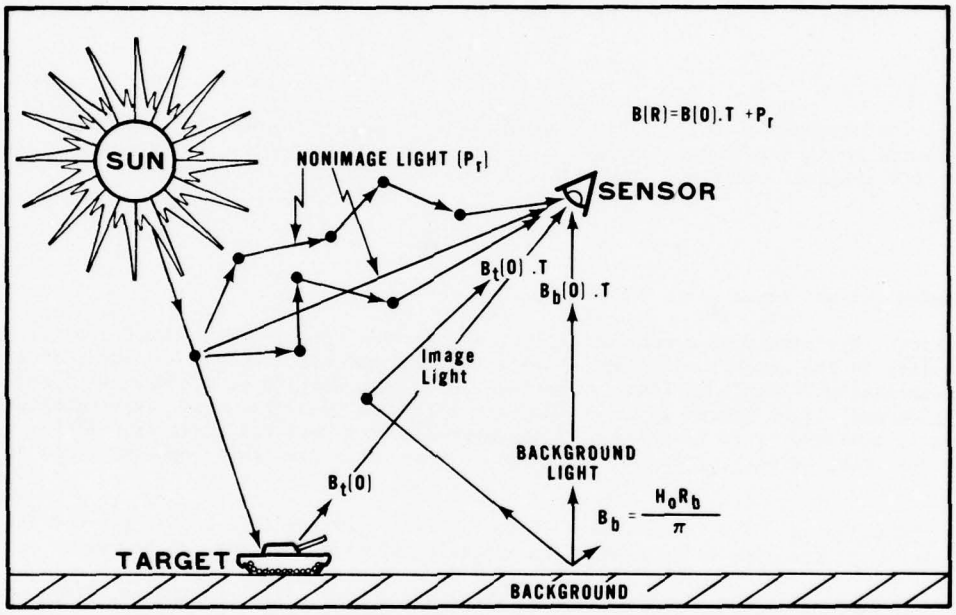

Figure A-3. Depiction of Contrast Transmission Parameters.

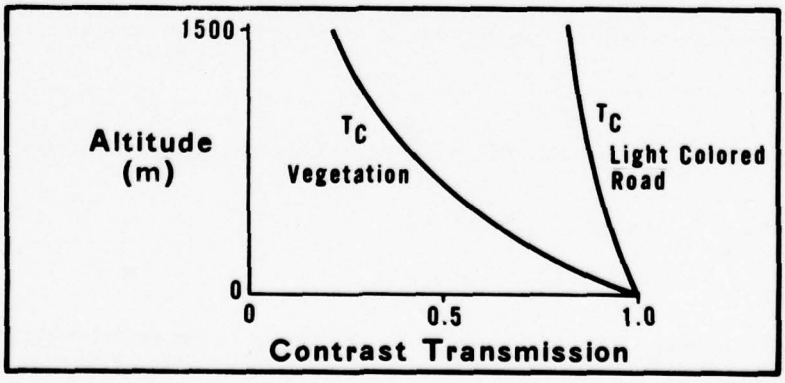

Figure A-4. Schematic Illustration of Contrast Transmission as a Function of Altitude and Vegetation/Terrain Type for the Same Target and Atmospheric Conditions.

A-6.1.2 Duntley (see Middleton [14], pp. 68-70) presents the general equation for contrast transmission as

$$C_R/C_o = [B_b(0)/B_b(R)]\, e^{-\tilde{b}R} \qquad \text{(A-25)}$$

where $B_b(R)$ is the background brightness at range R. In viewing an object against the horizon sky, the ratio $B_b(0)/B_b(R)$ approaches unity since both are brightnesses from the sky of "infinite" extent. Viewing a target from a downward looking sensor requires modification of (A-25) (see Middleton [14], pp. 68-73). The result is

$$C_R/C_o = [1 - (B_m/B_b(0))(1 - e^{\tilde{b}_o \bar{R}})]^{-1} \qquad \text{(A-26)}$$

where B_m is related to the component of the path radiance near the target divided by the value of the volume extinction coefficient $\tilde{b}_o$ in the vicinity of the target, and $\bar{R}$ represents the horizontal distance in a homogeneous atmosphere for which the extinction is the same as that actually encountered along the true path of length R. The ratio $B_m/B_b(0)$ is called the sky-ground ratio. Equation (A-26) is the theoretical foundation of Figures 26 and 27 where $B_m/B_b(0)$ equals 4.

A-6.2 Contrast Transmission for Middle through Far Far Infrared and Millimeterwave/Microwave Sensors. The radiance arriving from a target ($I_{t,\lambda}$) compared to the radiance arriving from the background ($I_{b,\lambda}$) is the important contrast in assessing the utility of most infrared and millimeterwave/microwave sensors. These radiances are composed of the energy emitted from the target ($I_{t,o,\lambda}$) and background ($I_{b,o,\lambda}$) and the energy emitted along the path between sensor and target/background (P_e), or scattered into the path in the direction of the sensor (P_s). For these sensors, the sum of P_e and P_s is path radiance (P_r). An adaptation of (A-20) that can be applied to both the target and background is

$$I_\lambda = I_{o,\lambda}\, \tau_\lambda + P_r \qquad \text{(A-27)}$$

where τ_λ is the atmospheric beam transmission over a homogeneous path and

$$\tau_\lambda = e^{-b\lambda R} \qquad \text{(A-28)}$$

where b_λ is the monochromatic volume attenuation (primarily absorption) coefficient, and R is the slant range. Absorption within the atmospheric windows can be substantial over long path lengths. Applying (A-27) to both the target and the background and subtracting results in

$$\Delta I_\lambda = (I_{t,\lambda} - I_{b,\lambda}) = (I_{t,o,\lambda} - I_{b,o,\lambda})\, \tau_\lambda \qquad \text{(A-29)}$$

Note that the path radiance term cancels. Hence, the term $(I_{t,o,\lambda} - I_{b,o,\lambda})$ is directly related to (A-38) (see next section) and the radiance difference (contrast) ΔI_λ between the target and background for most infrared and microwave frequencies is a function of the inherent radiance difference $(I_{t,o,\lambda} - I_{b,o,\lambda})$ and the beam transmission τ_λ. However, it should be noted that emissions of energy along the path from target to sensor might affect the maximum target acquisition/lock-on range (i.e., path radiance will not affect the apparent contrast, but could significantly attenuate energies which form the contrast over long path lengths).

A-7 Inherent Radiative Temperature Difference (ΔT_o^*) Between Target and Background. From Figure 9, Planck's Law may be combined with the monochromatic emissivities for the target and background to produce a representation for the energies emitted from the target and its background. The monochromatic energy emitted by a target and its background are given respectively as

$$E_{t,\lambda} = \varepsilon_{t,\lambda}\, (C_5/\lambda^5)/(e^{C_4/\lambda T_t} - 1) \qquad \text{(A-30)}$$

and

$$E_{b,\lambda} = \varepsilon_{b,\lambda}\, (C_5/\lambda^5)/(e^{C_4/\lambda T_b} - 1) \qquad \text{(A-31)}$$

where $\varepsilon_{t,\lambda}$ and $\varepsilon_{b,\lambda}$ are the respective monochromatic emissivities for the target and background, and T_t and T_b are respectively the physical temperatures of the target and background. The monochromatic target and background emissions given in (A-30) and (A-31) can be expressed without the emissivities if equivalent radiative temperatures are used in lieu of physical temperatures. Thus,

$$E_{t,\lambda} = (C_5/\lambda^5)/(e^{C_4/\lambda T_t^*} - 1) \quad \text{(A-32)}$$

and

$$E_{b,\lambda} = (C_5/\lambda^5)/(e^{C_4/\lambda T_b^*} - 1) \quad \text{(A-33)}$$

where T_t^* and T_b^* are the radiative temperatures. Solving (A-32) and (A-33) for T_t^* and T_b^* yields

$$T_t^* = C_4/\lambda \ln [1 + (C_5/E_{t,\lambda}\lambda^5)] \quad \text{(A-34)}$$

and

$$T_b^* = C_4/\lambda \ln [1 + (C_5/E_{b,\lambda}\lambda^5)] \quad \text{(A-35)}$$

Substituting (A-30) into (A-34) and (A-31) into (A-35) yields

$$T_t^* - (C_4/\lambda)/\ln [1 + (e^{C4/\lambda T_t} - 1)/\varepsilon_{t,\lambda}] \quad \text{(A-36)}$$

and

$$T_b^* = (C_4/\lambda)/\ln [1 + (e^{C_4/\lambda T_b} - 1)/\varepsilon_{b,\lambda}] \quad \text{(A-37)}$$

The difference between T_t^* and T_b^* is the inherent radiative temperature difference ΔT_o^* between the target and background and is expressed as

$$\Delta T_o^* = (C_4/\lambda) \{1/\ln [1 + (e^{C4/\lambda T_t} - 1)/\varepsilon_{t,\lambda}] - 1/\ln [1 + (e^{C_4/\lambda T_b} - 1)/\varepsilon_{b,\lambda}]\} \quad \text{(A-38)}$$

A-8 IR Method to Compute Lock-On Range. The rapid method (Paras. 4.3.1 and 4.3.2) for computing IR (8-12 μm) lock-on range was derived primarily from material presented by Huschke [8 (pp. 8 and 12-18)].

A-8.1 Figure 34a is based on Table 94 of List [11]. The saturation vapor pressure (e_s) is derived directly from the table based on a given temperature T. If a relative humidity (RH) is prescribed, then a dew-point temperature can be found by equating it to the temperature in Table 94 that corresponds to an actual vapor pressure (e) derived from the relationship

$$e = (RH)(e_s) \quad \text{(A-39)}$$

A-8.2 Figure 34b was based on the equations (corrected) at the bottom of page 13 and the top of page 15 of Huschke [8]. The curves are labeled with sensor altitudes that are twice the value used to calculate the data points for the curves. This was done to calculate absolute humidities for the middle of layers rather than at the tops of layers.

A-8.3 Figure 34c was based on the equation presented in the middle of page 15 of Huschke [8].

A-8.4 Figure 34d was based on the equation at the top of page 16 of Huschke [8].

A-8.5 Figure 35a is based on a simple modeling effort.

A-8.5.1 The lower atmosphere is divided into three layers:

A-8.5.1.1 The lowest layer (referred to as Region I) extends from the ground up to the base of the low-level inversion (or the top of the haze layer), H. Within Region I, the visibility V is assumed constant, and hence, the aerosol extinction coefficient $b_{a,I}$ is constant. Thus, the relationship

$$b_{a,I} = C/V \quad \text{(A-40)}$$

for $0 \leq z \leq H$ (km) and where C is a constant equal to 2.9, is used to define the relationship between $b_{a,I}$ and the surface visibility V.

A-8.5.1.2 The middle layer (referred to as Region II) extends from the top of the inversion to an altitude of 5 km. Within Region II, the aerosol extinction coefficient is assumed to decrease exponentially with altitude following the profiles shown in Figure 14 of McClatchey et al. [13] (see

also Jones et al. [9]). Generalizing the 5- and 23-km curves in Figure 24, the aerosol extinction coefficient for Region II is specified as

$$b_{a,II} = \exp\,[-\,3.5157366 + (5\text{-}z/5\text{-}H)(3.5157366 + \ln\, b_I)] \tag{A-41}$$

for $H < z < 5$ km.

A-8.5.1.3 Within the top layer (Region III), the aerosol extinction coefficient approximately follows Figure 14, and is defined by

$$b_{a,III} = \exp\,[0.05937218\,(20\text{-}z) - 4.4063193] \tag{A-42}$$

for $5 \leq z \leq 20$ km.

A-8.5.2 The total aerosol transmission T_{TOT} is estimated along a slant path between the ground and the sensor. A look angle of 45° is assumed. Through a numerical approach, the individual transmissions within the various regions up to the specified sensor altitude are calculated by means of the equation

$$T_k = \prod_{i=1}^{N_k} \exp\,(-\,b_{k,i}\,D_{k,i}) \tag{A-43}$$

where k is the region number, N_k is the number of sublayers within a region k, and $D_{k,i}$ is the increment of slant path within region k and sublayer i. And T_{TOT} is based on the relationship

$$T_{TOT} = \prod_{k=1}^{m} T_k \tag{A-44}$$

where m is the number of regions required to reach the sensor altitude.

A-8.5.3 The total aerosol extinction coefficient b_{TOT} along the total slant path D is estimated from

$$b_{TOT} = -\ln T_{TOT}/D \tag{A-45}$$

A-8.5.4 Finally, the slant range visibility V_s is estimated by

$$V_s = C/b_{TOT} \tag{A-46}$$

A-8.6 Figure 35b is based on the relationship

$$V_s = V/R_v \tag{A-47}$$

where R_v is the ratio of the surface visibility to the slant range visibility.

A-8.7 The curve in Figure 35c is derived from Huschke's ([8], p. 8) equation

$$b_a = 3.352/V_s \tag{A-48}$$

A-8.8 The curves presented in Figure 35d are derived from the equations presented by Huschke ([8], p. 18).

A-8.9 Finally, the IR lock-on range LOR_{IR} based on environmental parameters is derived from the equation

$$LOR_{IR} = -\ln T_{IRT}/b_{TOT} \tag{A-49}$$

where T_{IRT} is the sensor's threshold transmittance. The above equation is represented by the curves in Figure 36.

Appendix B

RAPID TV METHOD ILLUSTRATION AND WORKSHEET

B-1 Introduction. This appendix provides an example of the application of the rapid TV support method. Both blank and completed worksheets are included.

B-2 Manual Visual Example. Consider a TV guided missile to be launched against an OD painted tank moving across a background of dry vegetation at 1000Z. The tank is approximately 30 feet in size. The following factors are known:

Location is Central Europe (48°N, 10°E) in mid-June.

The 1000Z forecast for the target area is: 2/10 SC035, 6 miles in haze.

The base of a low-level inversion is 1 km.

Solar elevation angle is determined to be approximately 61° (from Appendix E).

Launch altitude will be 4000 feet.

Illumination thresholds required by the target acquisition and lock-on sensors is 100 ft-lamberts.

The pilot will acquire the target visually (contrast threshold is 0.02; assume a minimum resolvable subtense angle equal to 1 mrad), and the TV guided missile will lock on to the target with a contrast threshold of 0.2. The magnification factor for the acquisition system is 1.0 and for the lock-on system is 3.0. The lock-on system's minimum resolvable subtense angle is equal to 1 mrad; magnification is not included in this angle.

The background reflectance (albedo) from Table 8 is approximately 0.26 and the target reflectance is approximately 0.05.

STEP 1: Determine whether the natural illumination will be sufficient for target acquisition.

a. Knowing the solar elevation angle to be 61° and that the sun is relatively unobscured (only 2/10 cloud cover), then from Table 6, the available natural illumination (I) is about 9570 ft-candles.

b. Since the skies are partly cloudy, no modification is made to the available illumination; thus, I_c is 9570 ft-candles.

c. Use the larger value of the target and background reflectances, and calculate the approximate brightness.

$$B \simeq (0.26)(9570) = 2488 \text{ foot-lamberts}$$

d. Since both the target acquisition sensor and the lock-on sensor require only 100 foot-lamberts of illumination and 2488 are available, the answer is YES, and the natural illumination is sufficient.

STEP 2: Determine slant range visibility.

a. The ratio of the surface visibility to the slant range visibility is obtained from Figure 24.

$$R_v = V/V_s \simeq 0.90$$

b. Now, using 6 statute miles surface visibility:

$$V_s = V/R_v = 6/0.9 = 6.7 \text{ statute miles slant range visibility}$$

STEP 3: Determine the maximum target acquisition range.

a. The inherent contrast (C_o) from Figure 25 is 0.81 (ignore the negative sign). This considers the reflectance of both the OD painted tank and the dry vegetation background, i.e.,

$$C_o = (R_t - R_b)/R_b$$

b. With an inherent contrast of 0.81 and a slant range visibility of 6.7 statute miles, the maximum visual (eye) detection range from Figure 26 is approximately 4.2 statute miles.

c. Since the acquisition sensor's magnification factor is 1.0, there is no magnification for visual acquisition. The effective target size is the actual target size.

d. From Figure 28, for a 30-foot tank, the maximum slant acquisition range based on target size is about 5.7 miles (use 1 mrad line).

e. Although the maximum slant acquisition range is 5.7 statute miles based on target size, we are limited to seeing the target at a range of 4.2 statute miles (i.e., this range considers the effects due to eye contrast threshold, atmospheric aerosols, and path radiance).

STEP 4: Determine the maximum lock-on range.

a. With the inherent contrast of 0.81 and a slant range visibility of 6.7 statute miles, the maximum LOR from Figure 27 is approximately 1.0 statute miles.

b. The actual target size (i.e., L = 30 ft) multiplied by the magnification factor for the lock-on sensor (i.e., M_{LO} = 3.0) results in an effective target size of 90 feet.

c. From Figure 28, for a 90-foot target, the maximum slant lock-on range based on target size above is 17.5 miles.

d. The smaller value of 1.0 statute miles is the maximum LOR.

STEP 5: Determine CLOS at TAR and LOR.

a. The summation of cloud cover below the sensor altitude is 2/10.

b. Since the target may be visually acquired at 4.2 statute miles and at an altitude of 4000 feet, Figure 29 provides the look angle of 10 degrees.

c. Similarly, the TV sensor may lock on to the target at 1.0 miles and at an altitude of 4000 feet. Figure 29 provides the dive angle for the TV sensor of 55 degrees.

d. Based on the dive angle, the sky cover below the sensor altitude, and Table 9, the CLOS probability at TAR is approximately 0.76 and the CLOS probability at LOR is 0.90.

B-3 Worksheet for TV PGMs.

TARGET LOCATION_____ TIME OVER TARGET_____/_____Z

INPUT DATA

Astronomical Data (Source: Appendix E or Air Almanac) SA_____(degrees)

Forecast Weather:

V_____(stat mi) H_____(km)

Clouds:	N (tenths)	b (ft)	t_c (class)
	_____	_____	_____
	_____	_____	_____
	_____	_____	_____
	_____	_____	_____

Target Data (Source: Wing Targeting Shop and/or Table 7):

R_t_____ L_____(ft) R_b_____

Sensor Data (Source: Wing Targeting Shop):

h_____(ft)

Acquisition Sensor	Lock-On Sensor
I_T_____(ft-lamberts)	I_T_____(ft-lamberts)
C_{TA}_____	C_{LO}_____

M_{TA}_____ α_{TA}_____(mrad) M_{LO}_____ α_{LO}_____(mrad)

Step 1: Is $B > I_T$?

a. Using SA and Table 6, find I. I=_____(ft-candles)

b. Determine illumination level with forecast cloud cover, I_c :

(1) For clear and partly cloudy skies, set $I_c = I$. Go to Step 1c.

I_c = _____(ft-candles)

(2) For cloudy skies, use t_c and Table 7 to find R_c. R_c = _____(use the maximum value of R_c if more than one t_c is available). Multiply I by R_c.

$I_c = I \cdot R_c$ = (_____) • (_____) = _____(ft-candles)

c. Calculate the brightness value B. Use the maximum value of R_t and R_b, and multiply this maximum value by I_c to obtain B.

B ≈ Maximum · I_c = (_____) · (_____) = _____ (ft-lamberts)

d. Is $B > I_T$? Acquisition Sensor: Yes_____ No_____

Lock-On Sensor: Yes_____ No_____

If no, target can not be seen. If yes, continue to Step 2.

Step 2: Determine slant range visibility V_s.

a. Enter Figure 24 with the inversion height H and sensor altitude h to find the ratio of the surface visibility to the slant range visibility R_v.

R_v = _____

b. Use the surface visibility V to find V_s by dividing V by R_v.

$V_s = V / R_v$ = (_____) / (_____) = _____ (stat mi)

Step 3: Determine maximum Target Acquisition Range (TAR).

a. Enter Figure 25 with the target reflectance R_t and the background reflectance R_b to determine the inherent target-to-background contrast C_o.

C_o = _____

b. Enter Figure 26 (if C_{TA} = 0.02) or Figure 27 (if C_{TA} = 0.2) with C_o and V_s to determine a first estimate of the TAR.

TAR = _____ (stat mi)

c. Determine effective target dimension L_{TA} by multiplying the actual target dimension L by the system magnification factor M_{TA}.

$L_{TA} = M_{TA} \cdot L$ = (_____) · (_____) = _____ (ft)

d. Enter Figure 28 with L_{TA} and sensor type (or minimum subtended angle necessary for target acquisition) to determine a second estimate of the TAR based on target size.

TAR = _____ (stat mi)

e. Compare the TAR of Step 3b with the TAR of Step 3d, and use the smaller value as the maximum TAR.

* TAR = _____ (stat mi) Verification TAR_____

Step 4: Determine maximum Lock-On Range (LOR).

a. Enter Figure 26 (if C_{LO} = 0.02) or Figure 27 (if C_{LO} = 0.2) with C_o and V_s to determine a first estimate of the LOR.

LOR = _____ (stat mi)

b. Determine effective target dimension L_{LO} by multiplying the actual target dimension L by the system magnification factor M_{LO}.

$L_{LO} = M_{LO} \cdot L$ = (_____) · (_____) = _____ (ft)

c. Enter Figure 28 with L_{LO} and sensor type (or minimum subtended angle necessary for lock on) to determine a second estimate of the LOR based on target size.

LOR = _____ (stat mi)

d. Compare the LOR of Step 4a with the LOR of Step 4c, and use the smaller value as the maximum LOR.

* LOR = _____(stat mi) Verification LOR = _____

Step 5: Determine probabilities of clear line-of-sight, CLOS, at the TAR and the LOR.

a. Find the summation of cloud cover N_T below sensor altitude. N_T=_____(tenths)

b. Enter Figure 29 with TAR and h, and determine look (dive) angle at TAR, θ_{TAR}.

θ_{TAR}=_____(degrees)

c. Enter Figure 29 with LOR and h, and determine look (dive) angle at LOR, θ_{LOR}.

θ_{LOR}=_____(degrees)

d. Enter Table 9 with θ_{TAR} and N_T, and determine cloud-free line-of-sight, CFLOS at the TAR. At and within this maximum TAR, CLOS = CFLOS.

* $CLOS_{TAR}$ = _____ Verification $CLOS_{TAR}$_____

e. Enter Table 9 with θ_{LOR} and N_T, and determine CFLOS (i.e., CLOS) at the LOR.

* $CLOS_{LOR}$ = _____ Verification $CLOS_{LOR}$ _____

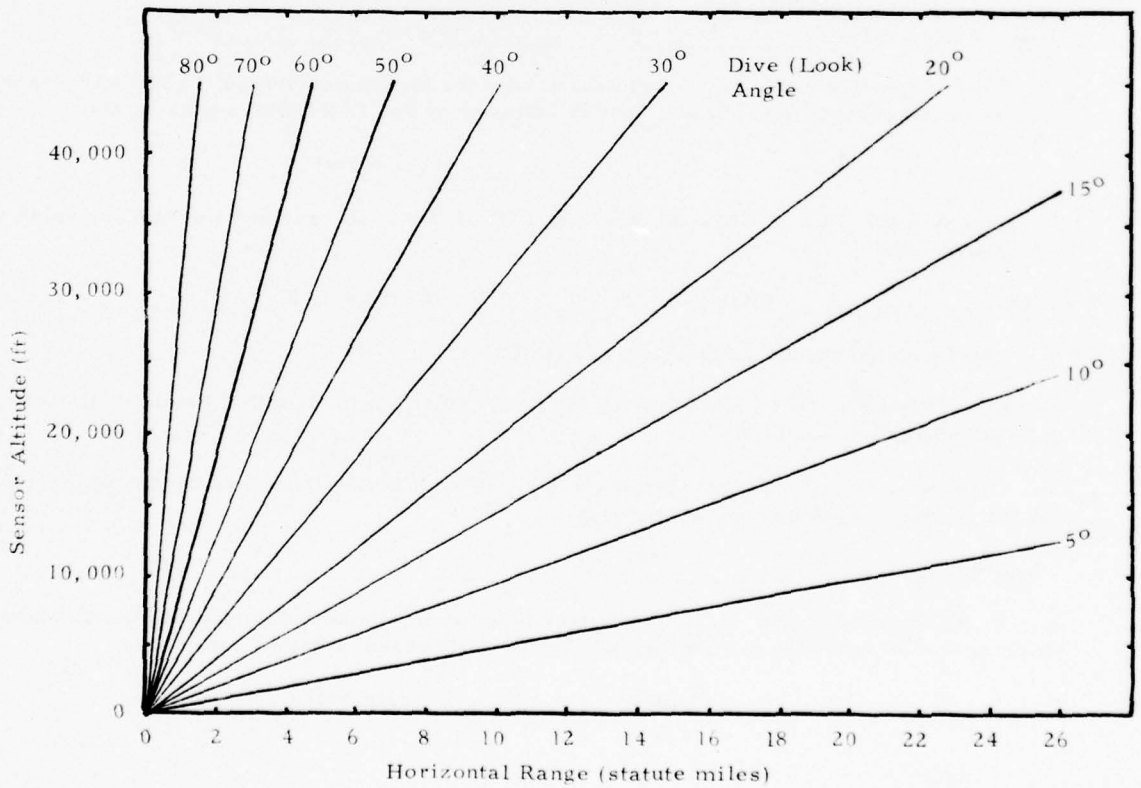

B-4 **Example of Completed Worksheet**

B-3 Worksheet for TV PGMs.

TARGET LOCATION 48°N 10°E TIME OVER TARGET 15 / 1000 Z

INPUT DATA

Astronomical Data (Source: Appendix E or Air Almanac) SA 61 (degrees)

Forecast Weather:

V 6 Hz (stat mi) H 1 (km)

Clouds:	N (tenths)	b (ft)	t_c (class)
	2	35	SC

Target Data (Source: Wing Targeting Shop and/or Table 7):

R_t 0.05 L 30 (ft) R_b 0.26

Sensor Data (Source: Wing Targeting Shop):

h 4000 (ft)

Acquisition Sensor	Lock-On Sensor
I_T 100 (ft-lamberts)	I_T 100 (ft-lamberts)
C_{TA} 0.02	C_{LO} 0.2
M_{TA} 1 α_{TA} 1 (mrad)	M_{LO} 3 α_{LO} 1 (mrad)

Step 1: Is $B > I_T$?

a. Using SA and Table 6, find I. I= 9570 (ft-candles)

b. Determine illumination level with forecast cloud cover, I_c :

(1) For clear and partly cloudy skies, set $I_c = I$. Go to Step 1c.

I_c = 9570 (ft-candles)

(2) For cloudy skies, use t_c and Table 7 to find R_c. R_c = _____ (use the maximum value of R_c if more than one t_c is available). Multiply I by R_c.

$I_c = I \bullet R_c$ = (_____) • (_____) = _____ (ft-candles)

c. Calculate the brightness value B. Use the maximum value of R_t and R_b, and multiply this maximum value by I_c to obtain B.

$B \approx \text{Maximum} \cdot I_c$ = (0.26) · (9570) 2488 (ft-lamberts)

d. Is $B > I_T$? Acquisition Sensor: Yes ✓ No _____

Lock-On Sensor: Yes ✓ No _____

If no, target can not be seen. If yes, continue to Step 2.

Step 2: Determine slant range visibility V_s.

a. Enter Figure 24 with the inversion height H and sensor altitude h to find the ratio of the surface visibility to the slant range visibility R_v.

R_v = 0.9

b. Use the surface visibility V to find V_s by dividing V by R_v.

$V_s = V / R_v$ = (6) / (0.9) = 6.7 (stat mi)

Step 3: Determine maximum Target Acquisition Range (TAR).

a. Enter Figure 25 with the target reflectance R_t and the background reflectance R_b to determine the inherent target-to-background contrast C_o.

C_o 0.81

b. Enter Figure 26 (if C_{TA} = 0.02) or Figure 27 (if C_{TA} = 0.2) with C_o and V_s to determine a first estimate of the TAR.

TAR = 4.2 (stat mi)

c. Determine effective target dimension L_{TA} by multiplying the actual target dimension L by the system magnification factor M_{TA}.

$L_{TA} = M_{TA} \cdot L$ = (1) · (30) = 30 (ft)

d. Enter Figure 28 with L_{TA} and sensor type (or minimum subtended angle necessary for target acquisition) to determine a second estimate of the TAR based on target size.

TAR = 5.7 (stat mi)

e. Compare the TAR of Step 3b with the TAR of Step 3d, and use the smaller value as the maximum TAR.

* TAR = 4.2 (stat mi) Verification TAR _____

Step 4: Determine maximum Lock-On Range (LOR).

a. Enter Figure 26 (if C_{LO} = 0.02) or Figure 27 (if C_{LO} = 0.2) with C_o and V_s to determine a first estimate of the LOR.

LOR = 1.0 (stat mi)

b. Determine effective target dimension L_{LO} by multiplying the actual target dimension L by the system magnification factor M_{LO}.

$L_{LO} = M_{LO} \cdot L$ = (3) · (30) = 90 (ft)

c. Enter Figure 28 with L_{LO} and sensor type (or minimum subtended angle necessary for lock on) to determine a second estimate of the LOR based on target size.

LOR = 17.5 (stat mi)

d. Compare the LOR of Step 4a with the LOR of Step 4c, and use the smaller value as the maximum LOR.

* LOR = 1.0 (stat mi) Verification LOR = _____

Step 5: Determine probabilities of clear line-of-sight, CLOS, at the TAR and the LOR.

a. Find the summation of cloud cover N_T below sensor altitude. N_T= 2 (tenths)

b. Enter Figure 29 with TAR and h, and determine look (dive) angle at TAR, θ_{TAR}.

θ_{TAR} = 10 (degrees)

c. Enter Figure 29 with LOR and h, and determine look (dive) angle at LOR, θ_{LOR}.

θ_{LOR} = 55 (degrees)

d. Enter Table 9 with θ_{TAR} and N_T, and determine cloud-free line-of-sight, CFLOS at the TAR. At and within this maximum TAR, CLOS = CFLOS.

* $CLOS_{TAR}$ = 0.76 Verification $CLOS_{TAR}$ _____

e. Enter Table 9 with θ_{LOR} and N_T, and determine CFLOS (i.e., CLOS) at the LOR.

* $CLOS_{LOR}$ = 0.9 Verification $CLOS_{LOR}$ _____

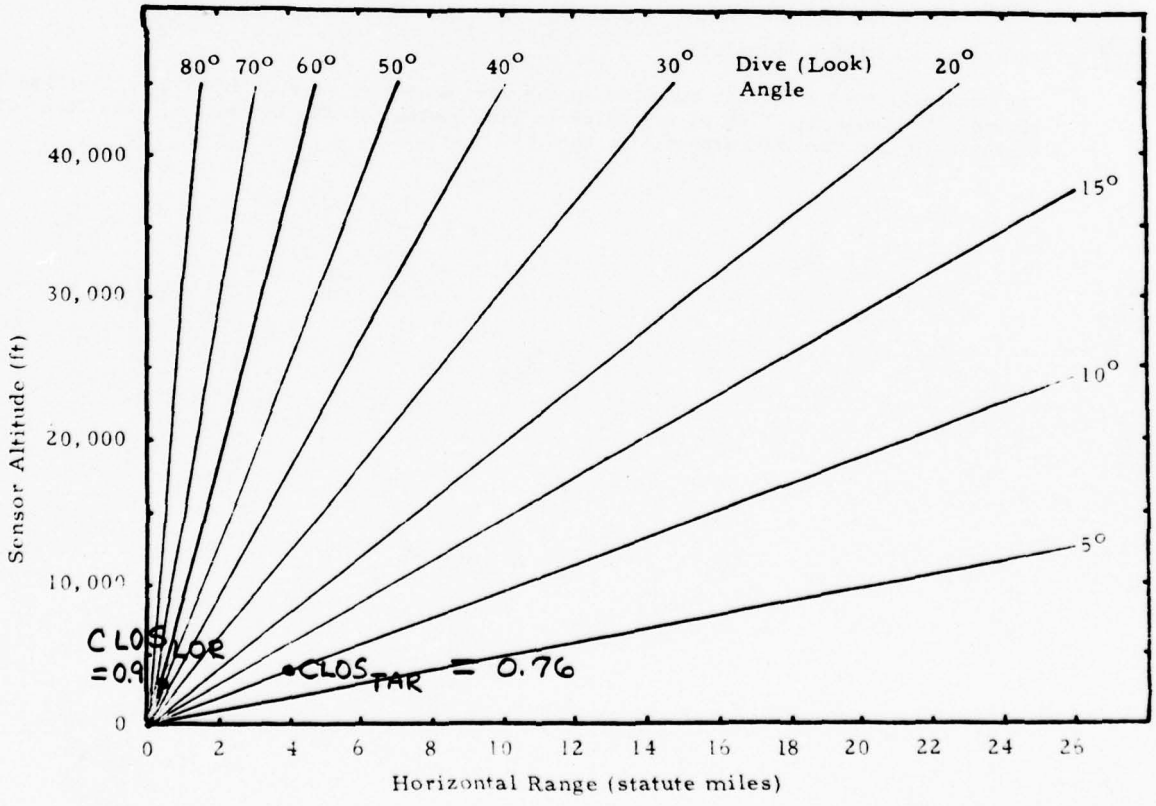

Appendix C

RAPID LASER METHOD ILLUSTRATION AND WORKSHEET

C-1 Introduction. This appendix provides an example of the application of the rapid laser support method. Both blank and completed worksheets are included.

C-2 Manual Laser Example. Using the data given for the manual visual illustration, determine the maximum practical laser lock-on range for a YAG - neodynium laser designator operating at a wavelength of 1.06 μm and the CLOS probability associated with the lock-on range.

STEP 1: Determine LLOR.

a. Assume the laser designator and receiver (sensor) are collocated at approximately the same altitude. We know the surface visibility is 6 miles in haze. The base of a low-level inversion is 1 km.

b. Using Figure 30 and an altitude of 4000 feet, we find the horizontal component (ground range) of the LLOR to be about 9.5 km.

c. Using the ground range and Figure 33, the LLOR is found to be 5.9 statute miles.

STEP 2: Determine the maximum practical LLOR.

If the target acquisition (TA) device is a visual sensor, the computed LLOR from Step 1 must be compared to the visual TAR in order to determine the minimum value (i.e., maximum practical LLOR). From the visual acquisition problem (Step 3, Appendix B), the TAR for the pilot's eyes was 4.2 miles. Therefore, in this case, the LLOR is limited by the pilot's eyes to 4.2 miles. If the pilot were using some other type of acquisition sensor, then the target acquisition ranges for these sensors must be compared to the computed LLOR. This could result in the maximum practical LLOR being smaller in value than the LLOR calculated above.

STEP 3: Determine the CLOS probability.

The probability of a CLOS is computed in the same manner as in the visual example (Step 5, Appendix B) except the LLOR of 4.2 miles is used instead of the visual TAR. The look (dive) angle is 10^{o} and the CLOS probability is 0.76.

C-3 Worksheet for Laser PGMs.

TARGET LOCATION _____ TIME OVER TARGET _____ / _____ Z

INPUT DATA

Forecast Weather:

V _____ (stat mi) Visibility Restriction _____

Clouds:	N (tenths)	b (ft)	t_c (class)
	_____	_____	_____
	_____	_____	_____
	_____	_____	_____
	_____	_____	_____

Low-Level Inversion Yes No (circle)

Sensor/Designator Data (Source: Wind Targeting Shop):

h _____ (ft) h_d _____ (ft)

Step 1: Determine laser lock-on range LLOR.

a. Are designator and receiver at approximately the same altitude?
(1) If NO, use Figure 32.
(2) If YES, choose (a) or (b) below:
(a) If visibility is restricted or a low level inversion is present, use Figure 30.
(b) Otherwise, use Figure 31.

Note Figure Number: _____

b. Using the figure number determined above, the sensor altitude h, and the surface visibility V, enter the appropriate figure and find the horizontal component (ground range) of the laser lock-on range.

Ground Range _____ (km)

c. Enter Figure 33 with sensor altitude h and ground range, and find the laser lock-on range.

* LLOR _____ (stat mi)

Step 2: Determine the maximum practical LLOR.

a. If a visual target acquisition device is used, compute the visual TAR using Appendix B (Steps 1, 2 and 3). If an IR target acquisition device is used, compute the IR TAR using the LOR_{IR} method from Appendix D (Steps 1 and 2).

TAR _____ (stat mi)

b. Select the minimum value of the TAR (visual or IR) and the LLOR from Step 1 above as the maximum practical LLOR.

** LLOR _____ (stat mi) Verification LOR _____

Step 3: Determine the CLOS probability for the maximum practical LLOR.

a. Find the summation of cloud cover N_T below sensor altitude. N_T = _____ (tenths)

b. Enter Figure 29 with the maximum practical LLOR and h, and determine look (dive) angle at LLOR.

θ_{LLOR} = _____(degrees)

c. Enter Table 9 with θ_{LLOR} and N_T, and determine CFLOS (CLOS) at LLOR.

* $CLOS_{LLOR}$ = _____ Verification $CLOS_{LOR}$_____

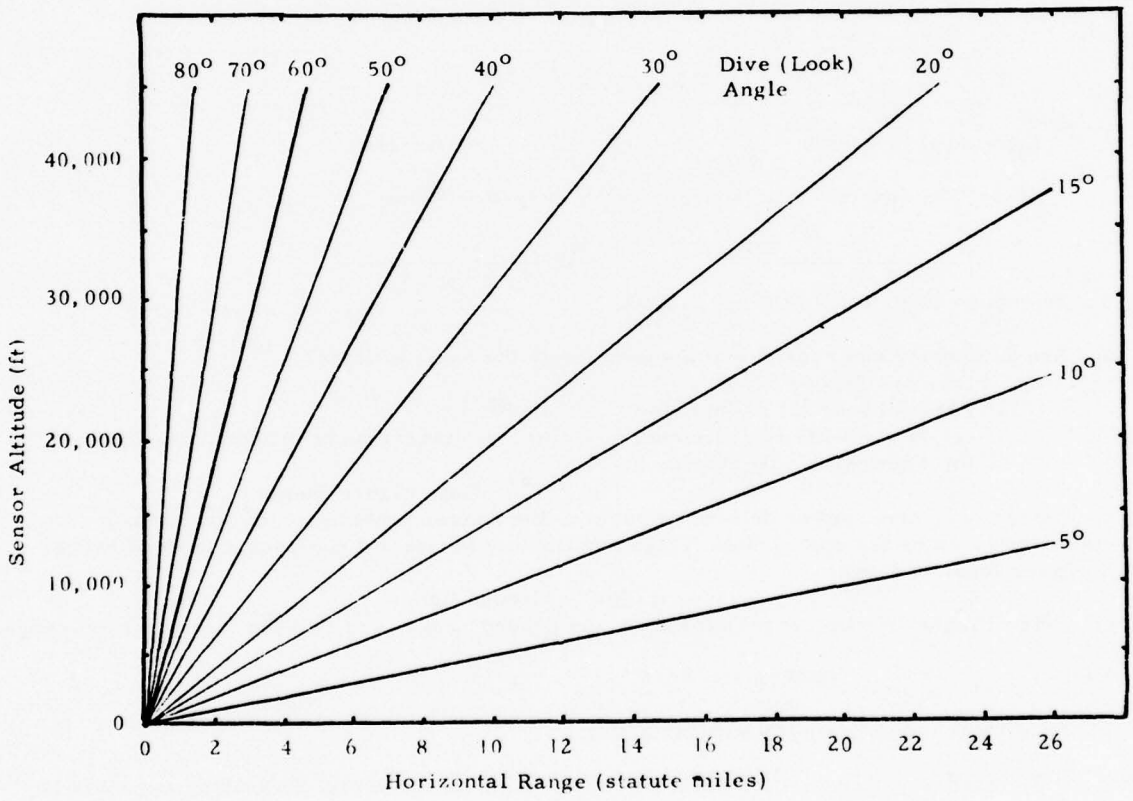

C-4 Example of Completed Worksheet.

C-3 Worksheet for Laser PGMs.

TARGET LOCATION CNTRL EUROPE (48°N) TIME OVER TARGET 05 / 1000 Z

INPUT DATA

Forecast Weather:

V 6 (stat mi) Visibility Restriction HZ

Clouds:	N (tenths)	b (ft)	t_c (class)
	2	35	SC

Low-Level Inversion (Yes) No (circle)

Sensor/Designator Data (Source: Wind Targeting Shop):

h 4,000 (ft) h_d 4,000 (ft)

Step 1: Determine laser lock-on range LLOR.

a. Are designator and receiver at approximately the same altitude?
(1) If NO, use Figure 32.
(2) If YES, choose (a) or (b) below:
(a) If visibility is restricted or a low level inversion is present, use Figure 30.
(b) Otherwise, use Figure 31.

Note Figure Number: 30

b. Using the figure number determined above, the sensor altitude h, and the surface visibility V, enter the appropriate figure and find the horizontal component (ground range) of the laser lock-on range.

Ground Range 9.5 (km)

c. Enter Figure 33 with sensor altitude h and ground range, and find the laser lock-on range.

* LLOR 5.9 (stat mi)

Step 2: Determine the maximum practical LLOR.

a. If a visual target acquisition device is used, compute the visual TAR using Appendix B (Steps 1, 2 and 3). If an IR target acquisition device is used, compute the IR TAR using the LOR_{IR} method from Appendix D (Steps 1 and 2).

TAR 4.2 (stat mi)

b. Select the minimum value of the TAR (visual or IR) and the LLOR from Step 1 above as the maximum practical LLOR.

** LLOR 4.2 (stat mi) VERIFICATION LOR _____

Step 3: Determine the CLOS probability for the maximum practical LLOR.

a. Find the summation of cloud cover N_T below sensor altitude. N_T = 2 (tenths)

b. Enter Figure 29 with the maximum practical LLOR and h, and determine look (dive) angle at LLOR.

θ_{LLOR} = 10 (degrees)

c. Enter Table 9 with θ_{LLOR} and N_T, and determine CFLOS (CLOS) at LLOR.

* $CLOS_{LLOR}$ = 0.76 VERIFICATION $CLOS_{LOR}$ _____

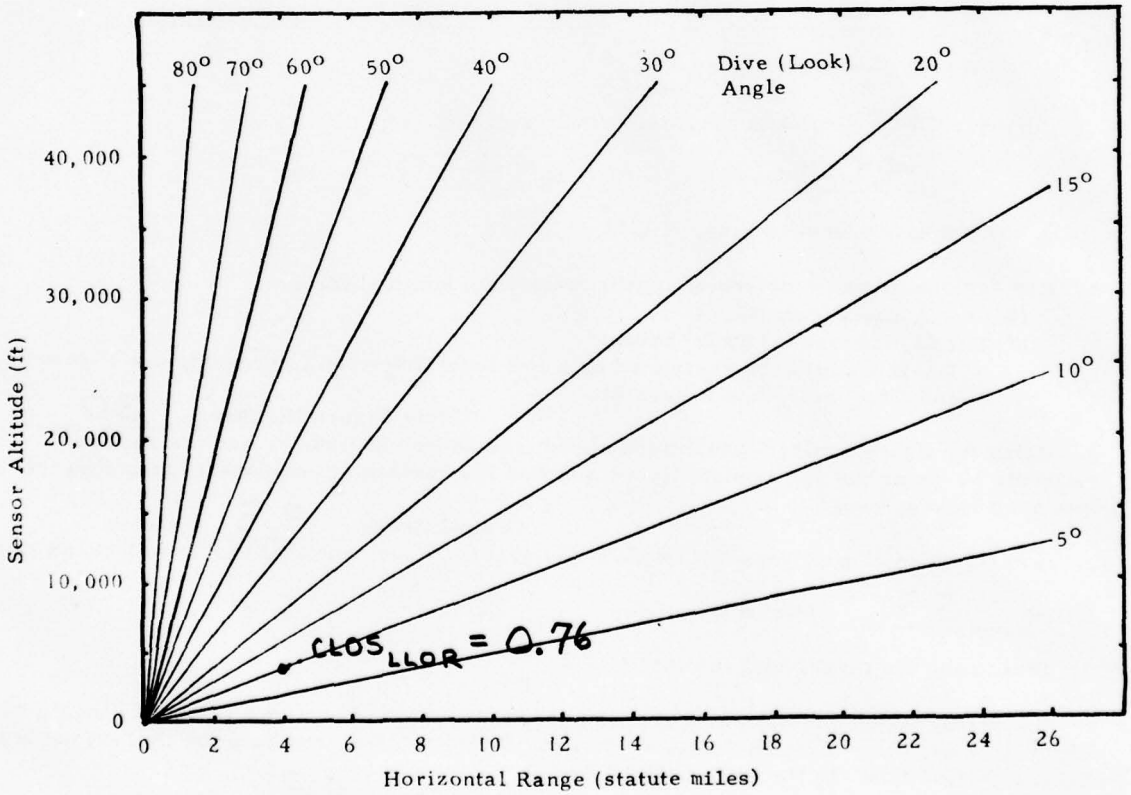

Appendix D

RAPID IR (8-12 μm) METHOD ILLUSTRATION AND WORKSHEET

D-1 Introduction. This appendix provides an example of the application of the rapid IR support method. Both blank and completed worksheets are included.

D-2 Manual IR Example. The data given below will be useful in determining the lock-on range and clear line-of-sight probability for an active tank using a forward looking infrared (FLIR) detector:

The target location is Central Europe (48°N, 10°E) on 15 June 1978 at 1000Z.

The vertically-averaged temperature (below inversion) is 23°C.

The vertically-averaged relative humidity (below inversion) is 70%.

Cloud forecast is 2/10 SC at 3500 feet.

Surface visibility is 6 statute miles in haze with haze layer topping at 1 km.

Radiative temperature contrast between tank and background is 10°C.

The size of the hot spot on the tank is 10 feet.

The sensor, located at 4000 feet AGL, is capable of detecting a minimum temperature contrast of 2.5°C, has a magnification factor of 3, and a minimum resolvable subtense angle of 1 mrad.

STEP 1: Determine the threshold transmittance T_{IRT}:

$$T_{IRT} = \Delta T^*_{RT}/\Delta T^*_o = 2.5/10 = 0.25$$

STEP 2: Find the maximum IR lock-on range LOR_{IR}.

a. Enter Figure 34a with $\overline{T}$ and $\overline{RH}$ to find $\overline{T}_d$ (the dew-point temperature). $\overline{T}_d$ equals 17°C. With $\overline{T}_d$ known, enter Figure 34b with $\overline{T}_d$ and h to obtain absolute humidity (equals 15.0 gm^{-3}). Enter Figure 34c with this value and obtain the molecular absorption coefficient of water vapor b_m at right of graph. With this value (b_m = 0.086 km^{-1}) and $\overline{T}$, enter Figure 34d to obtain the sum of the molecular and continuum absorption coefficients (b_w). Note the sum (b_w = 0.25 km^{-1}) on the worksheet.

b. Enter Figure 35a with the inversion height (or top of haze layer) (H) and the sensor altitude (h) to determine the ratio (R_V). With this value of R_V (R_V = 0.9) and V, enter Figure 35b to determine V_S. With this value of V_S (V_S + 6.5 stat mi), enter Figure 35c to determine the aerosol extinction coefficient at visible wavelengths on the right side of graph. Finally, with this value (0.32 km^{-1}) and $\overline{RH}$, determine the aerosol extinction coefficient for the 8-12 μm band (b_a). Note this value (b_a = 0.0077 km^{-1}) on the worksheet.

c. Sum the values of b_w and b_a to obtain the total extinction coefficient b_{TOT}. Note the result (b_{TOT} = 0.2577 km^{-1}) on the worksheet.

d. Enter Figure 36 with b_{TOT} and the threshold transmittance T_{IRT} obtained from Step 1. The maximum lock-on range LOR_{IR} based on environmental parameters is determined from this figure. LOR_{IR} = 5.5 km (or 3.3 stat mi).

e. Is the first estimate of lock-on range (Step 2d) within the maximum detection range of the target based on the target's size? Knowing the active target size is 10 feet and the sensor magnification factor is 3.0, effective target size is 30 feet. From Figure 28 (using α_{LO} = 1 mrad), the maximum detection range due to size is 6 statute miles.

f. Thus, the maximum LOR_{IR} equals 3.3 statute miles and is not limited by the target size resolution of the sensor.

STEP 3: Find the CLOS probability if the sensor could acquire the target at the LOR_{IR}.

a. Entering Figure 29 with a LOR_{IR} of 5.5 statute miles and an altitude of 4000 feet gives a look angle of 8°.

b. With a look angle of 8° and sky cover of 2/10 below the sensor, Table 9 gives a CFLOS probability of 0.74. At a lock-on slant range of 3.3 statute miles, this CFLOS probability is also the CLOS probability.

D-3 Worksheet for IR PGMs.

TARGET LOCATION _____ TIME OVER TARGET _____Z

INPUT DATA

Forecast Weather:

V_____(stat mi) H_____(km AGL)

Clouds:	N(tenths)	b (ft)	t_c (class)
	_____	_____	_____
	_____	_____	_____
	_____	_____	_____
	_____	_____	_____

$\overline{T}$_____(degrees Celsius) $\overline{T}_d$_____(degrees Celsius)

or $\overline{RH}$_____(percent)

Target Data (Source: Wing Targeting Shop or Customer/Observation/Experience):

ΔT_o^* _____(degrees Celsius) L_____(ft)

Sensor Data (Source: Customer or Wing Targeting Shop):

ΔT_{RT}^*_____(degrees Celsius) h_____(ft AGL)

M_{LO}_____ α_{LO}_____(mrad)

Step 1: Calculate threshold transmittance T_{IRT}.

$T_{IRT} = \Delta T_{RT}^*/\Delta T_o^*$ = (_____)/(_____) = _____

Step 2: Find the maximum IR lock-on range LOR_{IR}.

a. With $\overline{T}$ and $\overline{T}_d$ (or vertically averaged relative humidity), determine the water vapor absorption coefficient b_w from Figure 34

b_w = _____(km^{-1})

b. With H, h, V and $\overline{RH}$ (may be found in Figure 34a, given $\overline{T}$ and $\overline{T}_d$), determine the aerosol extinction coefficient b_a from Figure 35.

b_a = _____(km^{-1})

c. Add $b_w + b_a$ to obtain total extinction coefficient b_{TOT}.

b_{TOT} = (_____) + (_____) = _____(km^{-1})

d. Enter Figure 36 with b_{TOT} and T_{IRT} from Step 1 to determine LOR_{IR}.

* LOR_{IR} = _____(stat mi) _____(km)

e. Determine the effective target size L_{LO} and maximum detection range based on L_{LO} and α_{LO}.

$L_{LO} = M_{LO} \cdot L$ = (_____) · (_____) = _____(ft)

Enter Figure 28 with L_{LO} and α_{LO} and determine the maximum detection range (a second estimate of the LOR_{IR}).

* LOR_{IR} = _____(stat mi) _____(km)

f. **Select the minimum** LOR_{IR} value from Step 1d and Step 1e.

** LOR_{IR} = _____(stat mi) _____(km) VERIFICATION LOR_{IR}_____

Step 3: Determine the CLOS probability for this LOR_{IR}.

a. Using LOR_{IR} and h with Figure 29, determine sensor look (dive) angle θ_{LOR}.

θ_{LOR} = _____(degrees)

b. Find the summation of cloud cover N_T below sensor altitude.

N_T = _____(tenths)

c. Enter Table 9 with θ_{LOR} and N_T, and determine CFLOS (CLOS) at LOR_{IR}.

** $CLOS_{LOR}$ = _____ VERIFICATION $CLOS_{LOR}$_____

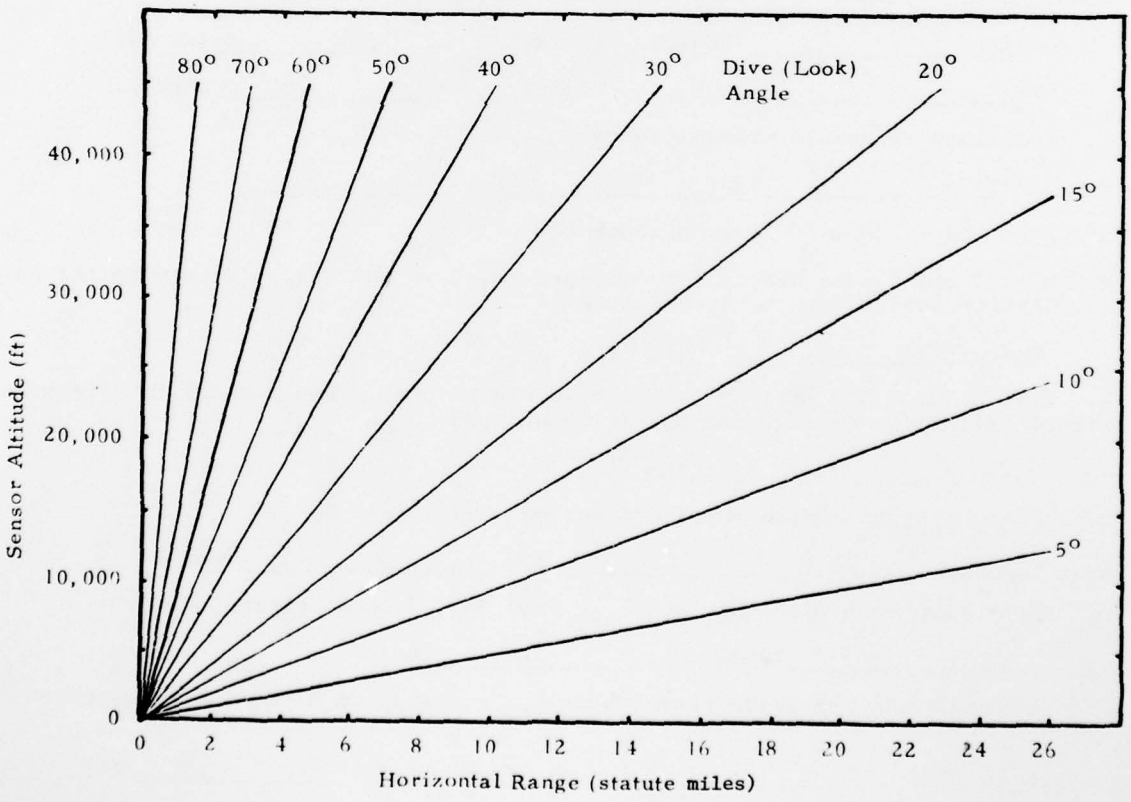

D-4 Example of Completed Worksheet

D-3 Worksheet for IR PGMs.

TARGET LOCATION 48°N 10°E TIME OVER TARGET 15/1000 Z

INPUT DATA

Forecast Weather:

V 6 (stat mi) H 1 (km AGL)

Clouds:	N(tenths)	b (ft)	t_c (class)
	2	3500	SC

$\overline{T}$ 23 (degrees Celsius) $\overline{T}_d$ 17 (degrees Celsius)

or $\overline{RH}$ 70 (percent)

Target Data (Source: Wing Targeting Shop or Customer/Observation/Experience):

ΔT^*_o 10 (degrees Celsius) L 10 (ft)

Sensor Data (Source: Customer or Wing Targeting Shop):

ΔT^*_{RT} 2.5 (degrees Celsius) h 4,000 (ft AGL)

M_{LO} 3 α_{LO} 1 (mrad)

Step 1: Calculate threshold transmittance T_{IRT}.

$T_{IRT} = \Delta T^*_{RT}/\Delta T^*_o$ = (2.5)/(10) = 0.25

Step 2: Find the maximum IR lock-on range LOR_{IR}.

a. With $\overline{T}$ and $\overline{T}_d$ (or vertically averaged relative humidity), determine the water vapor absorption coefficient b_w from Figure 34

b_w = 0.25 (km^{-1})

b. With H, h, V and $\overline{RH}$ (may be found in Figure 34a, given $\overline{T}$ and $\overline{T}_d$), determine the aerosol extinction coefficient b_a from Figure 35.

b_a = 0.0077 (km^{-1})

c. Add $b_w + b_a$ to obtain total extinction coefficient b_{TOT}.

b_{TOT} = (0.25) + (0.0077) = 0.2577 (km^{-1})

d. Enter Figure 36 with b_{TOT} and T_{IRT} from Step 1 to determine LOR_{IR}.

* LOR_{IR} = 3.3 (stat mi) 5.5 (km)

e. Determine the effective target size L_{LO} and maximum detection range based on L_{LO} and α_{LO}.

$L_{LO} = M_{LO} \cdot L$ = (3.0) · (10) = 30 (ft)

Enter Figure 28 with L_{LO} and α_{LO} and determine the maximum detection range (a second estimate of the LOR_{IR}).

* LOR_{IR} = 6.0 (stat mi) 9.6 (km)

f. **Select the minimum LOR_{IR} value from Step 1d and Step 1e.**

** LOR_{IR} = 3.3 (stat mi) 5.5 (km) VERIFICATION LOR_{IR} _____

Step 3: Determine the CLOS probability for this LOR_{IR}.

a. Using LOR_{IR} and h with Figure 29, determine sensor look (dive) angle θ_{LOR}.

θ_{LOR} = 14 (degrees)

b. Find the summation of cloud cover N_T below sensor altitude.

N_T = 2 (tenths)

c. Enter Table 9 with θ_{LOR} and N_T, and determine CFLOS (CLOS) at LOR_{IR}.

** $CLOS_{LOR}$ = 0.79 VERIFICATION $CLOS_{LOR}$ _____

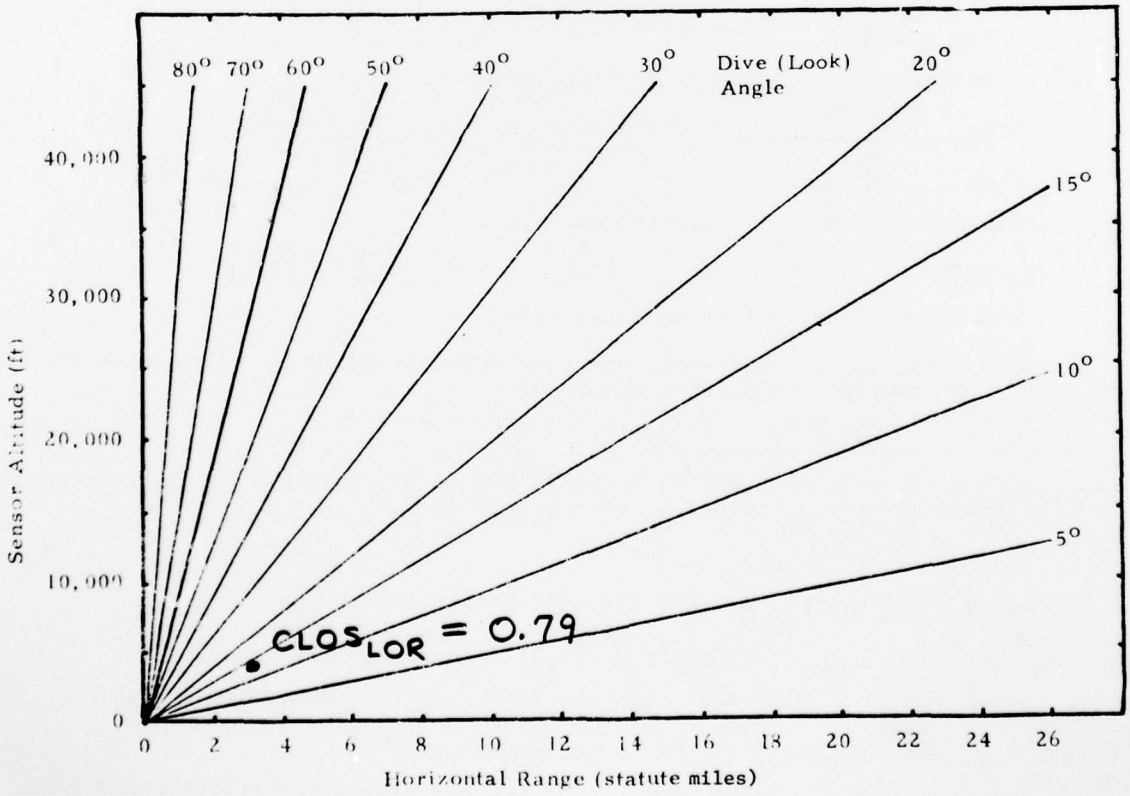

Appendix E

COMPUTATION OF SOLAR ELEVATION ANGLE

E-1 Introduction. The following graphical method for computing solar elevation angle (degrees above horizon) is based on Table 169 and (1) of Table 170 of List [11]. Calculations consider mean solar time only.

E-2 Input Data. Data required to compute solar elevation angle (SA) are:

Date (Greenwich Mean Time (GMT))

Time (Greenwich Mean Time (GMT))

Latitude (ϕ)

Longitude

E-3 Procedure (use worksheet in Para. E-5).

a. Enter Figure E-1 with date to find solar declination (δ). Follow date down graph to curve. From intersection with curve, follow graph to left to solar declination. Record solar declination on worksheet.

b. Enter Figure E-2 with the time and longitude to find local hour angle (A).

(1) Enter Figure E-2a with the GMT time and follow to right to curve. This intersection relates GMT time to the Greenwich hour angle (read values at upper edge of figure). From intersection with curve, follow graph down to lower graph edge.

(2) Using the Greenwich hour angle and the longitude, enter Figure E-2b to find local hour angle (A). Follow the Greenwich hour angle down the graph to the curve representing the longitude. From the intersection with the curve, move left along the graph until the local hour angle is determined. Record local hour angle on worksheet.

c. Enter Figure E-3 with solar declination, local hour angle, and latitude to find solar elevation angle.

(1) Figure E-3a produces two values. The curve labeled sin δ is used with Figure E-3b while the curve labeled cos δ is used with Figure E-3c. Enter Figure E-3a from the left with solar declination and intersect the curve labeled sin δ. Record value of sin δ (value at top of graph). With the same solar declination, intersect the curve labeled cos δ. Record value of cos δ (value at bottom of graph).

(2) With the value of sin δ from Figure E-3a, enter Figure E-3b and move upward until the appropriate latitude curve is intersection (interpolate linearly if necessary). Record value of sin ϕ sin δ.

(3) With the value of cos δ from Figure E-3a, enter Figure E-3c and move downward until the appropriate latitude curve is intersected (interpolate linearly if necessary). Use the determined value of cos ϕ cos δ and move to the right into Figure E-3d until the local hour angle is intersected. Record value of cos ϕ cos δ cos A.

(4) Finally, using the value just determined and the result of Figure E-3b (sin ϕ sin δ), enter Figure E-3e to find solar elevation angle (SA). Record solar elevation angle (SA).

E-4 Comments. More accurate values of solar elevation angle can be calculated using the Air Almanac with List's Equation (1). The true local hour angle would be calculated in lieu of the mean local hour angle in order to achieve better accuracy. However, for the purpose intended in this text, the described technique is generally adequate. In most daylight cases, the calculation of solar elevation angle to later infer solar illumination is probably unnecessary since adequate illumination will be available for most TV systems. However, near sunrise and sunset, and under extremely heavy cloudiness, calculations of solar elevation should be considered.

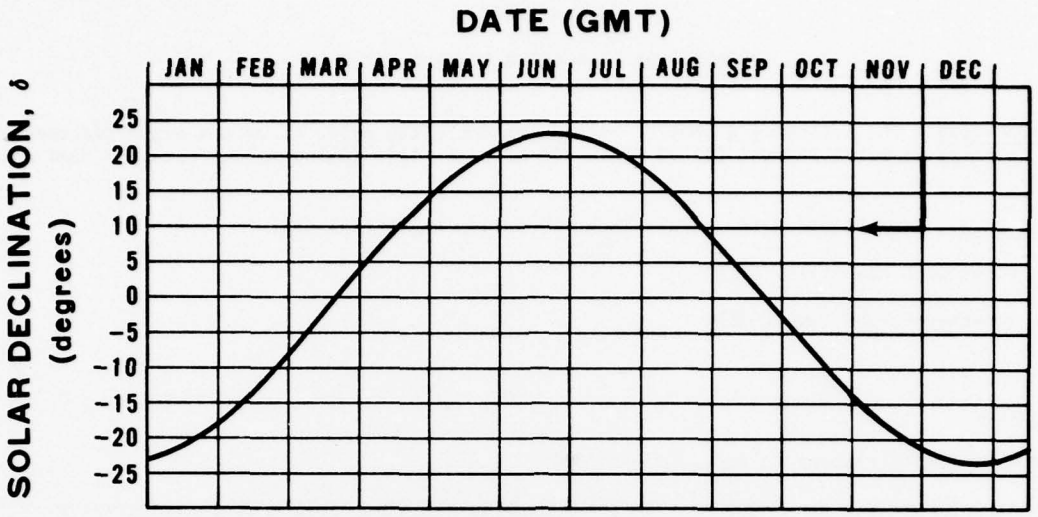

Figure E-1. Solar Declination as a Function of Data (Greenwich Mean Time).

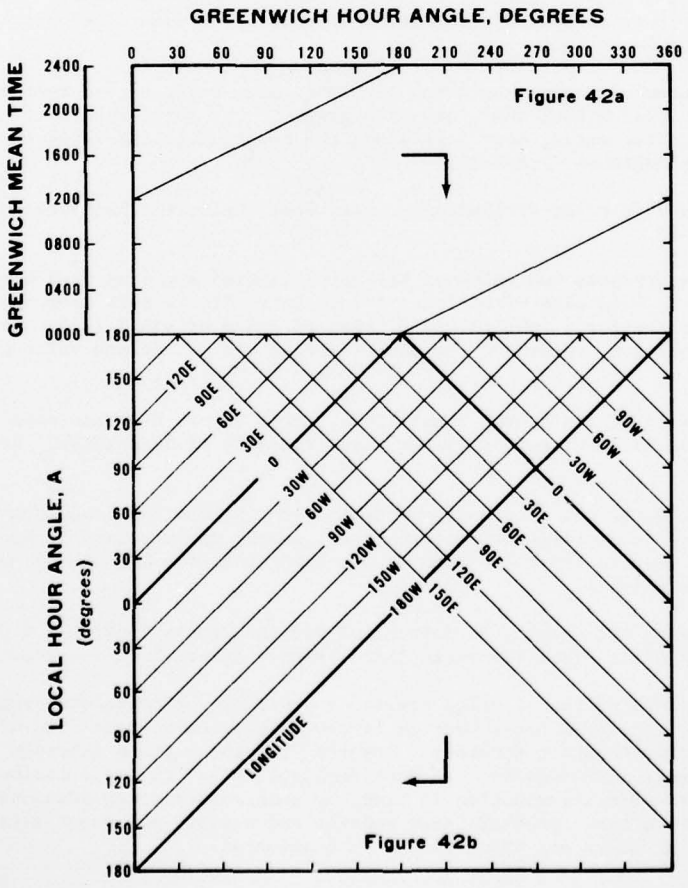

Figure E-2. Local Hour Angle as a Function of Greenwich Mean Time and Longitude.

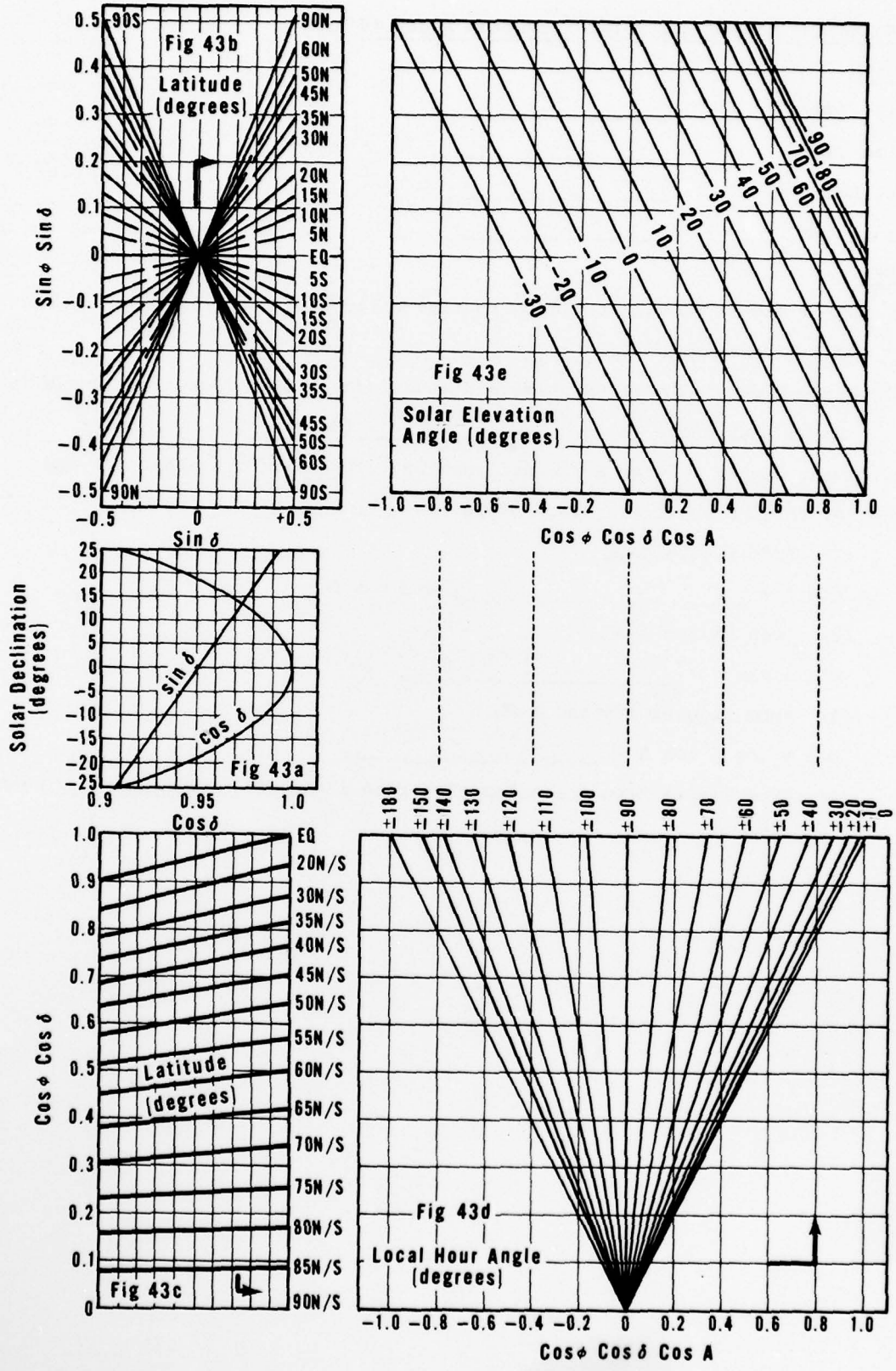

Figure E-3. Solar Elevation Angle as a Function of Solar Declination, Latitude, and Local Hour Angle.

E-5 Worksheet to Compute Solar Elevation Angle (SA).

INPUT DATA

Date (GMT) _____

Time (GMT) _____

Latitude (ϕ) _____

Longitude _____

PROCEDURE

a. Enter Figure E-1 with GMT date to find solar declination.

Solar declination (δ) _____(degrees).

b. Enter Figure E-2 with GMT time and longitude to find local hour angle (A).

Local hour angle (A) _____(degrees).

c. Enter Figure E-3 with solar declination (δ), local hour angle (A) and latitude (ϕ) to find solar elevation angle.

(1) From Figure E-3a,

$\sin \delta$ = _____, and $\cos \delta$ = _____.

(2) From Figure E-3b,

$\sin \phi \sin \delta$ = _____.

(3) From Figures E-3c and E-3d,

$\cos \phi \cos \delta \cos A$ = _____.

(4) From Figure E-3e, the solar elevation angle (SA) = _____(degrees).

E-6 Example of Completed Worksheet

E-5 Worksheet to Compute Solar Elevation Angle (SA).

INPUT DATA

Date (GMT) 15 JUN 78

Time (GMT) 1000 Z

Latitude (ϕ) 48 °N

Longitude 10 °E

PROCEDURE

a. Enter Figure E-1 with GMT date to find solar declination.

Solar declination (δ) + 23.3 (degrees).

b. Enter Figure E-2 with GMT time and longitude to find local hour angle (A).

Local hour angle (A) 20 (degrees).

c. Enter Figure E-3 with solar declination (δ), local hour angle (A) and latitude (ϕ) to find solar elevation angle.

(1) From Figure E-3a,

sin δ = 0.4, and cos δ = 0.92.

(2) From Figure E-3b,

sin ϕ sin δ = 0.295.

(3) From Figures E-3c and E-3d,

cos ϕ cos δ cos A = 0.58.

(4) From Figure E-3e, the solar elevation angle (SA) = 61 (degrees).

Appendix F

THIRD WEATHER WING SUPPORT FOR E-O SYSTEMS

Third Weather Wing (3WW) provides weather support to the Strategic Air Command (SAC) and has expanded their activities into providing weather support for E-O systems including the TV-GBU-15. Third Weather Wing has produced handouts to SAC and 3WW units on the subject of: "Meteorological Support for Electro-Optical Systems," "TV-GBU-15 SAC Support Seminar," "Impact of Atmospheric Considerations upon Military Electro-Optical Systems of the 1980s and 1990s," and "Meteorological Effects on Laser Transmission." In addition, a 3WW seminar is available on 35mm slides with cassette tape. Also, a SAC Pamphlet on weather support for the TV-GBU-15 Limited Operational Capability is available. This pamphlet describes the 3WW technique for forecasting CFLOS/LOR.

Office of primary responsibility for these documents is 3WW/DNC (or SAC/DOW), Offutt AFB, NE 68113.

GLOSSARY OF TERMS

ABLATION: The deterioration or erosion of a weapon's surface due to impaction with and abrasion by precipitation, aerosols, hail, and the like.

ABSOLUTE HUMIDITY: In a system of moist air, the ratio of the mass of water vapor present to the volume occupied by the mixture (Huschke [7]). Expressed usually in grams per cubic meter.

ABSORPTION: The process by which incident radiant energy is retained by a substance (Huschke [7]).

ABSORPTION COEFFICIENT: A measure of the decrease in radiation per unit distance (volume absorption coefficient) or per unit mass (mass absorption coefficient) due to absorption as the radiation passes through the atmosphere (or other medium).

ABSORPTIVITY: A measure of the amount of radiant energy absorbed by a given substance of definite dimensions; the ratio of the amount of radiant energy absorbed to the total amount incident upon that substance (Huschke [7]).

ACQUISITION: The detection, recognition, and identification of a target in sufficient detail to permit the effective employment of weapons.

ACQUISITION, AIDED VISUAL: Acquisition by means of direct viewing optical devices or by means of devices that present target information to an observer on a separate display.

ACQUISITION, DIRECT VISUAL: Acquisition by use of the unaided eye.

ACQUISITION SYSTEM: A system that assists an observer in one or more of the target acquisition cycle tasks.

ACTIVE GUIDANCE SYSTEM: (See Sensor, Active.)

AEROSOL: Small particles suspended within the air. Haze, smoke, and some small fog/cloud droplets are examples of aerosols. Water droplets are sometimes referred to as wet aerosols.

ALBEDO: The ratio of the amount of electromagnetic radiation reflected by a body compared to the amount incident upon it. Usually, the radiation is integrated over the visible spectrum, solar spectrum or the entire electromagnetic spectrum.

ANISOTROPIC: Not isotropic. Radiation is directionally dependent.

ANOMALOUS PROPAGATION: The transmission of energy when it arrives at a destination via a path significantly different from the normally expected path (Huschke [7]).

ATTACK ANGLE: In the context of targeting, the angle formed by the line passing through the longitudinal axis of the aircraft (or the line parallel to the aircraft flight path) and the horizontal plane.

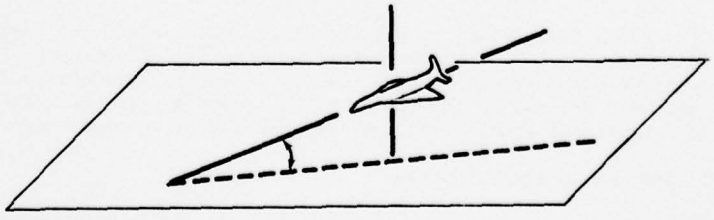

ATTENUATION: The decrease in intensity of a signal, beam, or wave as a result of absorption of energy and of scattering out of the beam or field of view of a detector by a medium such as the atmosphere.

ATTENUATION COEFFICIENT (b_λ): (See also, Extinction Coefficient.) The sum of the absorption coefficient and the scattering coefficient for a medium that absorbs and/or scatters radiation.

AZIMUTH: The length of the arc on the horizon (in degrees) intercepted between a line to a given point and an adopted reference direction, usually true north, and measured clockwise from the reference direction. Thus, azimuth is a horizontal direction expressed in degrees.

BACKSCATTER: A portion of the electromagnetic energy emitted from a source that is returned toward the source because of scattering with atmospheric particulates and other objects.

BLACK BODY: A hypothetical "body" which absorbs all of the electromagnetic radiation striking it; that is, one which neither reflects nor transmits any of the incident radiation.

BRIGHTNESS (B): Same as Luminance (Huschke [7]).

BRIGHTNESS, PHOTOMETRIC: Same as Luminance.

CANDLE: A unit of luminous intensity of a light source.

CANDELA: A unit of luminous intensity of a light source (SI units).

CLEAR LINE-OF-SIGHT (CLOS): That atmospheric condition in which a cloud-free line-of-sight exists between a sensor and target and the atmospheric attenuation of contrast (either visual or thermal) is not sufficient to reduce the apparent target and background contrast at the sensor location below a specified threshold level. The lock-on range defines the outer boundary of the clear line-of-sight.

CLEAR LINE-OF-SIGHT (CLOS) PROBABILITY: The probability that a clear line-of-sight exists between a sensor and target within the lock-on range under a given set of atmospheric conditions. The probability aspect of this parameter derives from the probability of a cloud-free line-of-sight under the specified cloud condition.

CLOSE AIR SUPPORT: Air attacks against hostile targets that are in close proximity to friendly forces and that require detailed integration of each air mission with the fire and movement of those forces.

CLOUD-FREE FIELD-OF-VIEW (CFFOV): Cloud-free line-of-sight applied to all possible lines-of-sight present within the field of view of a sensor and/or its display.

CLOUD-FREE LINE-OF-SIGHT (CFLOS): The absence of clouds on the line-of-sight between two points -- in this context between a target and sensor.

CLOUD-FREE LINE-OF-SIGHT (CFLOS) PROBABILITY: The probability that a cloud-free line-of-sight exists between two points, with a given set of cloud conditions. Estimate of this static probability assumes a random distribution of cloud elements. Dynamic cloud-free line-of-sight probability is the probability that a cloud-free line-of-sight will exist under a given cloud condition for a specified time interval between two points either or both of which may be moving.

CLUTTER: Objects, natural or artificial, other than the target, tending to hinder target detection.

COLLIMATED: Straight line, parallel beams of radiation.

CONTRAST, AERIAL: Defined as the ratio of the reflected visible radiation from the target to the reflected visible radiation from the background (B_t/B_b).

CONTRAST, APPARENT (C): For a given slant range, the difference between the luminance (or radiance or reflectance) of a target and the luminance (or radiance or reflectance) of the background, divided by the luminance (or radiance or reflectance) of the background; includes the effects of atmospheric attenuation. Defined as $(B_t-B_b)/B_b$ where B_t and B_b are the reflected visible radiation (luminance or brightness) from the target and background, respectively.

CONTRAST, BRIGHTNESS: Same as Apparent Contrast.

CONTRAST, INHERENT (C_o): For luminance (or radiance or reflectance) measurements taken close to the target (to avoid the effects of the atmosphere), the difference between the luminance (or radiance or reflectance) of a target and the luminance (or radiance or reflectance) of its background, divided by the background luminance (or radiance or reflectance).

CONTRAST, MODULATION: Defined as $(B_t-B_b)/(B_t+B_b)$ where B_t and B_b are the reflected visible radiation from the target and background, respectively.

CONTRAST THRESHOLD: The minimum target-to-background contrast at which a sensor can operate successfully.

CONTRAST TRANSMISSION: The ratio of the apparent target-to-background contrast to the inherent target-to-background contrast.

CROSSOVER, THERMAL: Various materials heat and cool at different rates. When the target and background radiative temperatures become equal, the inherent contrast becomes zero.

CUE: An item, feature, or signal that enhances target detection or acts as an indication of the nature of the object perceived.

CUING DEVICE: A device that receives and displays cues to an observer.

DENSITY, RADIANT FLUX: Same as Irradiance (Huschke [7]).

DELIQUESCENCE: The process by which a dry particle collects enough water molecules such that the particle goes into solution and becomes a droplet.

DEPTH, EXPONENTIAL MIXING: Refers to a surface turbulent mixing layer in which the distribution of a constituent decreases exponentially with height.

DEPTH, HOMOGENEOUS MIXING: Refers to a surface turbulent mixing layer in which the distribution of a constituent is constant with height.

DEPTH, OPTICAL: The mass of a given absorbing or emitting material lying along a geometric path of unit cross-sectional area.

DESIGNATOR: A device used to illuminate or irradiate a target or other object (e.g., a laser designator or a spotlight).

DESIGNATOR, LASER: A device capable of marking a target with a laser spot once the target has been acquired.

DETECTION, LIMINAL: Detection under conditions where the probability of success of 0.50.

DETECTION, TARGET: In the target acquisition cycle, an object is seen by the sensor.

ELEVATION ANGLE, SUN (SA): Same as Solar Angle.

EMISSION: The generation and sending out of radiant energy.

EMISSIVE POWER: Same as Emittance.

EMISSIVITY, SPECTRAL (ε_λ): The ratio of the emittance (emitted energy) of a given surface at a specified wavelength and temperature to the emittance of an ideal black body at the same wavelength and temperature.

EMITTANCE: (Same as Emissive Power.) A measure of the total radiant energy emitted per unit time per unit area of emitting surface; the total flux of electromagnetic radiation emitted by the unit surface area into a full hemisphere (2π steradians).

ENERGY, THERMAL: Heat. Energy transferred between systems because of differences in temperature, by radiation or by convection.

ENERGY, THRESHOLD: The minimum energy level at which a sensor can operate. Even if the energy contrast between target and background is great, the sensor cannot perceive the contrast if both the target or background energies are below the sensor's threshold energy.

ENVELOPE, BOMB: A sector which describes the maximum and minimum attack angle within which a bomb can be released based on the bomb's aerodynamic characteristics.

ENVELOPE, LAUNCH: A sector which describes the maximum and minimum attack angles within which a missile can be launched based on the missile's aerodynamic characteristics.

EROSION: Same as Ablation.

EXTINCTION COEFFICIENT: (See also, Attenuation Coefficient.) The sum of the absorption coefficient and the scattering coefficient for a medium that both absorbs and scatters radiation. Generally applies to visible radiation (Huschke [7]).

FLIGHT PROFILE: The flight path, airspeed, and altitude of an aircraft as a function of time.

FLUX: The rate of flow of some quantity (Huschke [7]).

FLUX DENSITY: The flux (rate of flow) of any quantity through a unit area of specified surface (Huschke [7]).

FLUX, LUMINOUS: The flux of visible radiation, so weighted as to account for the manner in which the response of the human eye varies with the wavelength of radiation.

FLUX, RADIANT: The rate of flow of radiant energy. Has dimensions of power per unit area.

FOOT-CANDLE (fc): A unit of illuminance. One lumen incident per square foot (Huschke [7]).

FOOT-LAMBERT: A unit of luminance or photometric brightness. $1/\pi$ candle per square foot (Huschke [7]).

FORWARD LOOKING INFRARED (FLIR): An acquisition system (designed to look forward from an aircraft) that senses radiation in either the 3 to 5 or 8 to 14 micrometer wavelength region of the electromagnetic spectrum.

FOVEA: The small rodless area of the central retinal region of the eye affording acute vision.

GLINT: A bright flash of light reflected from a surface.

IDENTIFICATION, TARGET: In the target acquisition cycle, an object can be described to the limit of the observer's knowledge (i.e., it is a motel, pickup truck, or policeman).

ILLUMINANCE: The total luminous flux received on a unit area of a given real or imaginary surface.

ILLUMINATION, GROUND: The luminous flux falling on a unit area of the ground from the sun, sky, moon, etc., possible units include lumens per square meter.

ILLUMINATION LEVEL: The amount of illumination falling upon a target/background scene. The amount depends mainly on the time of day, the degree of cloud cover, and the presence or absence of shadow.

IMAGE INTENSIFIER: (Also called image amplifier.) A device designed to amplify the brightness of visual displays through electrical methods.

IMAGING INFRARED (IIR or I^2R): A sensor which operates at infrared wavelengths and the accompanying display system which depicts a scene based on the sensor's data.

INSOLATION: Solar radiation received at the earth's surface. Also, the rate at which direct solar radiation is incident upon a unit horizontal surface at any point on or above the surface of the earth (Huschke [7]).

INTENSITY, LUMINOUS: The luminous flux per unit solid angle of a point source of radiation at visible wavelengths which has been adjusted to take into account the variable response of the human eye as a function of the wavelength of light.

INTENSITY, RADIANT: A measure of the radiant flux per unit solid angle emanating from some source (Huschke [7]).

INTERDICTION: The act of preventing or hindering, by any means, the enemy use of an area or route.

IRRADIANCE: (Same as Radiant Flux Density and Irradiation.) The total radiant flux received on a unit area of a given real or imaginary surface (Huschke [7]).

IRRADIATION: Same as Irradiance.

ISOTROPIC: Pertaining to a state of electromagnetic radiation in which the intensity is the same in all directions.

LASER: An acronym for light amplification by stimulated emitted radiation. Stimulating radiation excites the molecular structure of a material which initiates a coherent, collimated beam of electromagnetic radiation originating from within the material.

LOOK ANGLE, SENSOR: The angle formed by the line-of-sight of the sensor and the horizontal plane.

AD-A075 168 AIR WEATHER SERVICE SCOTT AFB IL F/G 4/1
ELECTRO-OPTICAL HANDBOOK. VOLUME I. WEATHER SUPPORT FOR PRECISI--ETC(U)
MAY 79 K G COTTRELL, P D TRY, D B HODGES
UNCLASSIFIED AWS/TR-79/002 NL

2 OF 2
ADA
075168

END
DATE FILMED
6-80
DTIC

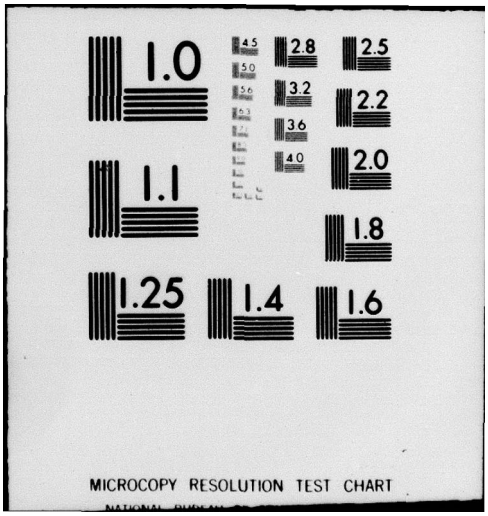
1.0
1.1
1.25
1.4
1.6
1.8
2.0
2.2
2.5
2.8
3.2
3.6
4.0
4.5
5.0
5.6
MICROCOPY RESOLUTION TEST CHART

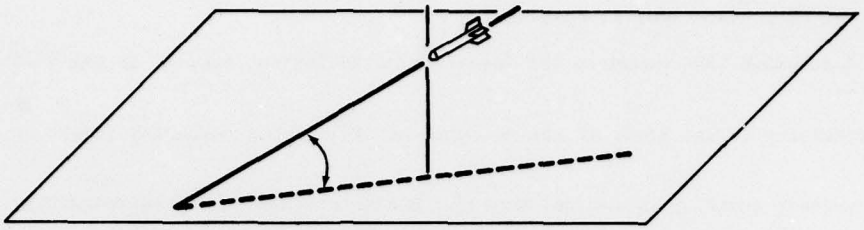

LOW LIGHT LEVEL TV (LLLTV): A television sensor system which views visible and very near IR wavelengths. Target-to-background contrasts are usually enhanced in the very near IR. The LLLTV possesses a photomultiplication capability which allows it to operate under low light level conditions; e.g., moonlit nights.

LUMEN: A unit of luminous flux. Equal to the luminour flux radiated into a unit solid angle (steradian) from a small source having a luminous intensity of one candle (Huschke [7]).

LUMINANCE: The photometric term corresponding to radiance; specifies the amount of power radiated from an extended body per solid angle and per projected area of radiating surface; expressed in lumens per steradian per square meter, or candle per square meter.

LUMINANCE, PATH: The amount of luminous flux scattered into the line-of-sight of an observer or emitted along the path.

LUMINANCE, SKY: The luminance of the sky at the horizon as measured in the same direction (azimuth) as the observer's line-of-sight.

LUMINOUS: Pertaining to the emission of visible radiation (Huschke [7]).

LUX: A unit of illuminance. One lumen incident per square meter (SI unit) (Huschke [7]).

MICROMETER (μm): One millionth of a meter.

MICRON (μ): Same as micrometer.

MODULATION TRANSFER FUNCTION: A characterization of an optical system in the spatial frequency domain -- specifically, the magnitude of the Fourier Transform of the line spread function (the line spread function describes the display of an extremely narrow straight line) as a function of spatial frequency.

MODULATION TRANSFER FUNCTION AREA: The area between the modulation transfer function of an acquisition system and the threshold-of-detectability curve of an observer.

MONOCHROMATIC: Pertaining to radiation of a single wavelength.

MONODISPERSED: Pertaining to a distribution of particulates which have a single radius.

NADIR: Straight down; opposite to zenith.

NEPHELOMETER: General name for an instrument which measures at more than one angle, the scattering function of particles suspended in a medium. Particle size and visual range can be determined from such measurements (Huschke [7]). An instrument that estimates the atmospheric extinction coefficient by shining a light through a sample of air and measuring the scattered light.

OCCULOMETER: An instrument that tracks the movement of an observer's eye.

OPTICAL TURBULENCE: Irregular and fluctuating gradients of optical refractive index in the atmosphere. Optical turbulence is caused mainly by mixing of air of different temperatures and particularly by thermal gradients which are sufficient to reverse the normal decrease in density with altitude.

ORIENTATION, TARGET: In the target acquisition cycle, an object is determined to be symmetric or asymmetric and its orientation may be discerned.

PARAFOVEAL VISION: Peripheral vision.

PARTICULATE: Any particle (liquid or solid) suspended in or falling through the atmosphere.

PASSIVE GUIDANCE SYSTEM: (See Sensor, Passive.)

PHOTOMETER: An instrument that measures the intensity of radiation, usually in the visible and near IR wavelengths.

PHOTOMETRIC: Pertaining to the study of the measurement of luminous intensity (light or visible radiation).

PHOTON: The elementary quantity of radiant energy. A discrete bundle of radiant energy.

PLANCK FUNCTION: An expression for the black body emittance as a function of temperature and the wavelength of emission.

POLYCHROMATIC: Pertaining to radiation of many wavelengths.

POLYDISPERSED: Pertaining to a distribution of particulates which have many different radii.

PRECIPITABLE WATER (PW): The total atmospheric water vapor contained in a vertical column of unit cross-sectional area extending between any two specified levels, commonly expressed in terms of the height to which that water substance would stand if completely condensed and collected in a vessel of the same unit cross-section.

PRECISION GUIDED MUNITION (PGM): A bomb or missile that is guided during its terminal phase.

PSEUDOTARGET: An object or image that might be mistaken for the true target; a group of pseudotargets appearing in a scene constitutes a form of clutter.

RADIANCE: The radiometric term specifying the amount of power radiated from an extended body per solid angle and per projected area of radiating surface expressed in watts per steradian per square meter.

RADIANCE, PATH: The radiant energy scattered into, or emitted in, the line-of-sight between the target and the sensor. This energy degrades the target-to-background contrast transmission along the line-of-sight by introducing nonimaging energy.

RADIANT ENERGY: The energy of any type of electromagnetic radiation.

RADIANT POWER: Same of Radiant Flux.

RADIATION: The transfer of energy by means of electromagnetic waves or particles.

RADIATIVE TEMPERATURE: (See Temperature, Radiative.)

RANGE: The distance between two points on the ground or the atmosphere.

RANGE, METEOROLOGICAL: The visual range at which the apparent contrast is a predetermined value. Usually, the value of 0.02 is used.

RANGE, TARGET ACQUISITION: A term which describes the range that is equivalent to the detection range, the orientation range, the recognition range, or the identification range.

RANGE, VISUAL: (Also called daytime visual range.) The distance, under daylight conditions, at which the apparent contrast between a specified type of target and its background becomes just equal to the threshold contrast of the observer (Huschke [7]).

RANGE GATED: A pulsed (over a time period) emission that is received by a sensor which is functioning only at the time that the radiation from a specific range interval between r and $r+\Delta r$ is arriving, where r is range.

RANGE MEASURING SYSTEM (RMS-2): A radio frequency system that collects data from which three-dimensional position as a function of time can be calculated for transponder instrumented aircraft and ground vehicles.

RATIO, CONTRAST: Same as Aerial Contrast.

RECOGNITION, TARGET: In the target acquisition cycle, the point at which the class to which an object belongs may be discerned (e.g., house, truck, man).

REFLECTANCE (R): The ratio of the luminous (or radiant) flux reflected from a surface to the total flux incident (illuminance) (or irradiance) upon that surface; varies according to the wavelength and angle of the incident radiation ($1 \geq R \geq 0$).

REFLECTIVITY: The ratio of the radiant energy reflected by a body to the total incident upon it.

REFRACTION: The process in which the direction of energy propagation is changed as the result of a change in density within the propagation medium, or as the energy passes through the interface representing a density discontinuity between two media (Huschke [7]). See Refractive Index.

REFRACTION, COMPLEX INDEX OF: An extension of the index of refraction to a consideration of the absorption of radiant energy by a substance.

REFRACTIVE INDEX: (Also called index of refraction.) A measure of the amount of refraction (a property of a dielectric substance). It is the ratio of the wavelength or phase velocity of an electromagnetic wave in a vacuum to that in a substance (Huschky [7]). It can be a function of wavelength, temperature, atmospheric pressure, and water vapor pressure.

REFRACTIVITY: Equal to (Refractive Index -1) X 10^6.

RESOLUTION: A measure of the smallest separation that a system can discriminate; often expressed as an angle in milliradians or minutes of arc.

SCATTERING: The process by which small particles suspended in a medium of a different index of refraction diffuse a portion of the incident radiation in all directions. In scattering, no energy transformation results, only a change in the spatial distribution of the radiation (Huschke [7]).

SCATTERING, ANOMALOUS: The spurious scattering of radiant energy which cannot be accounted for by Mie or Rayleigh scattering theory.

SCATTERING COEFFICIENT: A measure of the decrease in radiation (intensity) due to scattering as the radiation passes through the atmosphere (or other medium).

SCATTERING FACTOR: The ratio of the amount of radiation (at a specific wavelength) scattered by a substance (for example, haze) to the total amount of radiation (at a specific wavelength) incident on the substance. The values of the scattering factor range from zero to one. A value of one implies that all electromagnetic radiation incident on a substance is scattered.

SCATTERING, MIE: The distribution of energy which results from the interaction of energy incident on spherical particles whose radii are greater than approximately one tenth of the wavelength of the incident energy.

SCATTERING, MOLECULAR (Rayleigh): The distribution of energy which results from the interaction of energy incident on spherical particles whose radii are less than approximately one tenth of the wavelength of the incident energy.

SEEABILITY: The slant-range distance at which a sensor (e.g., human eye, TV, camera) is able to see, recognize, or lock onto a target through the intervening atmosphere which may contain clouds, haze, smoke, fog, precipitation, or dist. Furthermore, seeability is a function of target-to-background contrast, atmospheric parameters, direction, and type of illumination and sensor properties.

SEMIACTIVE GUIDANCE SYSTEM: (See Sensor, Semiactive.)

SENSOR, ACTIVE: An electro-optical sensor which also illuminates (or irradiates) a target or other object and senses the reflected (or scattered) energy coming from the target (e.g., a radar-guided missile).

SENSOR, ELECTRO-OPTICAL: The component of an electro-optical system which converts input electromagnetic by another part of the component. Examples include the human eye, a TV camera, or a photographic camera.

SENSOR, PASSIVE: An electro-optical sensor which preceives the emitted or reflected natural energy from a target or other object.

SENSOR, SEMIACTIVE: An electro-optical sensor which perceives the reflected energy from a target or other object. The reflected energy is created by illumination or irradiation by an unnatural source such as a laser designator.

SIGNAL-TO-NOISE RATIO (S/N): The ratio of the peak-to-peak amplitude of a signal to the root-mean-square amplitude of the noise superimposed on the signal.

SKY-GROUND LUMINANCE RATIO: The ratio of the luminance of the sky to the luminance of the ground.

SKY-GROUND RATIO: Same as Sky-Ground Luminance Ratio.

SLANT RANGE: The distance between a target or other object and a sensor within the atmosphere.

SOLAR ANGLE (SA): The angle between the line from the sun to the ground target and the line from the target to the horizon (contrast with sun angle).

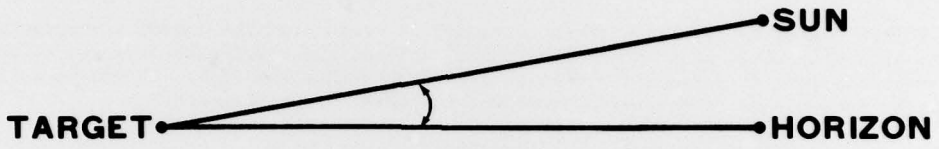

STEFAN-BOLTZMANN CONSTANT: A constant of proportionality between the radiant emittance of a black body and the fourth power of the body's absolute temperature.

SUN ANGLE: The angle between the line from the sun to the target and the line from the target to the sensor (contrast with solar angle).

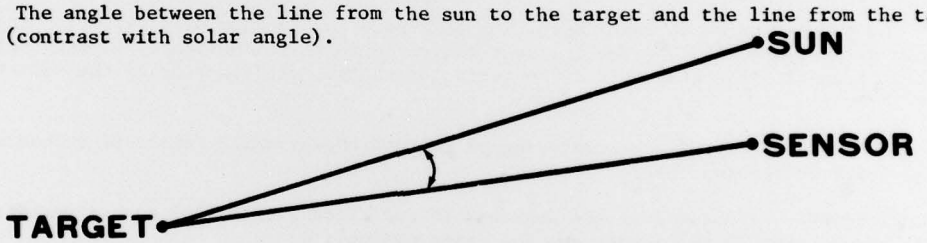

TARGET ACQUISITION CYCLE (CLASSICAL): A four-step cycle (after the target area is found) is illustrated by Johnson (Biberman [2]):

1. Detection - an object is present.
2. Orientation - the object is approximately symmetric or asymmetric and its orientation may be discerned.
3. Recognition - the class in which the object may be discerned (e.g., house, truck, man).
4. Identification - the target can be described to the limit of the observer's knowledge (e.g., motel, pickup truck, policeman).

TEMPERATURE, RADIATIVE (T*): The temperature an object appears to have based on the actual radiative emission of energy by the object. It is equivalent to the temperature that an object would appear to have if the object emitted black body radiation equal to the actual radiative emission.

TEMPERATURE, RADIOMETRIC: Same as Temperature, Radiative.

TERMINAL HOMING SYSTEM: The sensor and associated aerodynamic controls and surfaces used to guide a precision guided munition to a target.

THICKNESS, OPTICAL: Same as Depth, Optical.

THRESHOLD, ILLUMINATION (I_T): The minimum energy necessary to illuminate a target in order for a visual sensor to perceive the target/background scene. Even with sufficient target-to-background contrast, the target/background scene cannot be seen if the illumination is below the sensor's illumination threshold.

TRANSMISSIVITY (τ): The ratio of the radiant energy transmitted through part of the atmosphere (or other medium) to the total radiant energy incident upon a reference point within the atmosphere (or other medium) ($1 \geq \tau \geq 0$).

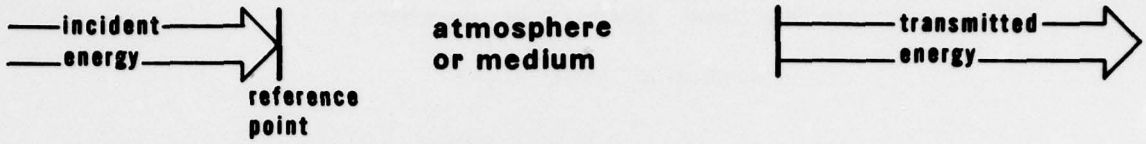

TRANSMITTANCE: Same as Transmissivity.

TRIBOELECTRIC EFFECT: The separation of electric charge on or near the surface of an object (e.g., a PGM) caused by the frictional interaction of the object with clouds of dust, ice crystals, and precipitation.

TURBIDITY, ATMOSPHERIC: A measure of the degree to which atmospheric constituents or processes (e.g., air molecules, particulates such as smoke, dust, and haze, and scintillation effects) reduce the transparency of the atmosphere to direct, usually visible or near IR, solar radiant energy. Cloudiness is excluded as an attenuating agent.

VISIBILITY (V): The observer to object distance at which the apparent contrast between the object and its surroundings equals the threshold contrast of the eye necessary for object identification.

WAVELENGTHS, FAR INFRARED: Electromagnetic radiation between 6 and 15 micrometers. (Both limits are arbitrary.)

WAVELENGTHS, INFRARED (IR): Electromagnetic radiation between 0.74 and 100 micrometers. (Upper limit is arbitrary.)

WAVELENGTHS, MICROWAVE (MW): Electromagnetic radiation between 1 centimeter and 100 centimeters. (Both limits are arbitrary.)

WAVELENGTHS, MIDDLE INFRARED: Electromagnetic radiation between 2 and 6 micrometers. (Both limits are arbitrary.)

WAVELENGTHS, NEAR INFRARED: Electromagnetic radiation between 0.74 and 2 micrometers. (Upper limit is arbitrary.)

WAVELENGTHS, SUBMILLIMETER: Electromagnetic radiation between 100 micrometers and 1000 micrometers (1 mm). (Both limits are arbitrary.)

WAVELENGTHS, ULTRAVIOLET: Electromagnetic radiation between 0.001 and 0.4 micrometers.

WAVELENGTHS, VISIBLE: Electromagnetic radiation between 0.4 and 0.74 micrometers.

ZENITH: The point that lies directly above an observer.

LIST OF ACRONYMS, ABBREVIATIONS, AND SYMBOLS

ACRONYMS AND ABBREVIATIONS

AA	antiaircraft
Ac	altocumulus
AFGL (formerly AFCRL)	Air Force Geophysics Laboratory
AFGWC	Air Force Global Weather Central
AGL	above ground level
AGM	air-to-ground missile
As	altostratus
AWS	Air Weather Service
BWS	base weather station
CFFOV	cloud-free field-of-view
CFLOS	cloud-free line-of-sight
Ci	cirrus
CLOS	clear line-of-sight
cm	centimeters
Cs	cirrostratus
DME	distance measuring equipment
EM	electromagnetic
EO or E-O	electro-optics
EOGB	electro-optically guided bomb
ETAC	Environmental Technical Applications Center
FAA	Federal Aviation Administration
FAC	forward air controller
fc	foot-candles
FLIR	forward looking infrared
FOV	field-of-view
g	gram
GBU	Guided Bomb Unit
GHz	Gigahertz
GLLD	ground located laser designator
IP	initial point
IIR	imaging infrared
I^2R	imaging infrared
IR	infrared
km	kilometer
LA	launch
LGB	laser guided bomb
LLLTV	low light level TV
LLO	laser lock on
LLOR	laser lock-on range
ln	natural logarithm
LO	lock on
LOR	lock-on range
LORAN	long-range navigation (equipment)
LOS	line-of-sight
LV	leave
MDR	maximum detection range
m	meter
mm	millimeter
MOS	model output statistics
mrad	milliradian
MSL	mean sea level
MTF	Modelation Transfer Function
MW	microwave
Ns	nimbostratus
OD	olive drab
PGM	precision guided munition
RPV	remotely piloted vehicle
R&D	research and development
SA	solar angle or solar elevation angle
SAM	surface-to-air missile
Sc	stratocumulus
SRV	slant-range visibility
St	stratus

stat mi	statute mile
SWO	staff weather officer
S/N	signal-to-noise
TA	target acquisition
TAR	target acquisition range
TV	television
WW	Weather Wing
USAFETAC	(See ETAC)
UV	ultraviolet
μm	micrometer

SYMBOLS

A	local hour angle
b	cloud height
B	brightness
b_a	aerosol volume extinction coefficient
$b_{aa,\lambda}$	monochromatic aerosol volume absorption coefficient
$b_{as,\lambda}$	monochromatic aerosol volume scattering coefficient
$b_{aa,o,\lambda}$	earth's surface value of $b_{aa,\lambda}$
$b_{as,o,\lambda}$	earth's surface value of $b_{as,\lambda}$
B_b, $B_b(O)$, $B_b(R)$	background brightness, background brightness at range equal to zero and at range equal to R, respectively
$b_{k,i}$	see section A-8
B_m	variable related to the component of the path radiance near the target divided by the value of the volume extinction coefficient b_o in vicinity of the target
$b_{ma,\lambda}$	monochromatic molecular volume absorption coefficient
$b_{ms,\lambda}$	monochromatic molecular volume (Rayleigh) scattering coefficient
B_t	target brightness
b_{TOT}	sum of b_a and b_w
b_w	water vapor volume absorption coefficient
B_λ	monochromatic decadic turbidity coefficient
b_λ	total volume monochromatic extinction or attentuation coefficient
$\tilde{b}$	volume extinction (attenuation) coefficient
b'_λ	monochromatic decadic extinction coefficient
$b'_{aa,\lambda}$	monochromatic volume absorption coefficient for aerosols
$b'_{as,\lambda}$	monochromatic volume scattering coefficient for aerosols

$b'_{ma,\lambda}(O_3)$	monochromatic decadic absorption coefficient for ozone
$b'_{ms,\lambda}$	monochromatic decadic scattering coefficient for air molecules
$\tilde{b}_o$	volume extinction coefficient in vicinity of the target
$\tilde{b}_\lambda$	representative monochromatic volume extinction coefficient
C	apparent contrast
C_{LO}	threshold contrast of lock-on sensor
$CLOS_{LOR}$	clear line-of-sight probability at lock-on range
$CLOS_{TAR}$	clear line-of-sight probability at target acquisition range
C_o	inherent contrast
C_R	apparent contrast at range R
C_{TA}	threshold contrast of acquisition sensor
C_1	constant for Junge's power law distribution
C_2, C_3	constants for Poliakova and Shifrin raindrop distribution
C_4, C_5	constants for Planck's Law
C_6	sum of $b'_{ms,\lambda}$ and $b'_{ma,\lambda}$
D	geometric path length
$D_{k,i}$	see section A-8
e	actual water vapor pressure
$E_{b,\lambda}$	energy emitted from background
e_s	saturation water vapor pressure
$E_{t,\lambda}$	energy emitted from target
E_λ	energy emitted at wavelength λ and temperature T
f	frequency
h, h_d	sensor and designator altitudes, respectively
H	low-level inversion base or top of haze layer
H_o	illumination at earth's surface
I	illumination level for cloudless sky
$I_{b,\lambda}$, $I_{b,o,\lambda}$	radiance arriving from background and inherent target radiance, respectively
I_c	illumination level for actual sky conditions
I_o	incident energy (intensity)
IR_{LOR}	infrared lock-on range

$I_{t,\lambda}$, $I_{t,o,\lambda}$	radiance arriving from target and inherent target radiance respectively
I_T	threshold illumination of target acquisition sensor
I_β	scattered energy (intensity)
I_λ	monochromatic beam intensity
$I_{\lambda,o}$	incident monochromatic beam intensity
k	Boltzmann constant
L	target dimension (overall size or hot-spot size)
L_{LO}	effective target dimension based on type of lock-on sensor
L_{TA}	effective target dimension based on type of target acquisition sensor
M	optical air mass
M_{LO}	lock-on sensor magnification factor
M_{TA}	acquisition sensor magnification factor
N	cloud amount
N'	number of aerosols per unit volume
$\tilde{N}$	number of molecules per unit volume
N_T	total cloud amount below sensor altitude
$\tilde{P}$	atmospheric pressure
P_r	path radiance or luminance (monochromatic or visible wavelength band)
Q	scattering area ratio (scattering efficiency)
r	particle radius
R	slant range
R_b	background reflectance
R_c	ratio of illuminance with overcast sky to illumination with cloudless sky
R_d	gas constant for dry air
RH	relative humidity
$\overline{R}$	horizontal distance in a homogeneous atmosphere for which the extinction is the same as that actually encountered along the true path of length R
$\overline{RH}$	representative low-level relative humidity
R_t	target reflectance
R_V	ratio of surface visibility to slant range visibility
r_o	minimum aerosol radius

r_1	maximum aerosol radius
S	speed of light
SA	solar elevation angle
T	temperature
T_b	background temperature (physical)
t_c	cloud type
T_{IRT}	threshold transmittance which is equal to $\Delta T^*_{RT}/\Delta T^*_o$
T_t	target temperature (physical)
$\overline{T}$	average low-level temperature (below inversion)
$\overline{T}_d$	average low-level dew point (below inversion)
T_{TOT}	see section A-8
T^*	radiative temperature
T^*_b	background radiative temperature
T^*_t	target radiative temperature
V, V_R	surface visibility and meteorological visual range, respectively
V_s	slant-range visibility
X	size parameter
z	independent variable for altitude
z'	aerosol scale height
α_{LO}	minimum resolvable subtense angle for lock-on sensor
α_{TA}	minimum resolvable subtense angle for target acquisition sensor
β	scattering angle
β_c	water vapor continuum volume absorption coefficient
β_m	water vapor molecular volume absorption coefficient
δ	solar declination
ΔI_λ	difference in target and background beam intensity
ΔT^*	radiative temperature difference between target and background
ΔT^*_o	inherent difference between target and background radiative temperatures
ΔT^*_{RT}	minimum detectable radiative temperature contrast of sensor
$\varepsilon_{b,\lambda}$	monochromatic background emissivity
$\varepsilon_{t,\lambda}$	monochromatic target emissivity

θ	look or dive angle
θ_{LLOR}	look angle at laser lock-on range
θ_{LOR}	look angle at lock-on range
θ_{TAR}	look angle at target acquisition range
λ	wavelength of radiation
ρ	air density
τ	beam transmission or transmissivity
τ_c	contrast transmission
τ_λ	monochromatic beam transmission or transmissivity
ϕ	latitude
Ω	solar elevation angle